AN OBSERVATIONAL INVESTIGATION OF LAKE-BREEZE FRONTAL MOVEMENT THROUGH THE CHICAGO AREA

BY

JASON M. KEELER

THESIS

Submitted in partial fulfillment of the requirements
for the degree of Master of Science in Atmospheric Sciences
in the Graduate College of the
University of Illinois at Urbana-Champaign, 2010

Urbana, Illinois

Adviser:

Adjunct Associate Professor David A. R. Kristovich

ABSTRACT

Lake- and sea-breezes have been extensively studied using observational, theoretical, numerical modeling, and laboratory techniques. Large population centers in coastal regions, such as Chicago, make predicting and understanding of these circulations particularly important due to their impacts on dispersion of pollutants, heat wave relief, and energy use. While recent numerical model simulations have suggested that sea- or lake-breezes should move more slowly through urban areas than in the surrounding suburbs due to the Urban Heat Island (UHI) circulation, there have been few fine-scale observations of the spatial and temporal variations in lake-breeze movement to evaluate these results. The goal of this research is to utilize high-resolution WSR-88D observations to evaluate the effect of the UHI on lake-breeze frontal movement through Chicago and nearby suburban areas. This was accomplished by identifying and analyzing a total of 44 lake-breezes which occurred during the April – September 2005 period.

During 2005 the monthly frequency of lake-breezes near Chicago gradually increased from 5 in April to 12 in August, despite a maximum in air-lake temperature differences in April. The August peak appears to be related to a decrease in the wind speed later in the warm season. A great deal of temporal and spatial variability of inland motion of the lake-breeze front (LBF) was noted. For example, while many LBF remained close to the shore, one LBF progressed more than 130 km inland.

The hourly position of the radar fine line was used to determine inland movement of the LBF along several shore-perpendicular cross-sections throughout the Chicago, IL,

area. This allowed for detailed analyses of the relationship between Chicago's UHI on lake-breeze frontal movement. The observed daytime UHI, which was substantially weaker than at night, did not have a statistically significant relationship with lake-breeze frontal movement through Chicago. However, the magnitude of the nighttime UHI preceding lake-breezes was found to decrease the speed of LBF movement as it progressed from downtown Chicago to its southwest suburbs. Physically, this relationship is consistent with previous studies of the diurnal evolution of UHI circulations.

TABLE OF CONTENTS

CHAPTER

1. BACKGROUND....1

1. Sea- and Lake-Breezes....1

a. Overview....1

b. Horizontal Variability of Sea- and Lake-Breeze Fronts....2

2. Urban Heat Islands....4

a. Thermal Structure....4

b. The Urban Heat Island Circulation....4

3. Sea- and Lake-Breeze Interaction with Urban Heat Islands....6

4. Summary....8

2. DATA AND METHODOLOGY....10

1. Selection of Lake-Breeze Cases....10

2. Analysis of Lake-Breeze Frontal Movement....13

a. Procedure....13

b. Validation....16

3. Surface Data....19

3. GENERAL LAKE-BREEZE CHARACTERISTICS....22

1. Forcing and Distribution of Lake-Breezes....22

2. Inland Motion of the Lake-Breeze Front.....28

a. Speed of Inland Motion.....28

b. Inland Penetration of the Lake-Breeze Front.....31

3. Case Studies.....34

a. Lake-Breeze Interaction with Cold Fronts.....34

b. Retrograding Lake-Breeze Fronts.....36

4. LAKE-BREEZE FRONTAL MOVEMENT THROUGH CHICAGO: EFFECTS OF THE URBAN HEAT ISLAND.....39

1. Chicago's Urban Heat Island.....39

a. Variation in Urban Heat Island Magnitude.....39

b. Evidence of an Urban Heat Island Circulation.....41

2. Urban Heat Island and Lake-Breeze Interaction.....46

3. Discussion.....52

5. CONCLUSIONS.....54

REFERENCES.....59

APPENDIX A: Hourly Lake-Breeze Front Locations.....63

AN OBSERVATIONAL INVESTIGATION OF LAKE-BREEZE FRONTAL MOVEMENT THROUGH THE CHICAGO AREA

BY

JASON M. KEELER

THESIS

Submitted in partial fulfillment of the requirements
for the degree of Master of Science in Atmospheric Sciences
in the Graduate College of the
University of Illinois at Urbana-Champaign, 2010

Urbana, Illinois

Adviser:

Adjunct Associate Professor David A. R. Kristovich

ABSTRACT

Lake- and sea-breezes have been extensively studied using observational, theoretical, numerical modeling, and laboratory techniques. Large population centers in coastal regions, such as Chicago, make predicting and understanding of these circulations particularly important due to their impacts on dispersion of pollutants, heat wave relief, and energy use. While recent numerical model simulations have suggested that sea- or lake-breezes should move more slowly through urban areas than in the surrounding suburbs due to the Urban Heat Island (UHI) circulation, there have been few fine-scale observations of the spatial and temporal variations in lake-breeze movement to evaluate these results. The goal of this research is to utilize high-resolution WSR-88D observations to evaluate the effect of the UHI on lake-breeze frontal movement through Chicago and nearby suburban areas. This was accomplished by identifying and analyzing a total of 44 lake-breezes which occurred during the April – September 2005 period.

During 2005 the monthly frequency of lake-breezes near Chicago gradually increased from 5 in April to 12 in August, despite a maximum in air-lake temperature differences in April. The August peak appears to be related to a decrease in the wind speed later in the warm season. A great deal of temporal and spatial variability of inland motion of the lake-breeze front (LBF) was noted. For example, while many LBF remained close to the shore, one LBF progressed more than 130 km inland.

The hourly position of the radar fine line was used to determine inland movement of the LBF along several shore-perpendicular cross-sections throughout the Chicago, IL,

area. This allowed for detailed analyses of the relationship between Chicago's UHI on lake-breeze frontal movement. The observed daytime UHI, which was substantially weaker than at night, did not have a statistically significant relationship with lake-breeze frontal movement through Chicago. However, the magnitude of the nighttime UHI preceding lake-breezes was found to decrease the speed of LBF movement as it progressed from downtown Chicago to its southwest suburbs. Physically, this relationship is consistent with previous studies of the diurnal evolution of UHI circulations.

TABLE OF CONTENTS

CHAPTER

1. BACKGROUND....1

1. Sea- and Lake-Breezes....1

a. Overview....1

b. Horizontal Variability of Sea- and Lake-Breeze Fronts....2

2. Urban Heat Islands....4

a. Thermal Structure....4

b. The Urban Heat Island Circulation....4

3. Sea- and Lake-Breeze Interaction with Urban Heat Islands....6

4. Summary....8

2. DATA AND METHODOLOGY....10

1. Selection of Lake-Breeze Cases....10

2. Analysis of Lake-Breeze Frontal Movement....13

a. Procedure....13

b. Validation....16

3. Surface Data....19

3. GENERAL LAKE-BREEZE CHARACTERISTICS....22

1. Forcing and Distribution of Lake-Breezes....22

2. Inland Motion of the Lake-Breeze Front.....28

a. Speed of Inland Motion.....28

b. Inland Penetration of the Lake-Breeze Front.....31

3. Case Studies.....34

a. Lake-Breeze Interaction with Cold Fronts.....34

b. Retrograding Lake-Breeze Fronts.....36

4. LAKE-BREEZE FRONTAL MOVEMENT THROUGH CHICAGO: EFFECTS OF THE URBAN HEAT ISLAND.....39

1. Chicago's Urban Heat Island.....39

a. Variation in Urban Heat Island Magnitude.....39

b. Evidence of an Urban Heat Island Circulation.....41

2. Urban Heat Island and Lake-Breeze Interaction.....46

3. Discussion.....52

5. CONCLUSIONS.....54

REFERENCES.....59

APPENDIX A: Hourly Lake-Breeze Front Locations.....63

CHAPTER 1

BACKGROUND

In order to put the current research in perspective of what is currently understood about the sea-breeze and urban heat island systems, a review of the literature is provided. This review will consist of overviews of sea-and lake-breezes, urban heat islands, and interactions between them.

1. Sea- and Lake-Breezes

a) *Overview*

Sea- and lake- breezes have a significant impact on local climate and air quality. For example, during the July 1995 Chicago heat wave, cooler air temperatures near the Lake Michigan shoreline were attributed to lake-breezes (Kunkel et al., 1996). Several authors have commented on the effect of coastal circulations on pollution. Emissions from Chicago and northern Indiana can be advected over Lake Michigan, and then transported inland by the lake-breeze circulation (Lyons and Cole, 1976). Keen and Lyons (1978) documented the recirculation of pollutants by a lake-breeze on the west shore of Lake Michigan.

A detailed review of the results of sea- and lake-breeze studies is provided by Miller et al. (2003). Sea- and lake-breezes are mesoscale circulations which result from temperature gradients in the vicinity of the land-water interface. On days with limited cloud-cover and adequate solar insolation, the land surface warms more quickly than the sea, which causes a temperature gradient to develop. This temperature gradient induces a

pressure gradient aloft, which causes a thermally-direct circulation. At the surface, this circulation causes cooler marine air from over the sea/lake to move inland. The leading edge of this cool, marine airmass is defined as the sea- or lake-breeze front. The upper portion of the lake-breeze circulation is referred to as the "return flow". Moroz (1967) was the first to observe the sea- or lake-breeze return flow in the mid-latitudes. This was done by tracking pilot balloons as they ascended through the lake-breeze circulation on the east shore of Lake Michigan. The observed onshore flow extended to a height of 750 m and exceeded 7 m s^{-1}. The return flow was twice as deep as the onshore flow and sometimes extended to a height of 2500 m.

A 15-year (1982 – 1996) climatology of lake-breezes occurring on Lake Michigan was conducted by Laird et al. (2001). Dates during which lake-breezes occurred were identified using hourly surface observations of wind and temperature. The peak frequency of lake-breezes by month was in August, with an average of 7.8 days. Laird et al. (2001) found that weak flow perpendicular to the lake shore in August allowed for the lake-breeze to penetrate inland more readily, despite the land-lake thermal contrast peaking earlier in the year. Similarly, Arritt (1993) found that sea-breezes are more likely to occur on days with weak offshore flow. Arritt also found that sea-breeze fronts and the sea-breeze circulation are poorly defined if the larger-scale flow is from the sea towards land.

b) ***Horizontal Variability of Sea- and Lake-Breeze Fronts***

The structure of sea-breeze systems can be complicated by the presence of bays, rivers, orographic features and other coastal irregularities. McPherson (1970) studied the impact of shoreline shape on sea-breezes. Based on simulations of a sea-breeze that

developed near an idealized version of Galveston Bay, McPherson showed that the leading edge of the sea-breeze followed the shoreline. This led to areas of convergence and divergence in the vicinity of convex and concave shores, respectively. Accordingly, near Chicago the overall concave shoreline should add a divergent component to the surface flow field when a lake-breeze is occurring. This divergence, however, could be offset locally, due to inland mesoscale circulation features, such as the Urban Heat Island circulation.

Wakimoto and Atkins (1994) documented small-scale perturbations in the horizontal structure of the sea-breeze front utilizing data collected during the Convection and Precipitation/Electrification (CaPE) experiment. Atkins et al. (1995) suggested that these irregularities were the result of the sea-breeze front intersecting with horizontal convective rolls within the boundary layer. Laird et al. (1995) conducted dual-Doppler analyses of the sea-breeze using radar data from CaPE and found that even small-scale coastal irregularities, such as rivers, can affect the structure of sea-breezes. A strong convergence line was observed behind intersecting segments of the sea-breeze front inland from a convex coastal area. A deeper sea-breeze circulation was present in the vicinity of this convergence line, which enhanced convective initiation. These papers indicate that the sea-breeze system is quite complex, even without the complicating effects of inland land cover variability, such as due to cities, and that there is much left to be learned about the sea-breeze system.

2. Urban Heat Islands

a) *Thermal Structure*

The Urban Heat Island is an urban – rural temperature perturbation that develops due to differences in thermal properties between urban and rural areas. Bornstein (1968) provided one of the first descriptions of the horizontal and vertical structure of the Urban Heat Island (UHI). Bornstein analyzed temperature data collected using an instrumented helicopter in the New York City area on 42 dates during the 1964 to 1966 period. On average, a positive temperature perturbation extended to a height of 300 m, relative to the temperature in the suburbs.

Ackerman (1985) developed a 30-year climatology of Chicago's UHI. The magnitude of the heat island was represented by the surface air temperature difference between Midway Airport and Argonne National Laboratory (located 23 kilometers to the southwest). The average UHI magnitude in Chicago was 1.85°C, and the maximum observed UHI magnitude was 9.3°C. A distinct diurnal cycle was observed, with a nighttime maximum and mid-day minimum. On the annual cycle, the UHI was weakest in April and strongest from July – September. On shorter time scales, the largest UHI magnitudes were observed when the wind was weak and there was limited or no cloud cover. Cloud cover was a less important factor when the wind was not weak (Ackerman, 1985). A similar approximation for the UHI magnitude will be used in this study, and is discussed in more detail in Chapter 2.

b) *The Urban Heat Island Circulation*

Similar to sea- or lake-breezes, Urban Heat Islands induce a thermally-driven mesoscale circulation with surface convergence centered on or near the urban area.

Utilizing a 2D linear model with a domain through a rural-city-rural cross-section, Vukovich (1971) found that larger-scale horizontal wind horizontally displaces the UHI circulation. This was verified by Wong and Dirks (1978), who analyzed UHI cases from summer 1975 utilizing data from the Metropolitan Meteorological Experiment (METROMEX) in St. Louis, MO. Wong and Dirks concluded that UHI circulations are displaced approximately 10 – 15 km downwind of the urban center when there is a uniform wind of 3 – 6 m s^{-1} throughout the mixing layer. On some occasions, other mesoscale circulations, such as the lake-breeze can displace the UHI circulation (Munn et al., 1969).

The UHI circulation is also known to have a diurnal cycle. While it may appear to be counterintuitive at first, previous research indicates that the maximum in the UHI circulation is during the daytime, despite stronger forcing occurring at night. This has been observed in at least two field campaigns (METROMEX: Vukovich et al., 1979; CAPITOUL: Hidalgo et al., 2008). Richiardone and Brusaca (1989) found that as the horizontal dimension of a city increases, the UHI circulation takes longer to develop. This could be an important factor in cities with a large areal extent, such as Chicago. Richiardone and Brusaca also found that decreased stability leads to a stronger and wider UHI circulation. Further, development of urban areas has been noted to increase the strength of UHIs over the course of multiple years (Comrie, 2000; Kusaka et al., 2000). Accordingly, as Chicago expands with time, one may expect its UHI and effect on lake-breezes to increase.

3. Sea- and Lake-Breeze Interaction with Urban Heat Islands

Over the past several decades, there have been many investigations of interactions between sea- or lake-breezes and Urban Heat Islands, based primarily on numerical simulations. Several studies have inferred the effect of urban areas on the sea-breeze circulation by removing a city or by changing its location and/or size in numerical simulations. Yoshikado (1992) simulated the UHI circulation in the vicinity of a sea-breeze over flat terrain using a 2D model. In his simulation the sea-breeze advanced inland more rapidly during its "growing" stage, and then slowed due to convergence of the sea-breeze and UHI inflow. The intensity of the sea-breeze front increased as a result of this convergence. In a similar 2D simulation, Sarkar et al. (1998) found that the presence of an urban area slightly decreased the inland penetration of the sea-breeze front (160 km versus 170 km). Stronger vertical velocities at the sea-breeze front and a deeper Thermal Internal Boundary Layer (TIBL) were observed in the simulation with a city. Additionally, Sarkar et al. found that increasing the heat flux from the city increased the strength of UHI circulation and the low-level flow associated with the sea-breeze.

Kusaka et al. (2000) ran 3D simulations of sea-breeze and UHI interactions in Tokyo based on the land use in 1900, 1950, and 1985. During that time frame the horizontal scale of Tokyo's urban area quadrupled from 10 to 40 km. Kusaka et al. found that the increase in Tokyo's size led to an increase in the magnitude of the UHI, slower inland movement of the sea-breeze, and a more clearly defined sea-breeze front. Specifically, in the simulation based on 1985 it took 2 more hours for the sea-breeze front to reach a specific inland location than it did in the 1900 simulation. Cedenese and Monti (2003) found that the UHI plume, the updraft portion of the UHI circulation, was shifted

by the sea-breeze in laboratory water tank experiments with a circular heater representing the city. The presence of an inland city (in addition to a coastal city) on the sea-breeze was simulated by Ohashi and Kida (2002). In this case the sea-breeze was able to penetrate further inland as a result of the inland UHI circulation.

Observational studies of the influence of UHI circulations on the sea-breeze are much more limited. Surface observations taken during 40 sea-breezes in the Boston, MA area were analyzed by Barbato (1978). Of the 40 cases analyzed, 62.5% remained in the lower topography near Boston. High topography inland of Boston limited the maximum inland penetration of the sea-breeze to 29.3 km. The average speed of inland penetration of the sea-breeze front between the shore and downtown Boston (Kenmore square) was 11.7 km hr^{-1}. Between downtown and the Waltham data site, located approximately 20 km inland, the sea-breeze front penetrated inland at 4.7 km hr^{-1}. Barbato suggested that the initial inland speed of the sea-breeze front was faster due to the high temperature gradient between the downtown area and the shore. The observed inland deceleration of the sea-breeze front could be due to higher topography west of Boston. Inland deceleration of the lake-breeze front due to topography would not be expected near Chicago, due to the relatively smooth topography of the Midwest compared to Massachusetts.

In New York City, Bornstein and Thompson (1981) deployed a high density network of anemometers in conjunction with the New York University/New York City (NYU/NYC) Urban Air Pollution Dynamics Project. These wind data were used to analyze the inland motion of the sea-breeze front for two Intensive Operation Periods (IOPs). During those IOPs, the inland motion of the sea-breeze front was notably slower

through the core of New York City, resulting in a higher concentration of pollutants in the Bronx, the northernmost borough of New York City. Bornstein and Thompson suggested that the observed slowing of the sea-breeze front through New York City was due to locally higher surface friction in New York City, relative to its surroundings. This contradicts the papers discussed earlier, which have suggested deceleration of sea-breeze is due to the Urban Heat Island circulation.

4. Summary

Sea- and lake-breezes are thermally driven mesoscale circulations that develop as the result of differential surface heating (Miller et al., 2003). During the day, the air over land warms more quickly than the marine airmass over the water; this induces a pressure gradient which causes the marine airmass to move inland. The inland transport of the marine airmass can provide relief from heat waves (Kunkel et al., 1996), and affects pollution concentrations in the vicinity of the circulation (Keen and Lyons, 1978; Lyons and Cole, 1976). The leading edge of the sea-breeze, or sea-breeze front, is more clearly defined when weak opposing flow is present, and is poorly defined when the large scale flow is from the water toward land (Arritt, 1993).

Urban Heat Islands are urban – rural temperature perturbations that develop as a result of differences in thermal properties of the surface (Bornstein, 1968). This temperature perturbation has a diurnal cycle with a nighttime maximum and daytime minimum (Ackerman, 1985). As with the sea-breeze, this temperature perturbation induces a mesoscale circulation, which is stronger during the day (Vukovich et al., 1979; Hidalgo et al., 2008).

Interactions between the UHI and sea-breeze circulations are hypothesized to have key implications on the inland motion of the sea-breeze front. Numerical simulations have suggested that after an initial acceleration to the urban center (UHI circulation updraft), the sea-breeze front moves inland more slowly than it would if the city were not there (Yoshikado, 1992; Sarkar et al., 1998; Kusaka et al., 2000). This deceleration has been hypothesized to ultimately reduce the inland penetration of the sea-breeze in the vicinity of urban areas (Sarkar et al., 1998). To date, no studies have attempted to validate these recent hypotheses utilizing high-resolution observations of sea- or lake-breezes. The goal of this research is to relate high-resolution observations of lake-breezes in the vicinity of Chicago to observed surface data in order to evaluate these recent hypotheses.

CHAPTER 2

DATA AND METHODOLOGY

1. Selection of Lake-Breeze Cases

In order to fully understand the effect of the Urban Heat Island on the motion of the lake-breeze front through the Chicago, IL, area, a large sample of lake-breezes needed to be selected and analyzed. This was accomplished by identifying dates during which lake-breezes developed in the vicinity of the KLOT WSR-88D radar (Figure 2.1) throughout the warm season of 2005. For the purposes of this study, the warm season was considered March 1 through November 30.

As an initial filter, archived visible satellite images were examined in order to eliminate days which were overcast, since lake-breezes rarely occur during overcast conditions (Laird et al., 2001). These satellite images, archived by the Illinois State Water Survey Center for Atmospheric Sciences, were obtained courtesy of the Aviation Digital Data Service (ADDS, 2005). Of the initial 275 dates in the March 1 through November 30 period, 59 dates were eliminated as potential cases due to overcast conditions. An additional 6 dates were eliminated due to the presence of banded cloud formations originating over the Great Lakes, indicative of lake-effect precipitation. Since lake-effect precipitation requires the boundary layer over the involved lake to be much warmer than that of the ambient environment, lake-breezes would be unlikely to have occurred on those dates.

Radar fine lines have been used to identify sea-breezes since the 1950s (Atlas, 1960). An example of a radar fine line is shown in Figure 2.1. Advances in radar

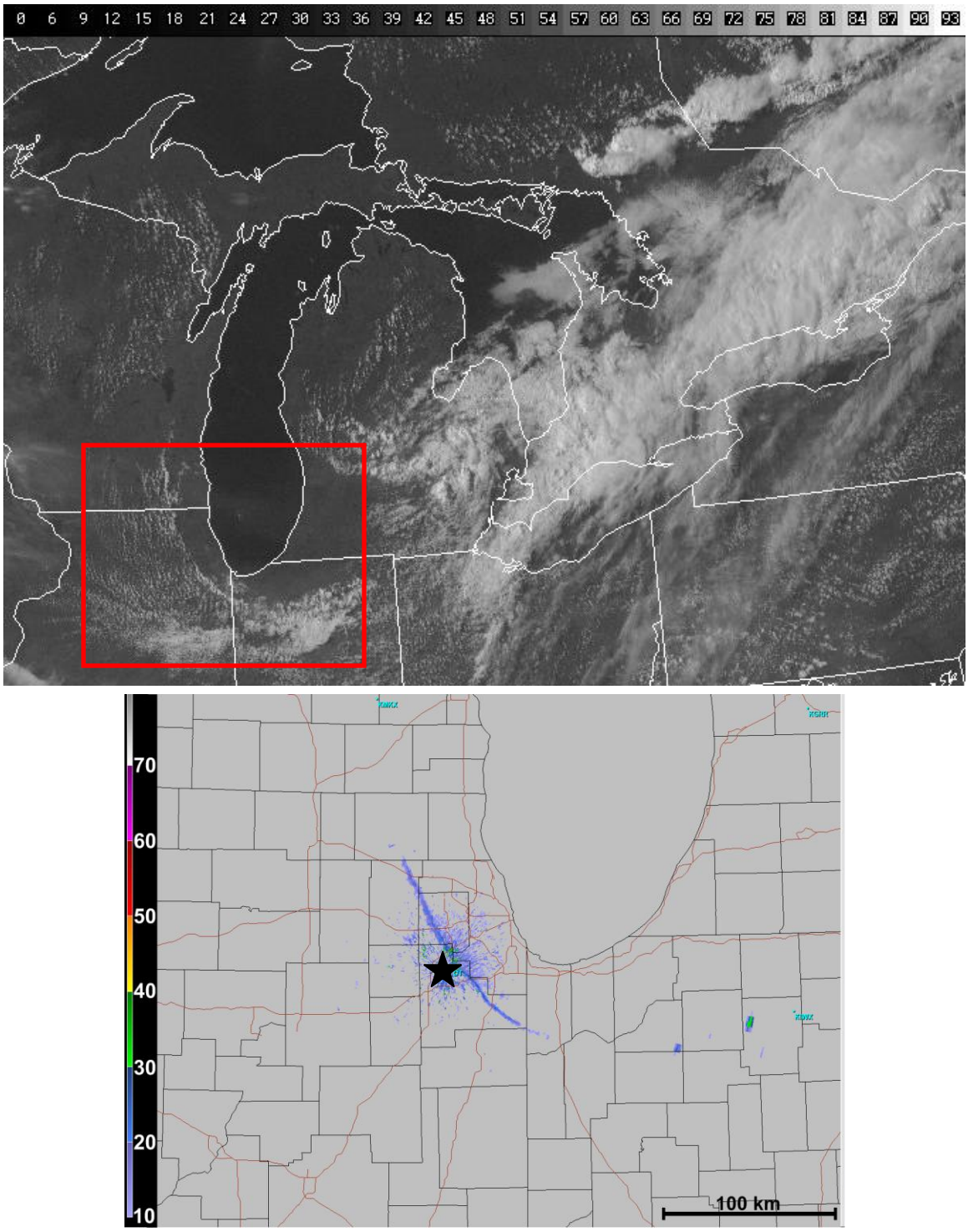

Figure 2.1. Example of a lake-breeze as seen by visible satellite (top; source: Aviation Digital Data Service, 2005), and radar base reflectivity (bottom, dBZ) for approximately 2115 UTC 21 June 2005. The domain of the radar image is marked by a red box in the top panel. The location of the KLOT WSR-88D radar is indicated by the black star in the bottom panel.

technology, utilized in the upgrade from the WSR-57 to WSR-88D network increased the ability of these radars to detect mesoscale boundaries (Crum and Alberty, 1993), such as lake-breeze fronts, boundary layer rolls, convective outflows, etc. After the initial filter using satellite data, Level II data from the KLOT WSR-88D radar (NCDC, 2008) were analyzed using GR2Analyst software (Gibson Ridge, Version 1.44) for the presence of

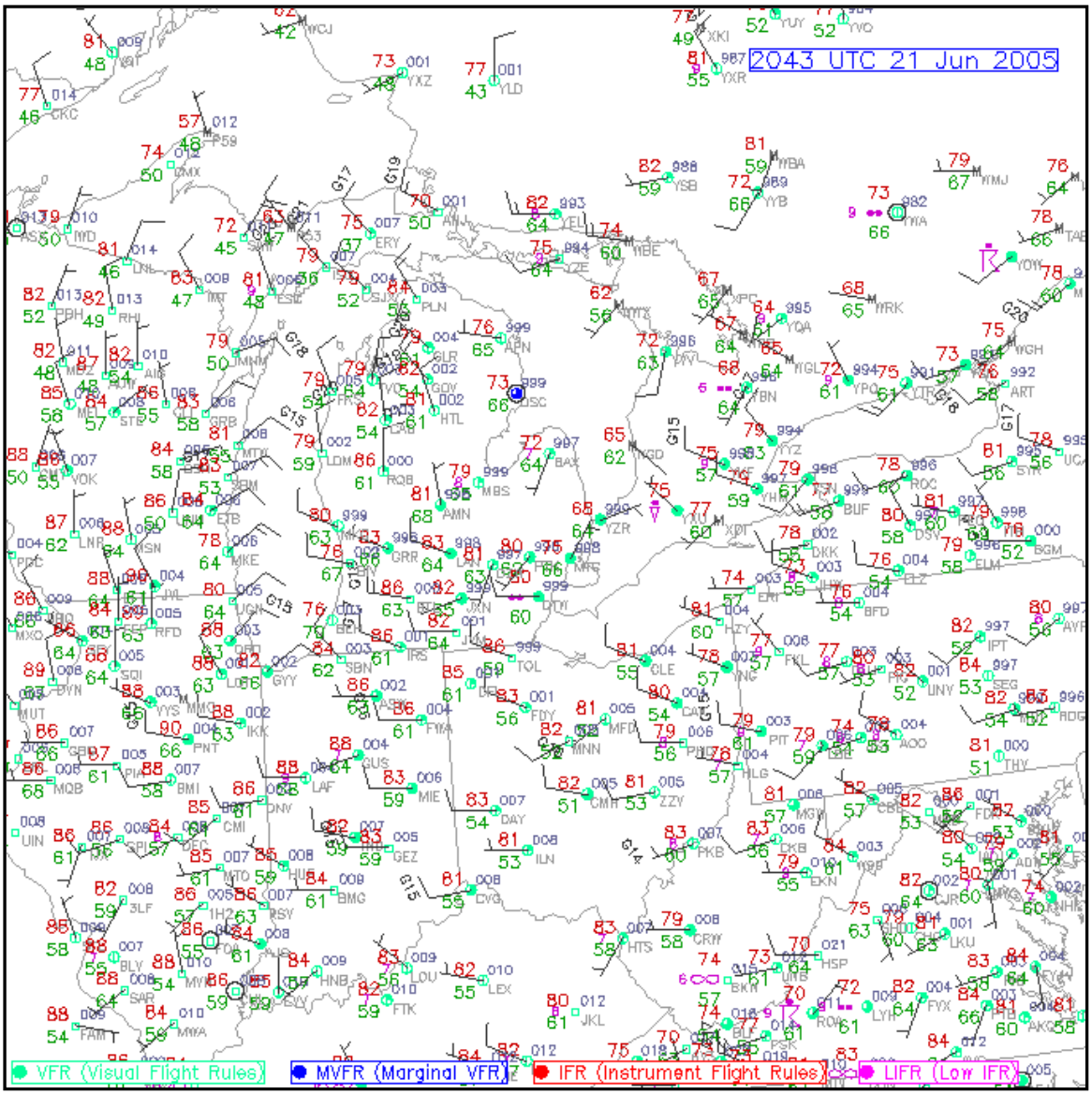

Figure 2.2. Example of surface conditions during a lake-breeze off of Lake Michigan. Note the divergence over Lake Michigan, convergence on the west side of Chicago, and cooler temperatures along the shore of Lake Michigan. Source: University Corporation for Atmospheric Research – Research Applications Laboratory, 2008.

fine lines (in reflectivity, velocity, or spectral width fields) on the remaining 210 dates. An additional 109 dates were eliminated due to a lack of radar fine lines and 7 dates were eliminated due to no radar data being available for that day.

Surface temperature and wind data from the remaining 94 dates were examined to determine if the observed fine lines were lake-breeze fronts, rather than horizontal convective rolls and/or outflow from convection. In order to be considered a lake-breeze front, the fine line must have been collocated with a surface convergence zone, and cooler surface temperatures had to be present on the side of the fine line closer to Lake Michigan. Both of these criteria can be seen along the west coast of Lake Michigan in the example surface map shown in Figure 2.2. A total of 49 lake-breeze cases met all of the above criteria during the warm season of 2005.

2. Analysis of Lake-Breeze Frontal Movement

a. *Procedure*

The hourly locations of the lake-breeze front, indicated by radar fine lines, were documented along several approximately shore-perpendicular cross sections through the Chicago, IL, area (Figure 2.3). These cross sections were selected so that the speed of inland movement of the lake-breeze front could be quantified through downtown Chicago and the surrounding suburbs. Inland motion of the lake-breeze front along cross sections outside of downtown Chicago provided a baseline, so that the effect of Chicago on the lake-breeze could be better understood. The seven cross sections, spaced by approximately 15 km along the coast, cover the domain where the lake-breeze front can

typically be seen by the WSR-88D radar in Romeoville, IL. The locations of the cross sections in Figure 2.3 were used for all cases.

Along each cross section, the distance which the lake-breeze front progressed was divided by the time lapse between the radar images in order to determine the average hourly speed of the inland motion of the lake-breeze front. This allowed for analysis of

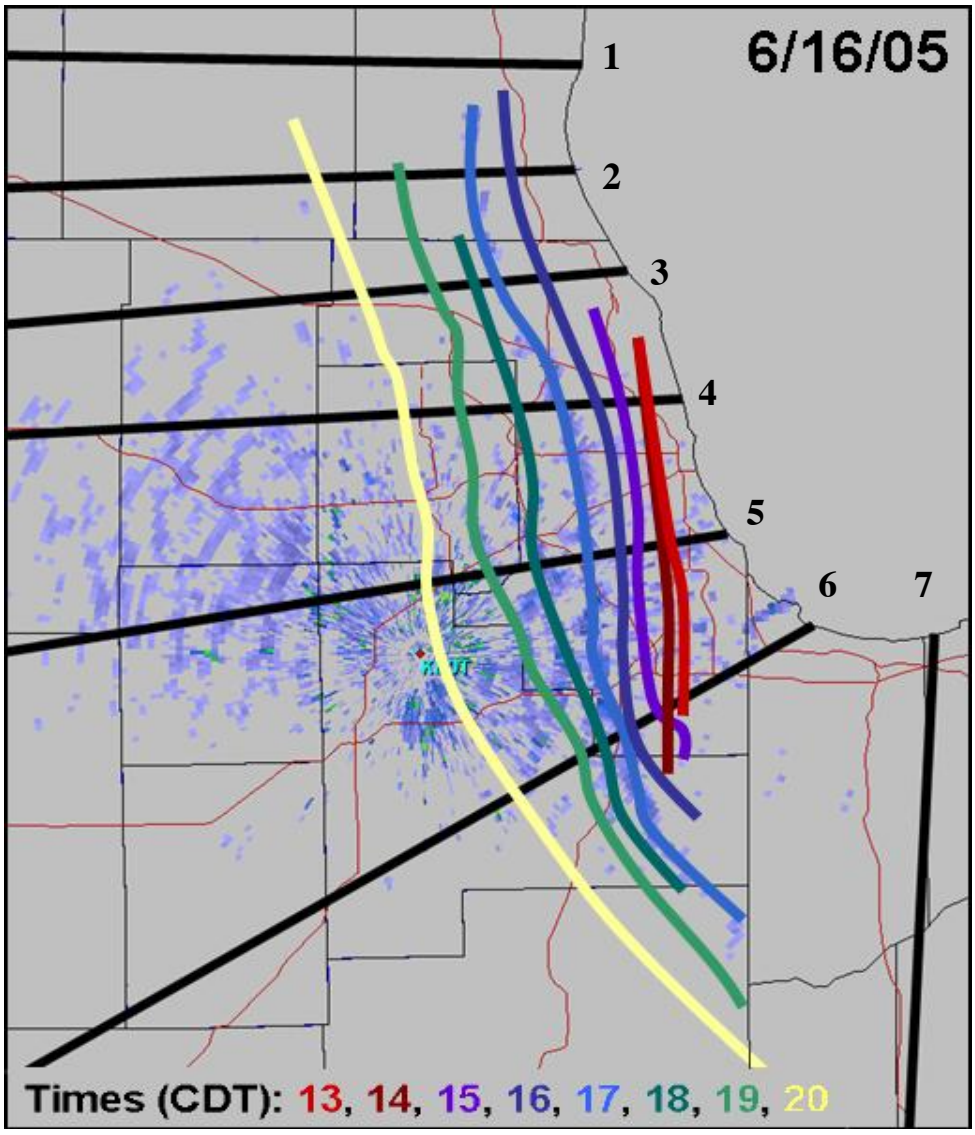

Figure 2.3. KLOT WSR-88D base reflectivity at approximately 1700 CDT on 16 June 2005. Hourly locations of the lake-breeze front for the full duration of the case are shown with colored lines. Cross sections through the Chicago, IL area are shown, numbered 1 – 7.

differential motion of the lake-breeze front, both spatially and temporally. However, for lake-breeze fronts which persisted for less than 3 hours, analysis of hour-to-hour accelerations of lake-breeze frontal movement was not completed. Cases eliminated from our analysis based on lack of data from, or analysis of, radar observations are shown in Table 2.1. Five cases were eliminated, which resulted in a total of 44 cases that were analyzed using this method.

Date	Reason for Elimination
June 13, 2005	Convective outflow interacted with lake-breeze
June 17, 2005	Short-lived (less than 3 hours)
July 3, 2005	Radar data missing
August 9, 2005	Short-lived (less than 3 hours)
August 17, 2005	Radar data missing for 6 hours of lake-breeze

Table 2.1. Summary of lake-breezes eliminated from the dataset based on lack of data from, or analysis of, the KLOT WSR-88D. (shown in gray in Figure 3.1).

Gaps in the fine line as seen in individual base reflectivity Plan Position Indicator (PPI) images were filled using base velocity or spectral width data. If small gaps in the fine line (approximately 10 km or less) were present in all radar products used in this research (radar reflectivity, velocity and spectral width), the location of the lake-breeze front was manually interpolated between segments of the fine line. Interpolation of the position of the lake-breeze front was not performed if data for a particular cross section was missing for at least one hour. This averaging would have indicated temporally uniform inland motion of the lake-breeze front regardless of any frontal acceleration which may have occurred during the data gap.

b. ***Validation***

It was necessary to determine if the cross section method could accurately depict differences in speed of inland motion of the lake-breeze front from cross section to cross

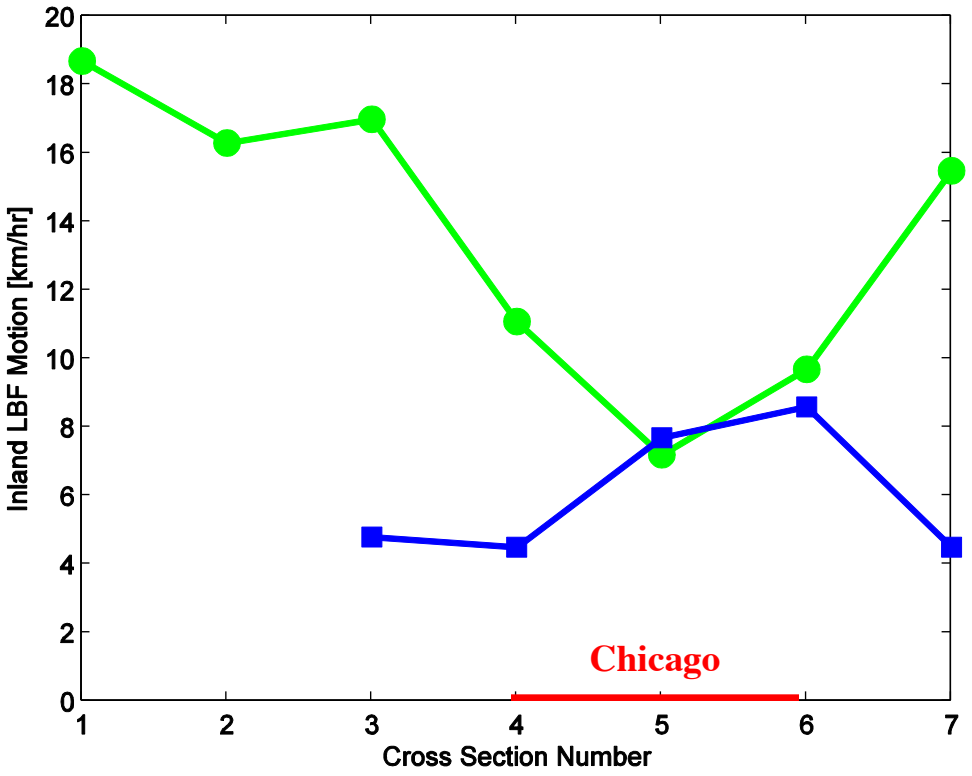

Figure 2.4. Speed of inland motion of the lake-breeze front along each of the cross sections (Fig. 2.3) for two case studies (6/21/05, 13-14 CDT, green; 8/28/05, 15-16 CDT, blue). The approximate location of downtown Chicago shown in red.

section. Plots of inland motion along each cross section for two cases (Figure 2.4) indicate that differential movement between cross sections can be detected. At 13-14 CDT on 21 June (green line in Figure 2.4) the lake-breeze front moved more slowly through Chicago compared to the suburbs. Conversely, at 15-16 CDT on 28 August 2005 (blue line in Figure 2.4) the lake-breeze front moved more quickly through Chicago compared to the suburbs. Data from the two cases shown suggests that Chicago does not always have the same affect on the lake-breeze. The hourly position of lake-breeze front

for all cases, shown in Appendix A, confirms that the inland motion of the lake-breeze front through the Chicago area varies widely from day to day.

It was also necessary to determine if the method above accurately depicted the overall motion of the lake-breeze front before proceeding with further analyses. Since it is well known that overall sea breeze frontal movement is related to large-scale pressure and wind fields, synoptic composite charts of mean sea-level pressure were generated for fastest and slowest moving 1/3 of cases (Figure 2.5). North American Regional Reanalysis (NARR) data (Mesinger et al., 2006) were analyzed using the NOAA Earth Systems Research Laboratory web interface (2008) to generate these charts. These charts suggest that results using the cross section method described in section 2.a. make physical sense, since these pressure fields support stronger opposing flow to the lake-breeze for cases during which the lake-breeze front moved inland more slowly.

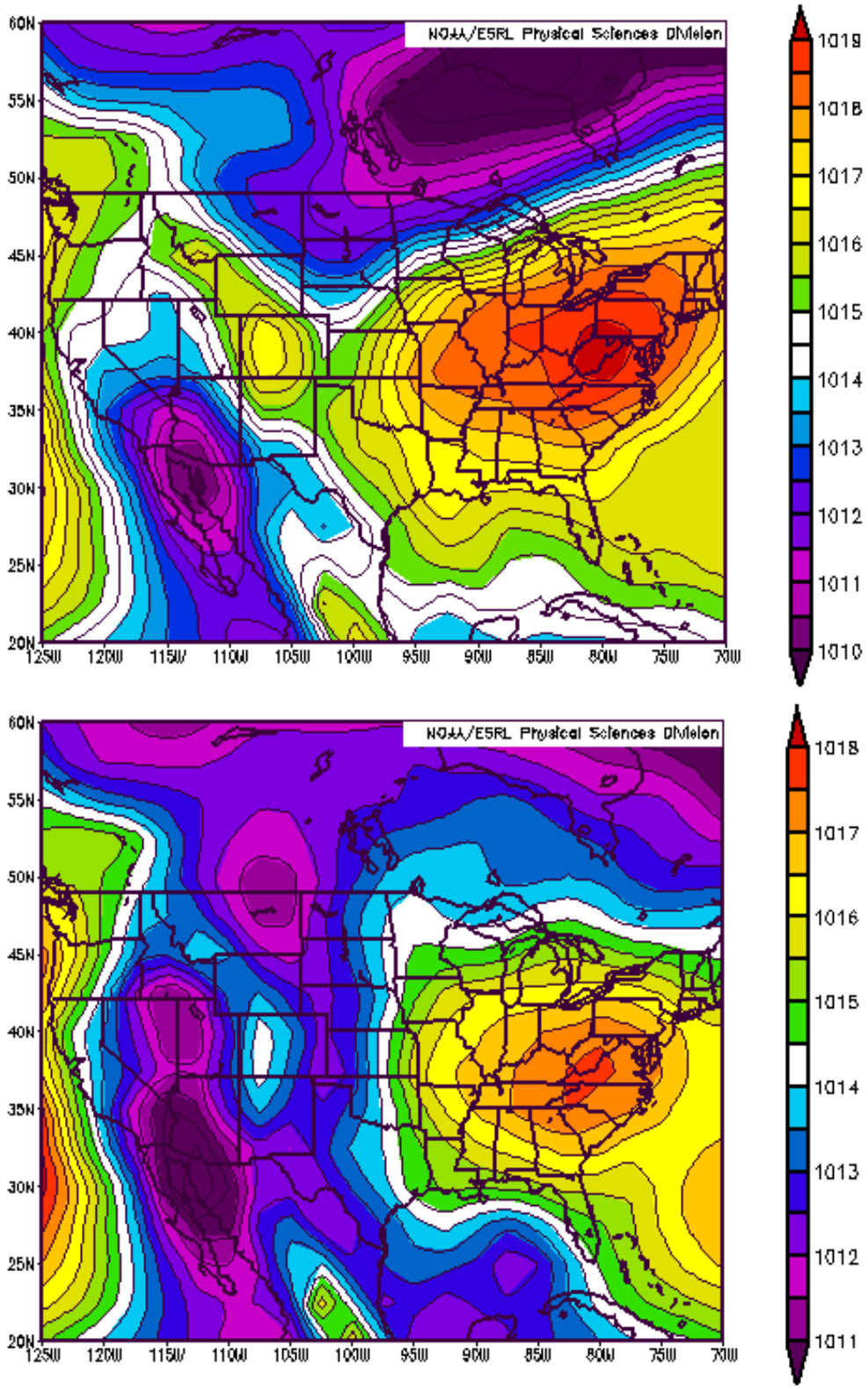

Figure 2.5. Composite mean sea-level pressure (hPa) for days with slow (14 cases, top) and fast (14 cases, bottom) lake-breeze front movement. Source: National Oceanic and Atmospheric Administration Earth Systems Research Laboratory.

3. Surface Data

Locations of hourly surface data from selected Automated Surface Observing Stations (MRCC, 2008) and buoy data from central Lake Michigan (National Data Buoy Center, NDBC; 2008) are shown in Figure 2.6. These data allowed for a comparison of surface conditions to the motion of the lake-breeze front. In particular, the effect of the Urban Heat Island (UHI) on lake-breeze circulations was of interest. Since there are no direct measurements taken of the urban heat island and lake-breeze circulations independent of each other, and the large scale wind, their strength was approximated by the temperature differences which drive them. NDBC buoy 45007 was chosen to represent the air temperature over Lake Michigan due to its mid-lake location. Buoys

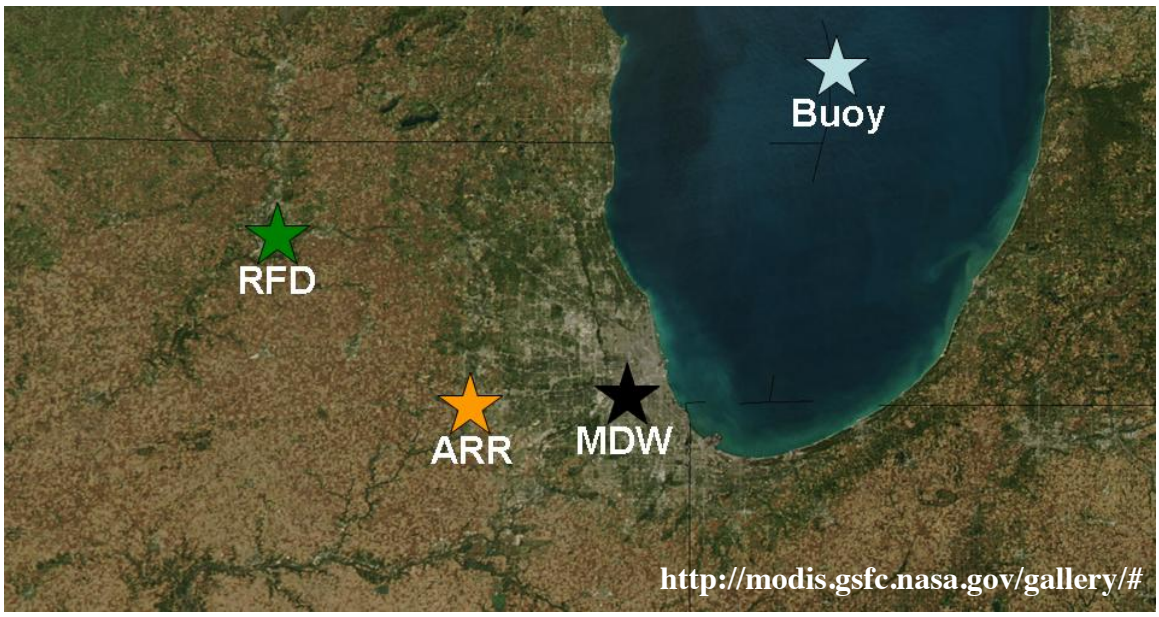

Figure 2.6. Aqua MODIS (Moderate Resolution Imaging Spectroradiometer) true-color image of southern Lake Michigan taken on October 5, 2002 (MODIS, 2010). Locations of surface data stations used to calculate $UHI_{forcing}$ and $LB_{forcing}$ are indicated by stars (ARR: Aurora, MDW: Midway, RFD: Rockford, Buoy: National Data Buoy Center Buoy # 45007).

closer to the shore are likely to be more representative of continental air and less representative of the maritime boundary layer than a mid-lake location. Rockford, IL, was chosen to represent the inland temperature since it is well-removed from both Lake Michigan and the Chicago urban center.

Midway was chosen to represent the air temperature within Chicago's heat island since it consistently had warmer temperatures than surrounding ASOS on nights preceding lake-breezes examined in this study. Midway was also chosen by Ackerman (1985) to represent the temperature within Chicago's UHI in her climatological study. While temperature data taken at Argonne National Laboratory were used by Ackerman (1985) to represent the rural temperature, Chicago's suburbs have expanded since the time of her study. Accordingly, data from Aurora, which is 15 km further west, was used to represent the air temperature outside of Chicago's UHI. The mean temperature perturbation in Aurora, relative to nearby surface data sites, for all identified lake-breeze dates in this study is shown in table 2.2. It should be noted that Aurora exhibits a cold bias compared to the nearby locations. Compared to less urban locations, namely DuPage and Rockford, IL, Aurora is only slightly cooler (less than a 0.5 °C perturbation). This cold bias is believed to be due to topography, since Aurora is located at a lower elevation than its surroundings (Eric Lenning, National Weather Service – Romeoville, IL, personal communication, 2010). This suggests that a large portion (nearly 75%) of the Midway Airport – Aurora temperature difference may be due to the UHI.

Midway Airport	O'Hare Airport	DuPage, IL	Gary, IN	Rockford, IL
-1.82	-1.09	-0.47	-0.75	-0.48

Table 2.2. Mean temperature perturbation at Aurora, IL [°C] relative to several observation sites in the Chicago area for dates with lake-breezes during the April – September 2005 period.

The equations used to represent the forcing of the UHI and lake-breeze circulations are as follows:

$$UHI_{forcing} = T_{airMDW} - T_{airARR}$$

$$LB_{forcing} = T_{airRFD} - T_{airBUOY}$$

where T_{airMDW}, T_{airARR}, T_{airRFD}, and $T_{airBUOY}$ are the surface air temperatures at Midway, Aurora, Rockford and NDBC Buoy 45007, respectively.

CHAPTER 3

GENERAL LAKE-BREEZE CHARACTERISTICS

1. Forcing and Distribution of Lake-Breezes

Forty-four days with lake-breezes during April – September 2005 were identified using methods described in Chapter 2. The number of lake-breezes by month, shown in Figure 3.1, gradually increased from 5 in April to 12 in August then decreased to 10 in September. The late summer peak in lake-breezes occurred despite stronger lake-breeze forcing earlier in the season (Figure 3.2). Stronger winds in the spring and early summer may have acted as a stronger opposing force to the formation of lake-breezes (Figure 3.2, see, for example, Arritt, 1993). Laird et al. (2001) also hypothesized that stronger winds earlier in the warm season led to a late season peak in lake-breeze frequency from Lake

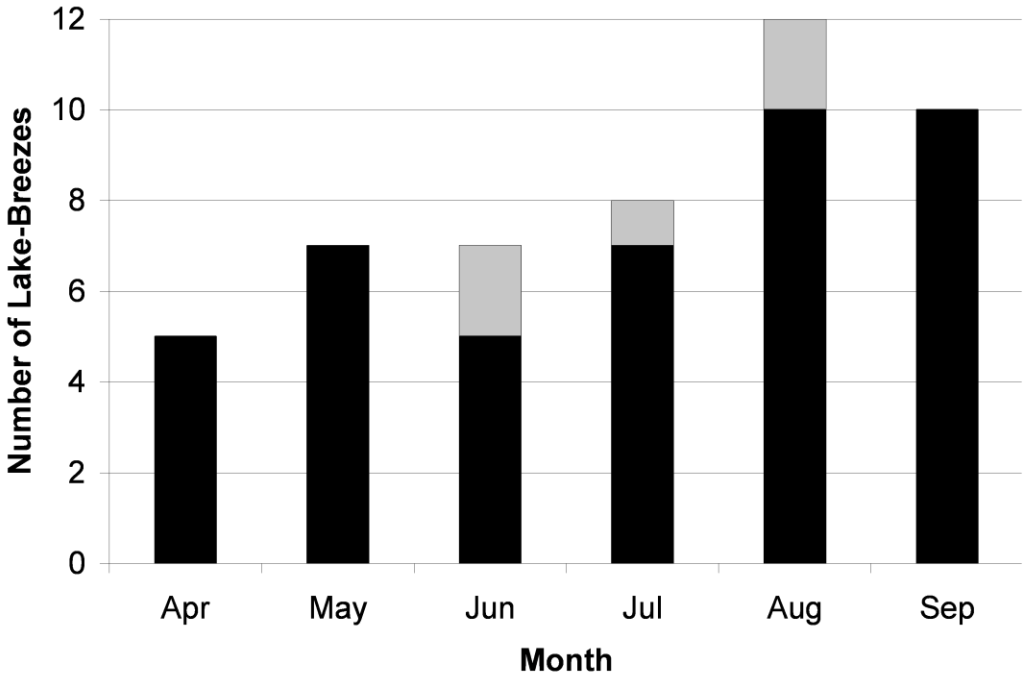

Figure 3.1. Distribution of lake-breeze days by month during the April – September, 2005 period. Lake-breeze days eliminated from the dataset (shown in table 2.1) are shown in grey.

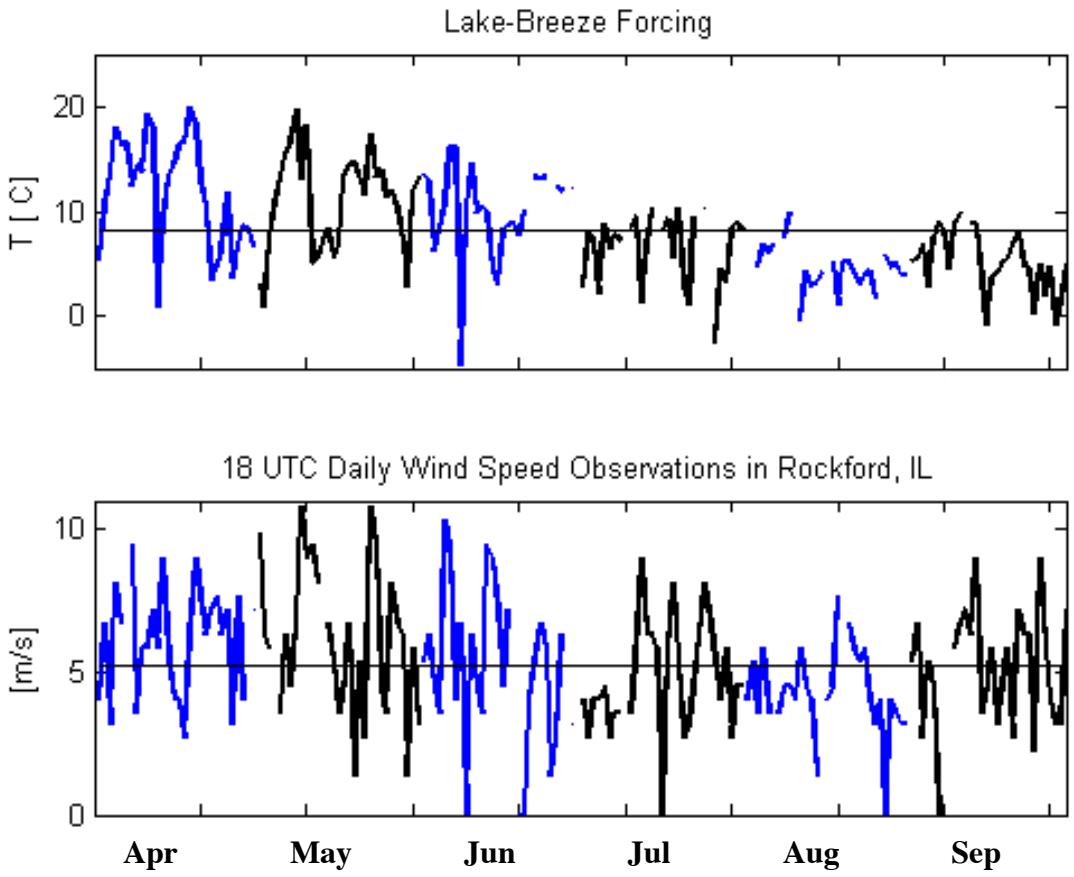

Figure 3.2. Daily lake-breeze forcing ($LB_{forcing} = T_{airRFD} - T_{airBUOY}$) at 18 UTC (top), and daily wind speed observations at 18 UTC in Rockford, IL (bottom) for 1 April – 30 September, 2005. The mean value of lake-breeze forcing and wind speed at 18 UTC are shown by the horizontal black lines. The data shown in the figure alternate between blue and black by month, so that the individual months are more clearly discerned.

Michigan. An alternative explanation may be an early-season lack of scatterers (such as insects) needed for radar observations of the lake breeze. The agreement with Laird et al., however, is evidence that it isn't due to the observation technique, since they used surface observations rather than radar.

Analysis of the daily u and v components of the wind in Rockford, IL (Figure 3.3) may help explain the monthly distribution of lake-breezes in 2005. The u component of the wind remained negative for a substantial portion of April. This would cause inland

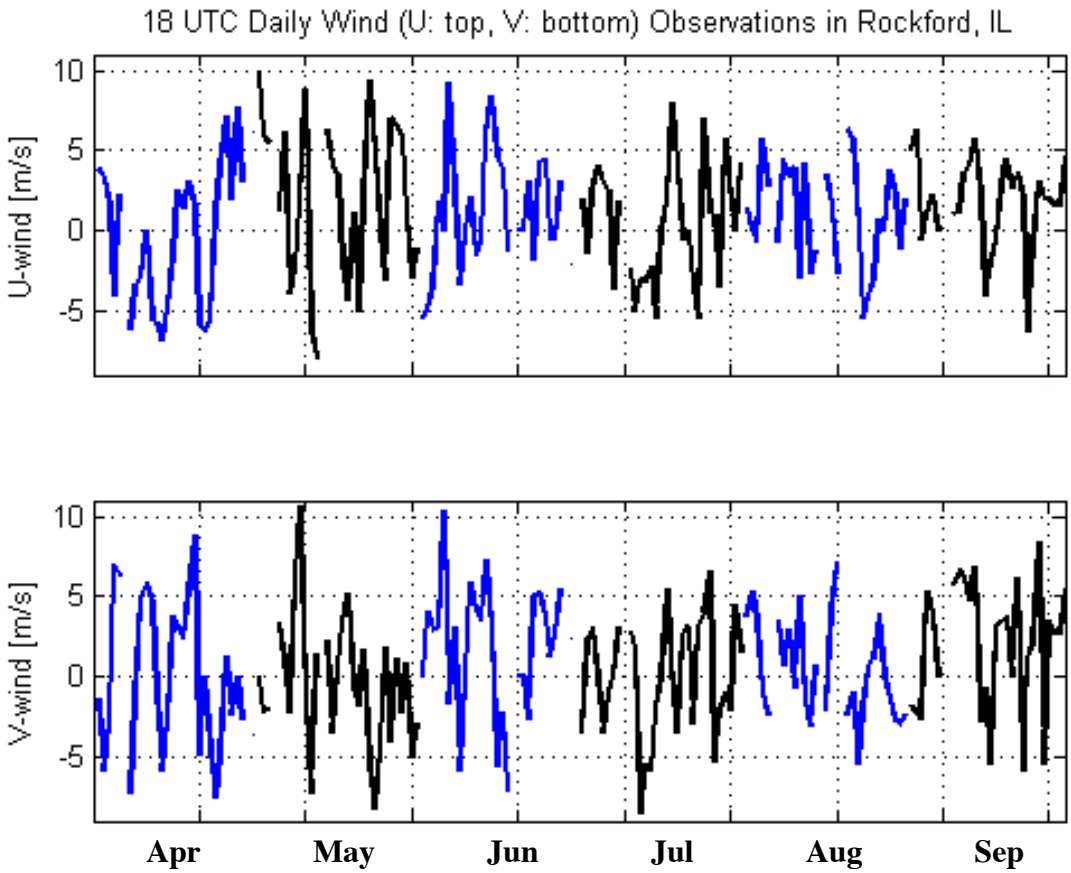

Figure 3.3. Daily U (top) and V (bottom) components of the wind at 18 UTC in Rockford, IL from 1 April – 30 September, 2005. The data shown in the figure alternate between blue and black by month, so that the individual months stand out more clearly.

advection of the marine airmass, as opposed to a clearly distinguishable lake-breeze circulation. This could explain the low number of lake-breezes in April, despite April having the strongest lake-breeze forcing. Four of the five lake-breezes in April occurred in the second half of the month, after the u component of the wind became positive. However, no lake-breezes occurred in April when the u component of the wind exceeded 3.1 m s^{-1}. There was no evident trend in the v-component of the wind during the April – September 2005 period.

In general, the mean wind speed decreased from late June through September, the time period in which 32 of the lake-breezes (approximately 73%) occurred. The half-

month mean 18 UTC wind speed in Rockford, IL was above 3.5 m s^{-1} through the first half of June (Figure 3.4); after that time, the mean wind speed remained near or below 3.0 m s^{-1}. This decrease in wind coincided with an increase in the frequency of observed lake-breezes.

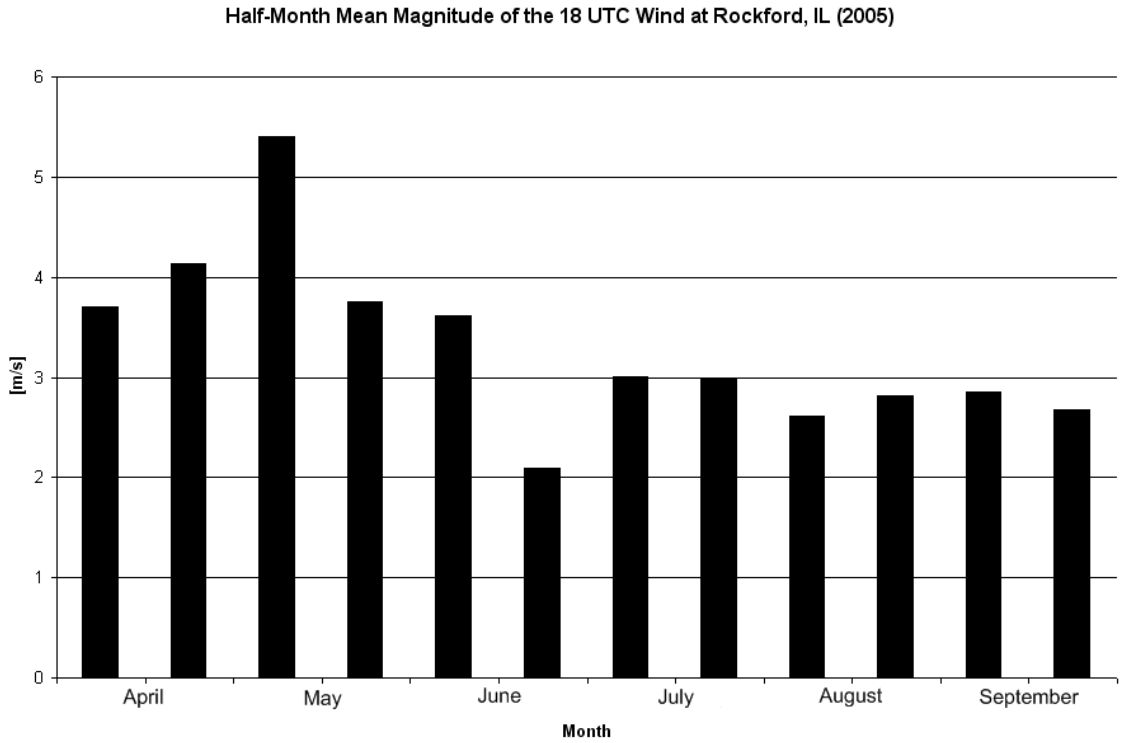

Figure 3.4. Mean magnitude of the 18 UTC wind speed in Rockford, IL for each half month during 2005. The first half of the month was defined as day 1 to 15, and the second half was defined as day 16 to the end of the month.

The lake-breeze index, ε (Biggs and Graves, 1962; Laird et al., 2001), has been used as a predictor of lake-breeze occurrence and is calculated as follows:

$$\varepsilon = U^2/C_p\Delta T$$

where U is the mean wind speed from 10 to 16 CDT [m s^{-1}], ΔT is maximum inland air - surface water temperature difference [°C] during the same time frame, and C_p is the specific heat of dry air at constant pressure. The lake-breeze index was calculated for all

dates in the April – September 2005 period, utilizing the observed surface conditions in Rockford, IL and the water temperature at the National Data Buoy Center buoy #45007 (location shown in Chapter 2).

Typically dates with a lake-breeze index of less than 3 are considered favorable for the occurrence of lake-breezes. Of the 49 dates with lake-breezes during the April – September 2005 period, 15 had lake-breeze indices above 3, eight of which had lake-breeze indices above 4. All of these 8 lake-breeze days behaved differently than the remainder of the cases: 3 were eliminated from the dataset (3 of the 5 lake-breezes shown in table 2.1), 3 made limited inland penetration, and 2 retrograded.

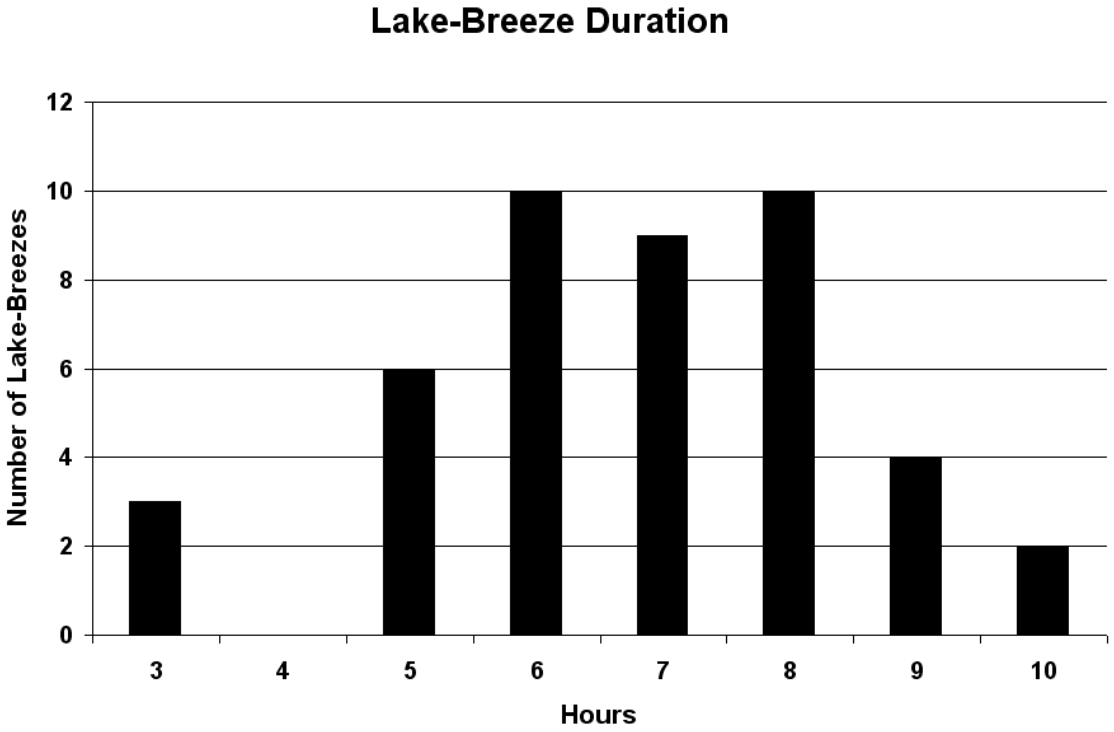

Figure 3.5. Duration of lake-breezes observed during 2005, defined as the number of hours the radar fine line was discernable. As explained in Chapter 2, lake-breezes with radar fine lines visible for less than 3 consecutive hourly observations (6/17 and 8/9) were not included in this investigation.

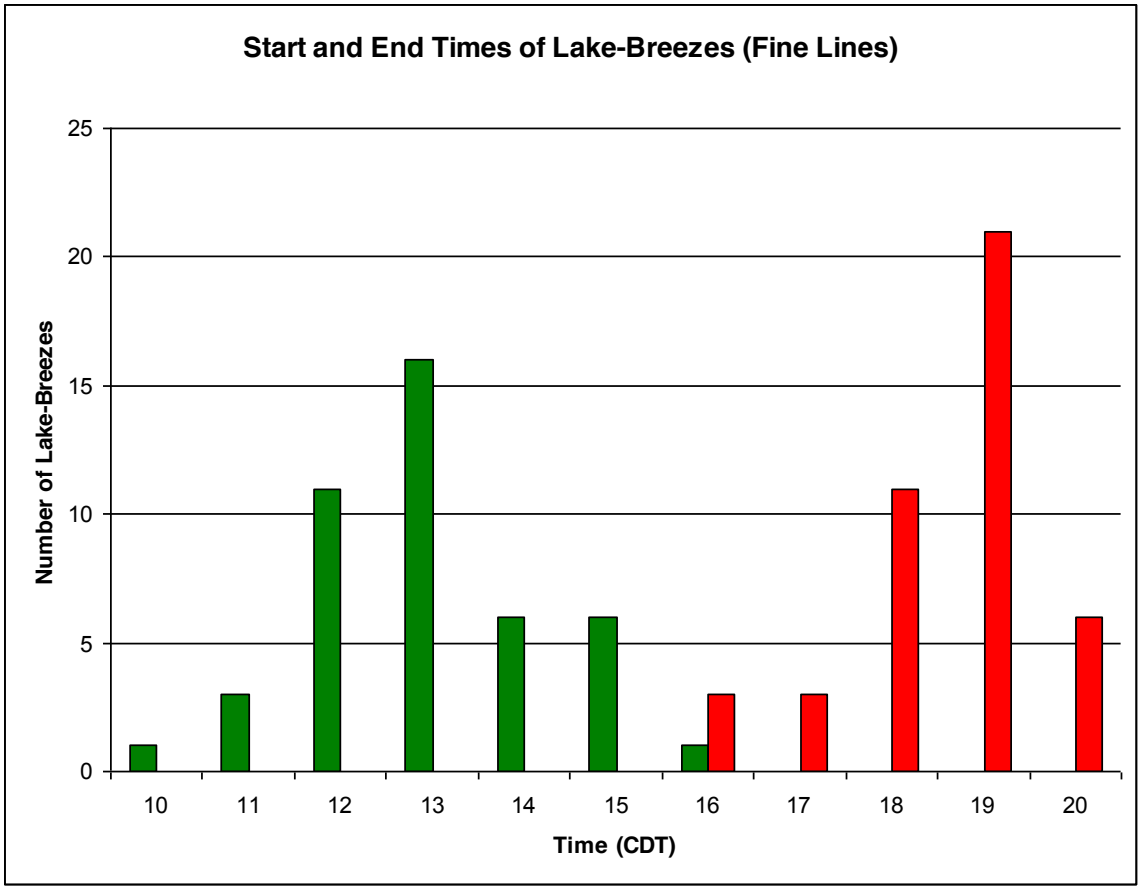

Figure 3.6. Distribution of lake-breeze start and end times shown by green and red bars, respectively. The start and end times were defined as the first and last hourly radar observations in which a fine line was present.

Lake-breeze duration, defined as the number of hours the fine line was discernable in radar data, ranged from 3 to 10 hours (Figure 3.5). Lake breezes which persisted for less than 3 hours were not included in this study, as was explained in Chapter 2. Day- to-day variation in the duration of the lake-breeze was large, and no discernable seasonal trend in duration was evident (not shown). Start and end times of lake-breezes (Figure 3.6) also varied significantly, with peak start and end times of 1300 and 1900 CDT, respectively.

One might expect that the u-component of the wind would affect the start time of the lake-breeze, as well as its duration. For stronger u-components of the wind, the lake-breeze circulation would have to overcome stronger opposing flow before moving inland, thus delaying its start time. Strong opposing flow would also cause the lake-breeze to end earlier that it would have otherwise, thus reducing its duration. To test these hypotheses, the lake-breeze start time and duration were correlated with the 12 UTC (7 CDT) u-component and overall magnitude of the wind in Rockford, IL (Table 3.1). While these correlations are of the expected sign, they are not statistically significant, suggesting that there might be a weak relationship, but that other factors likely play more important roles.

Variables	Correlation	Significance
Start time and 12 UTC u-component	0.16	0.69
Duration and 12 UTC u-component	-0.14	0.61
Start time and 12 UTC wind magnitude	0.05	0.23
Duration and 12 UTC wind magnitude	-0.17	0.72

Table 3.1. Pearson's linear correlation coefficient between the 12 UTC wind speed in Rockford, IL (u-component and overall magnitude), and lake-breeze characteristics (start time and duration). Significance is defined as 1-P[correlation due to random chance].

2. Inland Movement of the Lake-Breeze Front

a. *Speed of Inland Motion*

The speed of inland movement of the lake-breeze front was calculated based on the hourly location of the radar fine line along seven cross-sections (Chapter 2). The overall average speed at which the lake-breeze front moved inland was 5.0 km hr^{-1} during 2005. This is slower than was found for the Boston, MA area (Barbato, 1978): 11.7 km hr^{-1} from the coast to the center of Boston, then slowed to 4.7 km hr^{-1} west of Boston

based on analysis of 40 cases. It is unknown why the lake-breeze moved inland more slowly in Chicago in 2005 than the sea-breeze in Boston in Barbato's study.

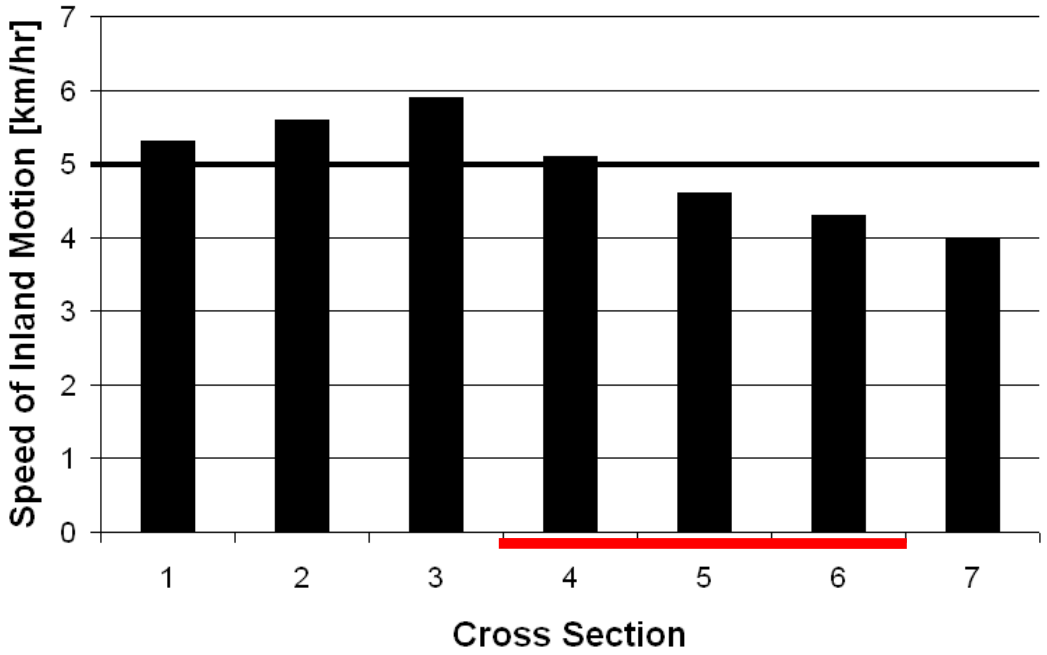

Figure 3.7. Average speed of inland motion of the lake-breeze front along each of the cross sections. See figure 2.3 for the location of cross sections 1 – 7. The overall average speed that the lake-breeze front moved inland, 5.0 km hr^{-1} is highlighted by the bold line. The approximate location of Chicago is noted by the horizontal red line.

In general, the lake-breeze front moved inland more quickly north of Chicago (cross sections 1-3, Figure 3.7) than near or south of the city. Along cross section 3, just north of Evanston, IL, the lake-breeze front moved inland at an average speed of 5.9 km hr^{-1}. On the south end of Lake Michigan, along cross section 7, the lake-breeze front moved inland at an average speed of 4.0 km hr^{-1}.

We have chosen to use Rockford, IL (more than 100 km from Lake Michigan) to represent the large scale flow since the lake-breeze front rarely made it that far inland in 2005 (less than 5% of identified lake-breezes). At Rockford, the average 18 UTC wind velocity on lake-breeze days examined in this study was 236° at 0.8 m s^{-1}. One would

expect the lake-breeze front's inland motion to be the same or slightly slower to the north of Chicago than to the south of Chicago due to shoreline shape since the u (east-west) component of the wind is stronger than the v (north-south) component of the wind (0.7 and 0.5 m s^{-1}, respectively). This unexpected difference in lake-breeze frontal movement, and the influence of Chicago on the movement of the lake-breeze front, and will be investigated in detail in Chapter 4.

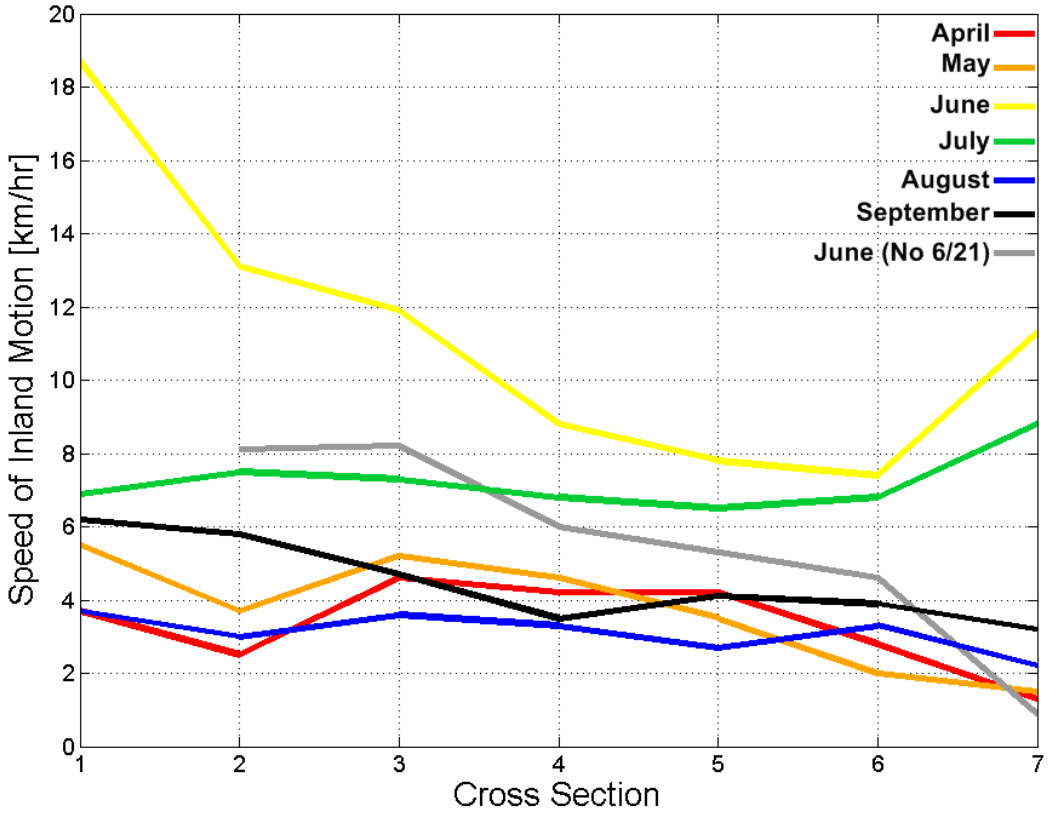

Figure 3.8. Average speed of inland motion of the lake-breeze front by month along each individual cross section (shown in Figure 2.3).

The lake-breeze front moved inland more quickly in June and July than any other month, as shown in Figure 3.8. The high average inland motion of the lake-breeze front during June was affected by a lack of substantial lake-breeze front retrogression (see

section 4.b.) and the rapid inland movement of the lake-breeze front on 6/21/05. The 6/21/05 case, which interacted with a cold front resulting in rapid inland motion of the lake-breeze front, is discussed in more detail in section 4.a. However, even after removing 6/21/05 from the June average (gray line in Figure 3.8), the inland motion of the lake-breeze front was quicker than most other months. The weakest half-month average wind speed in Rockford, IL (2.09 m s^{-1}) was observed in the second half of June (Figure 3.4). Weak wind, combined with lake-breeze forcing which had not dropped substantially between April and June likely contributed to the quicker inland motion of the lake-breeze front during June. The mean wind speed in Rockford, IL increased slightly in July, and then decreased during August and September, when lake-breeze forcing was weaker and the frequency of lake-breezes was at its peak (Figure 3.4).

b. ***Inland Penetration of the Lake-Breeze Front***

Figure 3.9 shows the maximum inland penetration of the lake-breeze front for every case, based on positions along each of the cross sections. In general, the lake-breeze front penetrated further inland on the north side of Chicago than the south side. Approximately 60% of the lake-breeze fronts observed in 2005 remained within 15 km of the shore in the vicinity of downtown Chicago (Figure 3.9: 41.75 N, -87.75 W). Further inland, nearly 30% of lake-breeze fronts penetrated beyond the WSR-88D located at the National Weather Service office in Romeoville, IL (approximately 50 km inland).

The mean sea level pressure for dates with lake-breezes that penetrated further than 50 km inland, the distance from Lake Michigan to the Romeoville, IL WSR-88D, was calculated using North American Regional Analysis (NARR) data (Figure 3.10). This was done in order to investigate the possibility that a particular pressure field

promoted further inland penetration of the lake-breeze front. The mean sea level pressure field over North America includes distinct features such as an area of high pressure over the Ohio River Valley/Central Appalachian Mountains, a ridge extending from the upper Midwest into central Canada, and a trough extending southwestward from eastern Canada into the Great Lakes region. Troughs were evident in this average location in NARR data on 9 of the 13 dates included in the composite (Figure 3.10), and 11 of the 13 dates had a westward synoptic scale pressure gradient that would support an easterly component of the wind, thus accelerating the lake-breeze front inland.

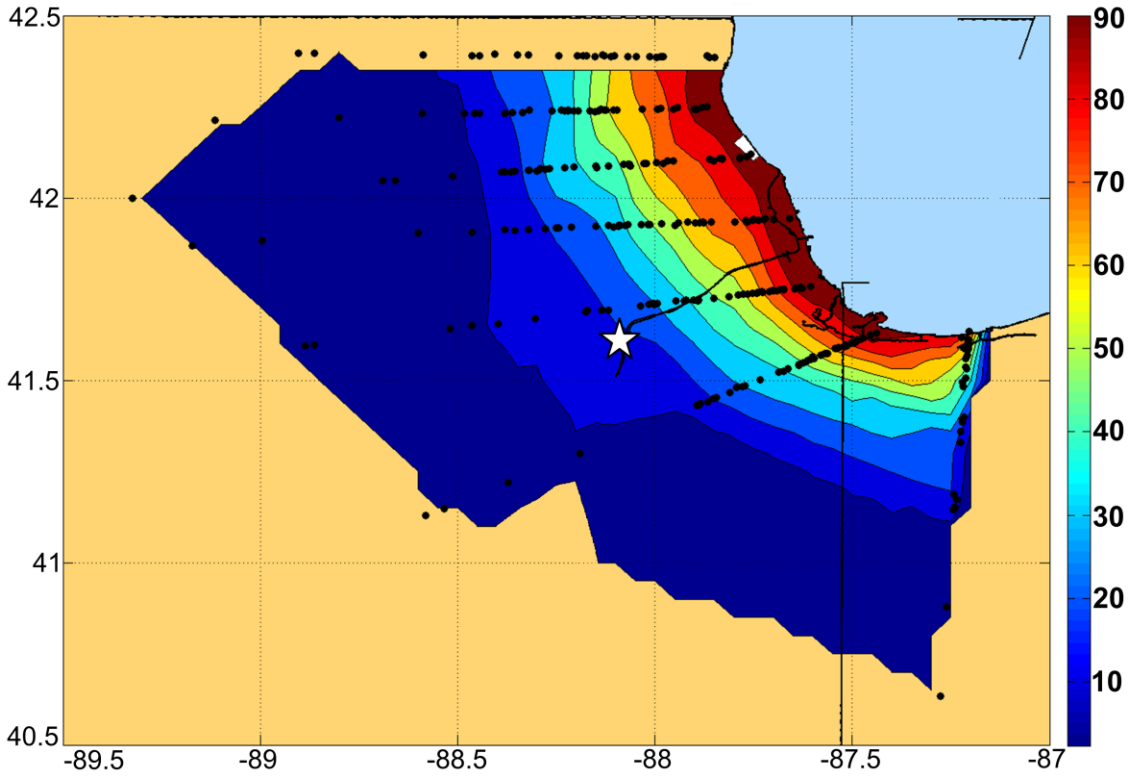

Figure 3.9. Maximum inland penetration of lake-breeze fronts along the cross sections discussed in Chapter 2 during 2005 (black dots). Color shading represents the percent of lake-breeze fronts which terminated inland of specific geographic locations. The white star indicates the location of the WSR-88D radar, whose data were used in this study.

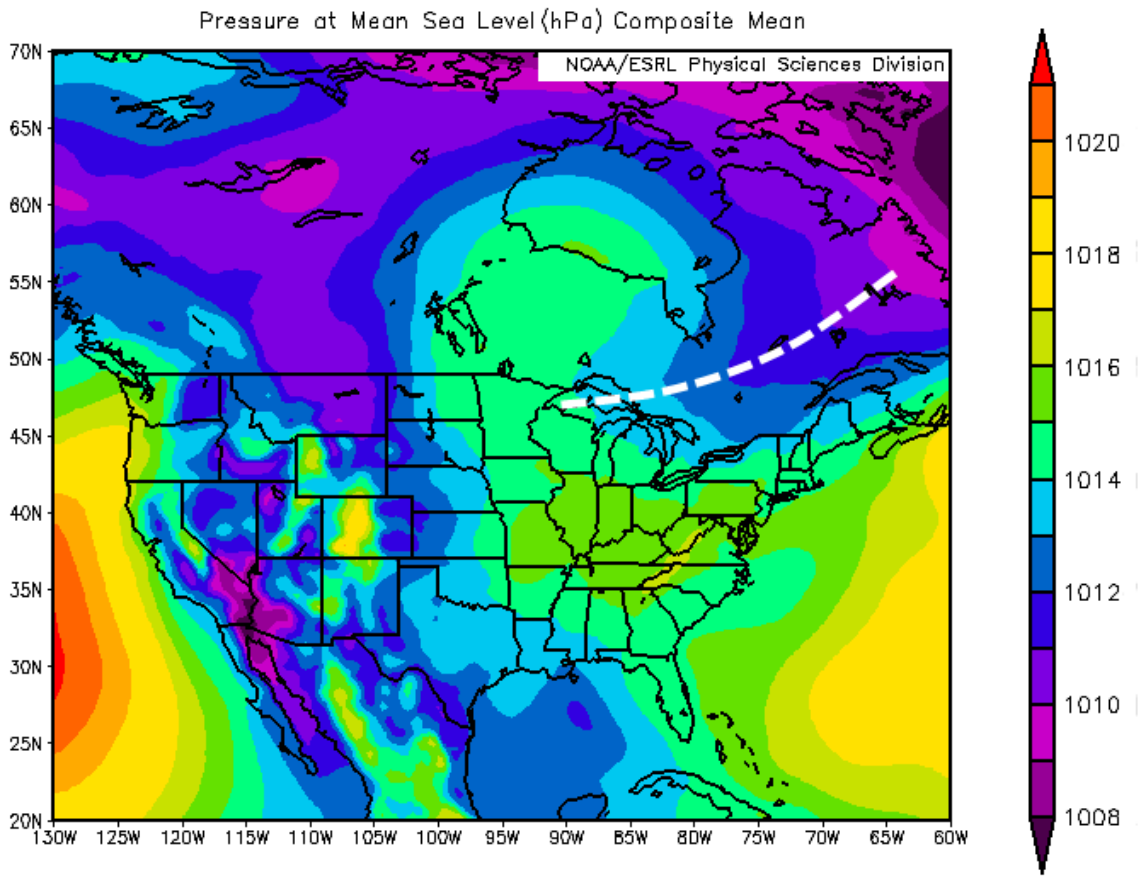

Figure 3.10. Mean sea level pressure for dates when the lake-breeze penetrated further inland than the Romeoville, IL WSR-88D (approximately 50 km from Lake Michigan). A trough axis through the upper Great Lakes is indicated by the dashed white line. The dates used in the composite are as follows: 4/10, 5/3, 5/23, 6/16, 6/21, 6/28, 7/5, 7/9, 7/29, 8/10, 8/28, 8/29, and 9/3/2005. Source: NOAA/ESRL, www.esrl.noaa.gov/psd/cgi-bin/data/narr/plotday.pl.

The mean sea level pressure for dates on which the lake-breeze front didn't penetrate beyond the I-294 corridor near downtown Chicago (approximately 25 km inland) was also calculated using NARR data (Figure 3.11). This analysis suggests that surface high pressure centered to the southwest of Chicago is associated with less inland motion of the lake-breeze front. This makes physical sense, as stronger opposing flow to the lake-breeze is favored by this pressure field.

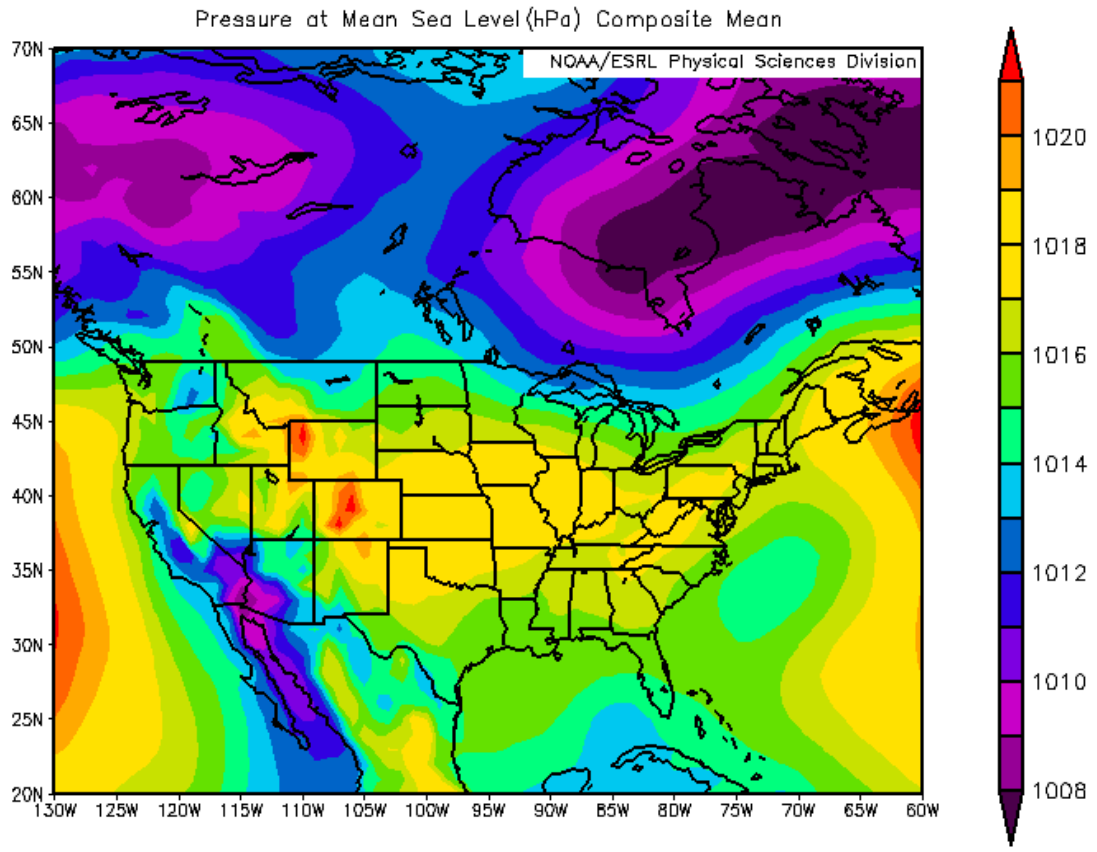

Figure 3.11. Mean sea level pressure for dates when the lake-breeze did not penetrate beyond the I-294 corridor (approximately 25 km from Lake Michigan in downtown Chicago). The dates used in the composite are as follows: 4/16, 5/26, 7/28, 8/1, 8/21, 8/27, and 9/29/2005. Source: NOAA/ESRL, www.esrl.noaa.gov/psd/cgi-bin/data/narr/plotday.pl.

3. Case Studies

As previously discussed, day-to-day variability in lake-breeze frontal movement was quite large. These variations, highlighted in Appendix A, motivated further investigation of particular cases. These cases, namely interaction with cold fronts and frontal retrogression, will be discussed in this section.

a. *Lake-Breeze Interaction with Cold Fronts*

Cold frontal passage occurred in the early afternoon on June 21, 2005, as indicated by a wind shift in the base velocity from WNW to NNW inland of the lake-

breeze front (Figure 3.12). A similar persistence of the lake-breeze despite the passage of a cold front was observed on August 28, 2005. On both of these dates the lake-breeze front made substantial progress inland (132 and more than 50 km, respectively). Other cold fronts or troughs interacted with, or were located within approximately 500 km inland of lake-breezes on 4/16, 5/3, 5/5, 5/23, 5/26, 6/20, 6/28, 7/1, 7/5, 7/19, 7/28, 7/29, 8/8, 8/10, 8/19, 8/21, 8/26, 8/27, 9/1, 9/2, 9/6, 9/20, and 9/29/2005 (Laird and Maliawco, 2010, personal communication) based on their analysis of surface data.

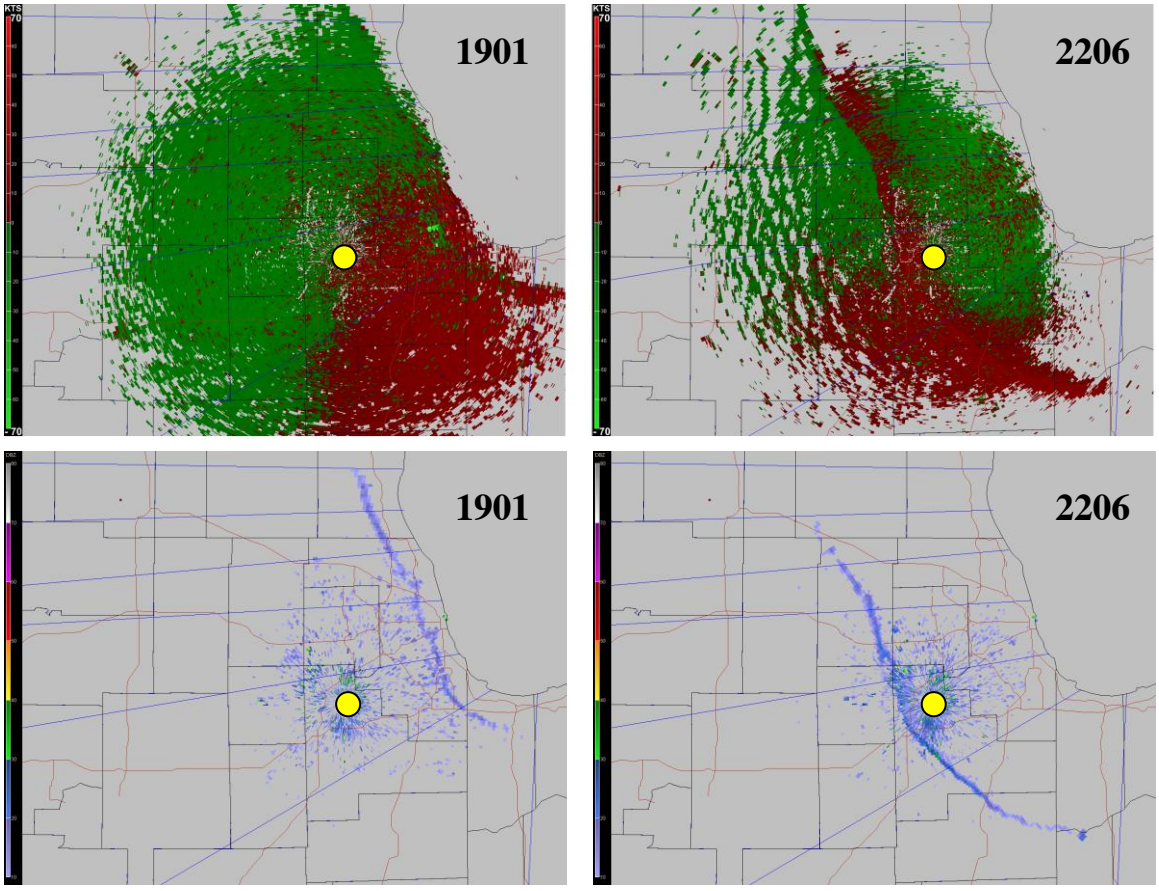

Figure 3.12. Base velocity (top) and base reflectivity (bottom) from June 21, 2005 at 1401 (left) and 1706 (right) CDT. A cold front passed through Chicago between those two times. The location of the Romeoville, IL WSR-88D radar is shown by the yellow circle.

Recall that in section 2.b., there were 13 cases where the lake-breeze front propagated more than 50 km inland, past the KLOT WSR-88D radar. In that section, it was hypothesized that upwind fronts or troughs had an effect on the lake-breeze front's inland movement. While the inland motion of the lake-breeze front was only slightly faster overall on cold front/trough days listed above (within the 25th to 75th percentiles of hourly lake-breeze frontal movement), 8 of the 13 lake-breezes which penetrated beyond the Romeoville, IL WSR-88D (noted in Figure 3.10 caption) were cold front/trough days. The reverse is not necessarily true, however, as there were many dates with smaller inland penetration of the lake-breeze front, despite inland cold fronts or troughs.

b. ***Retrograding Lake-Breeze Fronts***

Retrograding lake-breeze fronts were observed on several dates during 2005 (5/8, 5/26, 7/28, 8/1, 8/7, 9/1, and 9/2/05). The lake-breeze with the largest extent of retrogression occurred on 7/28/05 (Figure 3.13). The substantial amount of lake-breeze front retrogression which occurred that afternoon was likely due to a pairing of weak lake-breeze forcing (defined in Chapter 2) and an increasing u-component of the wind. The u-components of the wind at 09 and 13 CDT (14 and 18 UTC) were 1.7 and 5.8 m s^{-1}, respectively. The increase in the opposing flow to the lake-breeze between 09 and 13 CDT (14 and 18 UTC) appears to have caused the movement of the lake-breeze front to decelerate, and eventually reverse direction. Between 14 and 15 CDT (18 and 19 UTC), the wind shifted from westerly to southwesterly (Figure 3.14), which directly opposed the inland motion of the lake-breeze front. Of the 44 dates with lake-breezes analyzed, this case falls in the 8th percentile of lake-breeze forcing (3.2 °C) and 93rd percentile of the 13 CDT (18 UTC) u-component of the wind (5.8 m s^{-1}). This lake-

breeze was also the only lake-breeze with a fine line visible over Lake Michigan at any time, and was also the only lake-breeze with most clear retrogression (greater than a few km and over multiple hours). Therefore, little can be concluded regarding how this case applies to other retrograding lake-breezes at this time.

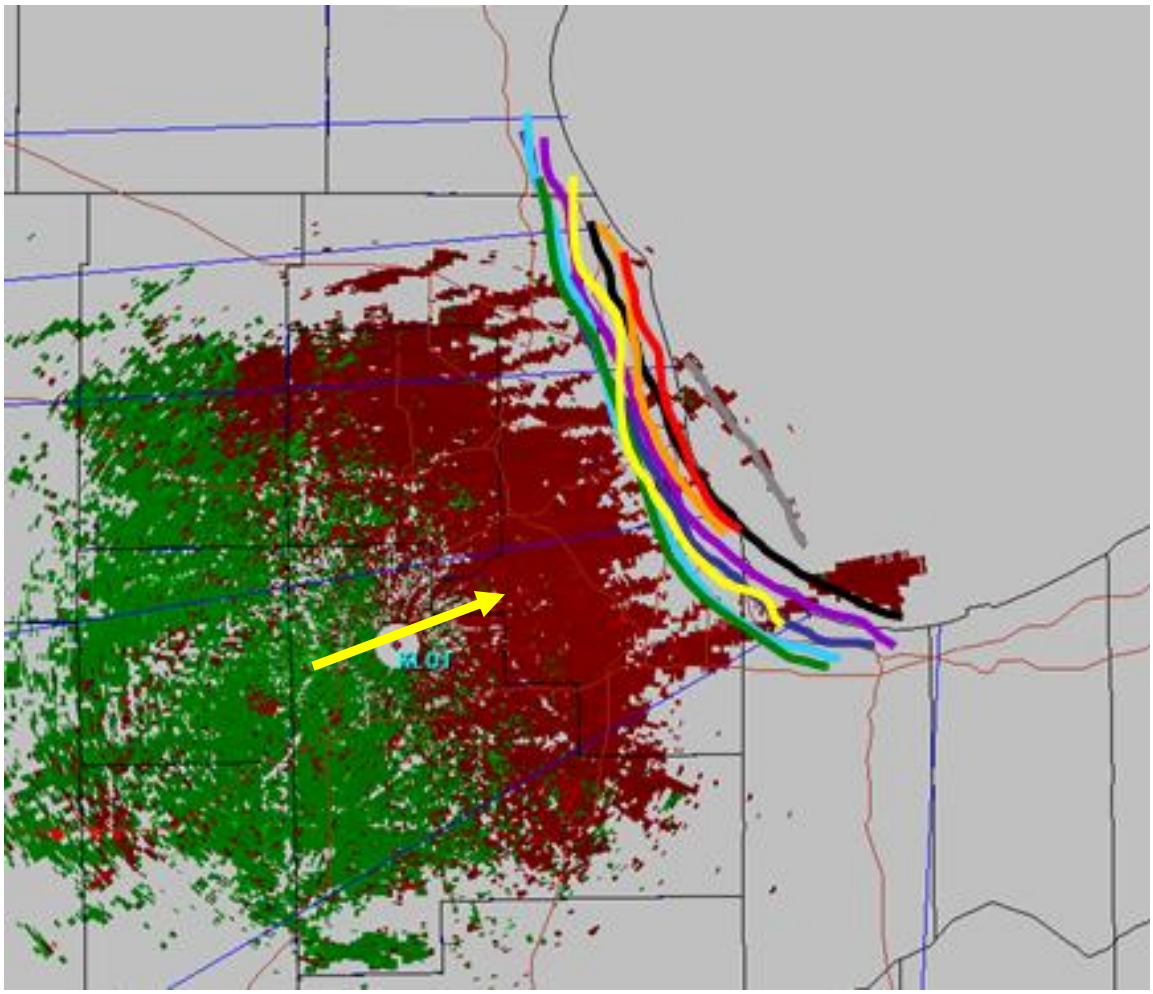

Figure 3.13. Hourly locations of the lake-breeze front on 7/28/05 overlaid on a base velocity radar image from 2003 CDT on that day. Note that after 1400 – 1500 CDT the lake-breeze front began to move lakeward. The mean wind direction (based on BVEL) is shown by the yellow arrow.

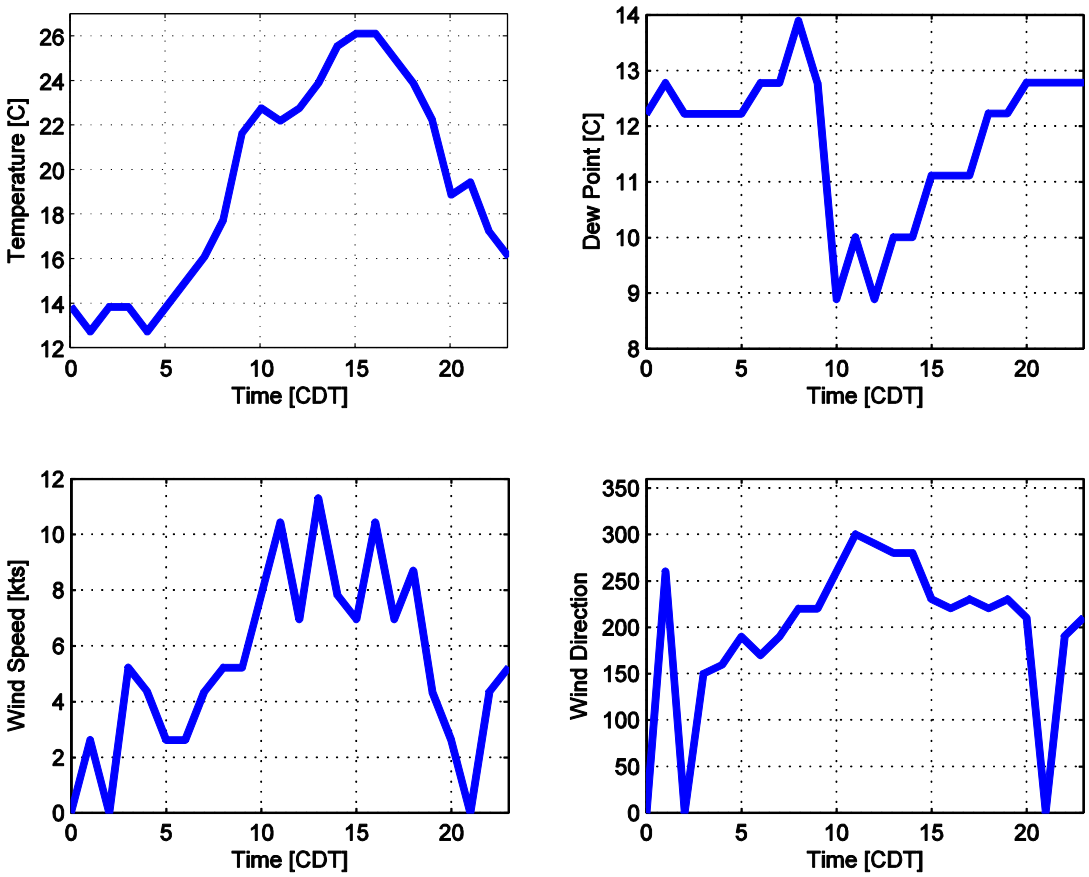

Figure 3.14. Time series of temperature, dew point, wind speed and wind direction observed in Rockford, IL on 7/28/05. Note the wind shift between 14 and 15 CDT (18 and 19 UTC) from westerly to southwesterly.

CHAPTER 4

LAKE-BREEZE FRONTAL MOVEMENT THROUGH CHICAGO: EFFECTS OF THE URBAN HEAT ISLAND

1. Chicago's Urban Heat Island

a. *Variation in Urban Heat Island Magnitude*

In order to test our hypothesis that Chicago's UHI circulation decreases the speed of inland motion of the lake-breeze front through Chicago and its inland suburbs, the hourly magnitude of Chicago's Urban Heat Island (UHI) was approximated by the air temperature difference between Midway Airport (MDW) and Aurora, IL (ARR). A similar approximation, used by Ackerman (1985), is discussed in Chapter 2.

The diurnal variability of the UHI magnitude (Figure 4.1) consists of a peak in the pre-dawn hours and a minimum in the afternoon. The UHI magnitude rapidly decreases between about 06 and 10 CDT, and rapidly increases between 19 and 02 CDT. On days when a lake-breeze was observed, the peak magnitude of the UHI was approximately 1.5°C higher than on days without a lake-breeze. The stronger UHI magnitude observed on days with lake-breezes is not surprising, since the synoptic scale conditions favorable for UHI development (clear skies and light winds) are also favorable for lake-breeze development. The average UHI magnitude remains positive until 14 CDT, when 18% (8 out of 44) of lake-breeze fronts have passed through Midway Airport. Once the lake-breeze front passes through Midway Airport, the air generally becomes cooler than it is further inland in Aurora. This relative cooling of the air at Midway Airport shows up as a

drop in the average UHI magnitude after around 15 CDT on days with a lake-breeze, when 34% (15 out of 44) of lake-breeze fronts have passed through Midway Airport.

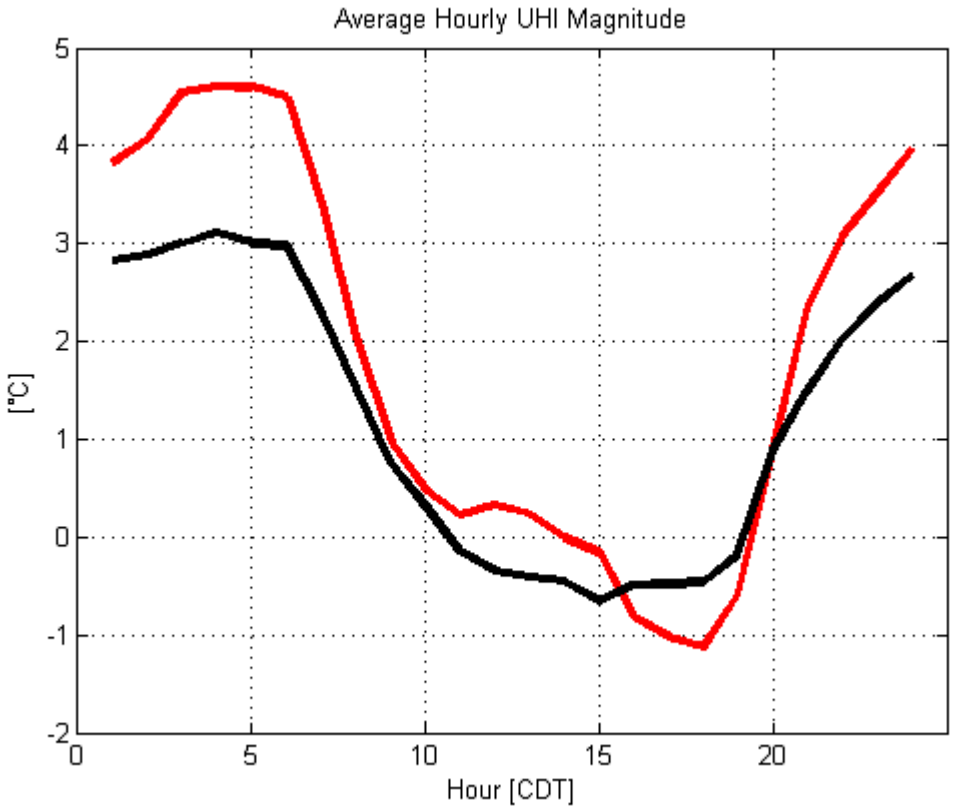

Figure 4.1. Diurnal variability of the UHI magnitude on days with and without lake-breezes (red and black lines, respectively) during the April – September, 2005 period.

Negative UHI magnitudes, observed in the afternoon of non-lake-breeze days (Figure 4.1), would theoretically lead to a reverse UHI circulation, with a divergent surface flow field over Chicago. This reverse circulation was not observed in surface data, which is not surprising considering the weak magnitude of the UHI circulation. Negative heat islands have been observed during the warm season in mid latitude cities, possibly due to albedo differences (Baltimore, MD: Mitchell, 1961; Edmonton, Alberta:

Hage, 1972; Seoul, South Korea: Kim and Baik, 2005). This could also be explained by large-scale flows off the lake or lake-breezes that couldn't be seen with radar.

b. ***Evidence of an Urban Heat Island Circulation***

Urban Heat Island circulations are extremely difficult to observe with standard surface observations due to their weak magnitude and location in areas with strong microscale circulations (induced by obstructions, buildings, etc.). In order to attempt to observe the UHI circulation directly, the surface wind observations in Aurora, IL were analyzed. This site was chosen due to its proximity to Chicago, since the UHI circulation typically exists over an area 2 – 3 times the size of its parent city (Hidalgo et al., 2008). Convergence of the near surface flow field on the urban center is a key characteristic of the UHI circulation. In Aurora, IL, to the west of Chicago, one would expect that a UHI circulation would contribute to a positive u component of the wind. Figure 4.2 shows correlation values and their statistical significance between the hourly UHI magnitude (UHIt) and u-component of the winds at Aurora. From midnight until 04 CDT the UHI magnitude and u component of the wind had a correlation near 0.2 with a significance ranging from approximately 0.7 to 0.9. Lower correlation coefficients and significance were present near and shortly after dawn. The late morning through early afternoon hours were characterized by an increase in correlation coefficient and significance, as shown by examples of scatter plots in Figures 4.3 and 4.4. Correlation coefficients and significance near 0.1 – 0.3 and 0.6 – 0.9, respectively, were observed during that time frame which suggests that the UHI could have a weak influence on the wind in Aurora, IL.

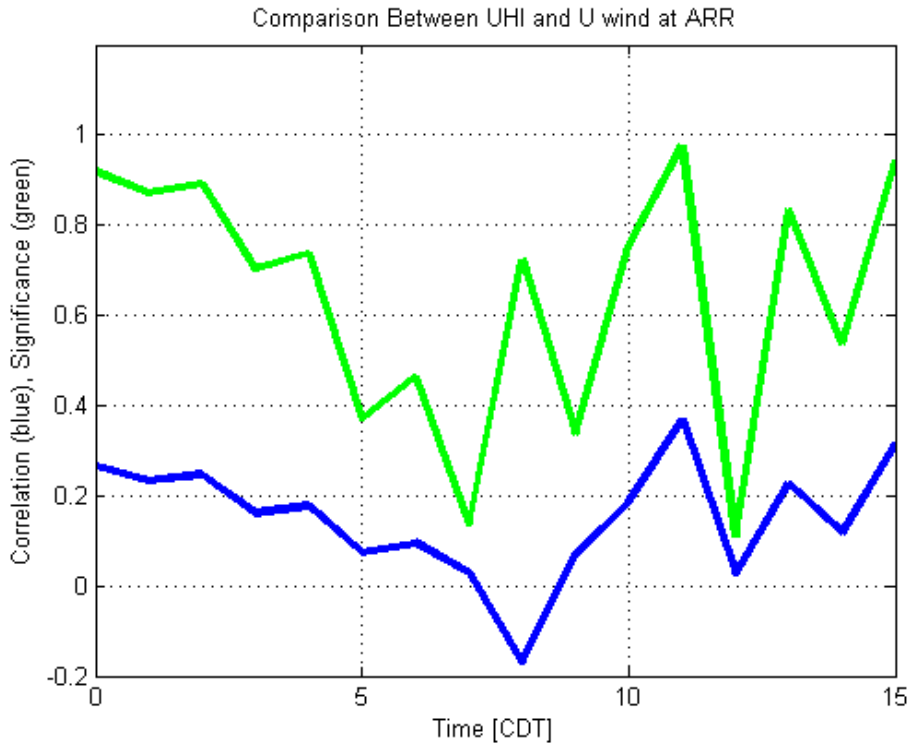

Figure 4.2. Comparison between the UHI magnitude and the u component of the wind in Aurora for days with lake-breezes. Pearson's linear correlation coefficient is shown by the blue line and the significance (1 – P[correlation by random chance]) is shown by the green line.

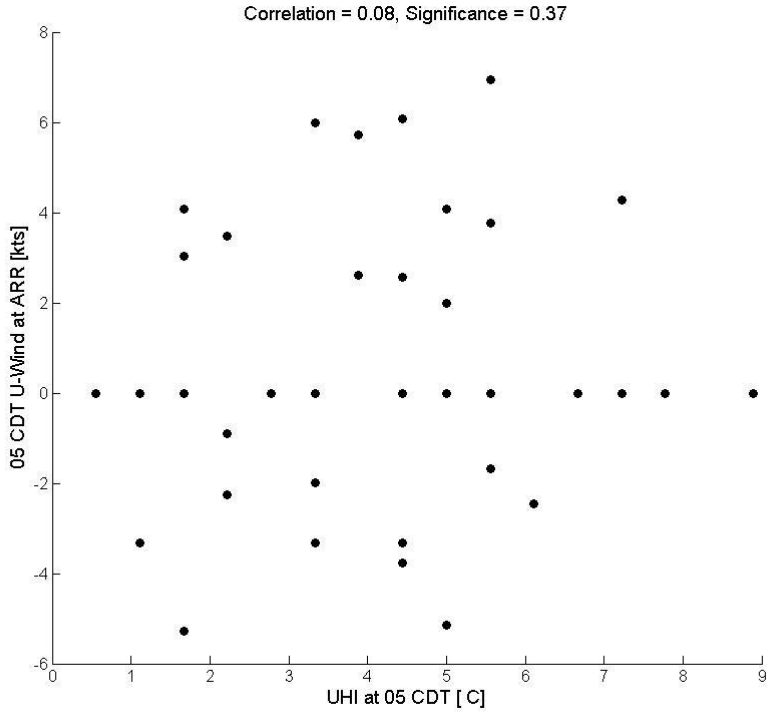

Figure 4.3. Scatter plot of the UHI magnitude and u-component of the wind in Aurora at 05 CDT for all lake-breeze dates. See Figure 4.2 for a summary of 00 – 15 CDT.

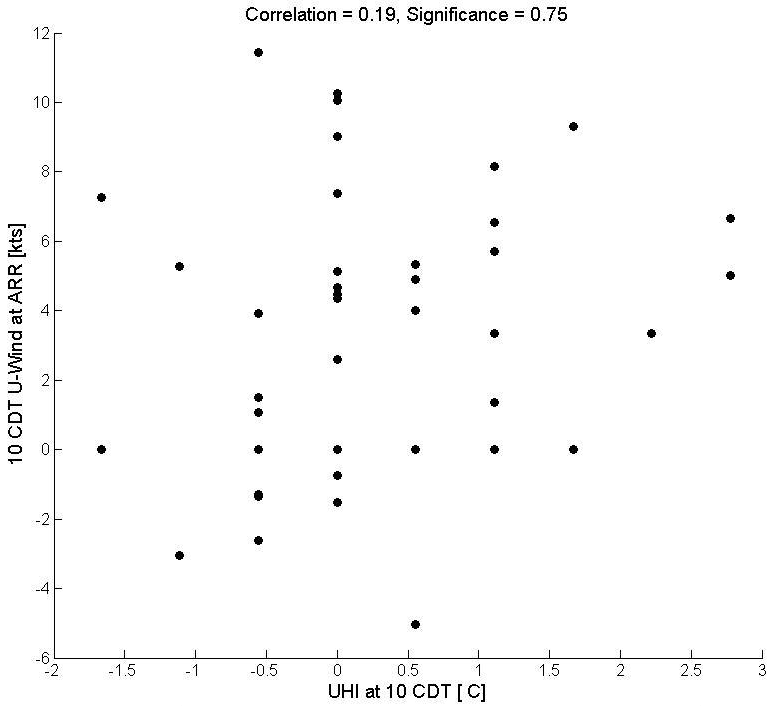

Figure 4.4. Scatter plot of the UHI magnitude and u-component of the wind in Aurora at 10 CDT for all lake-breeze dates. See Figure 4.2 for a summary of 00 – 15 CDT.

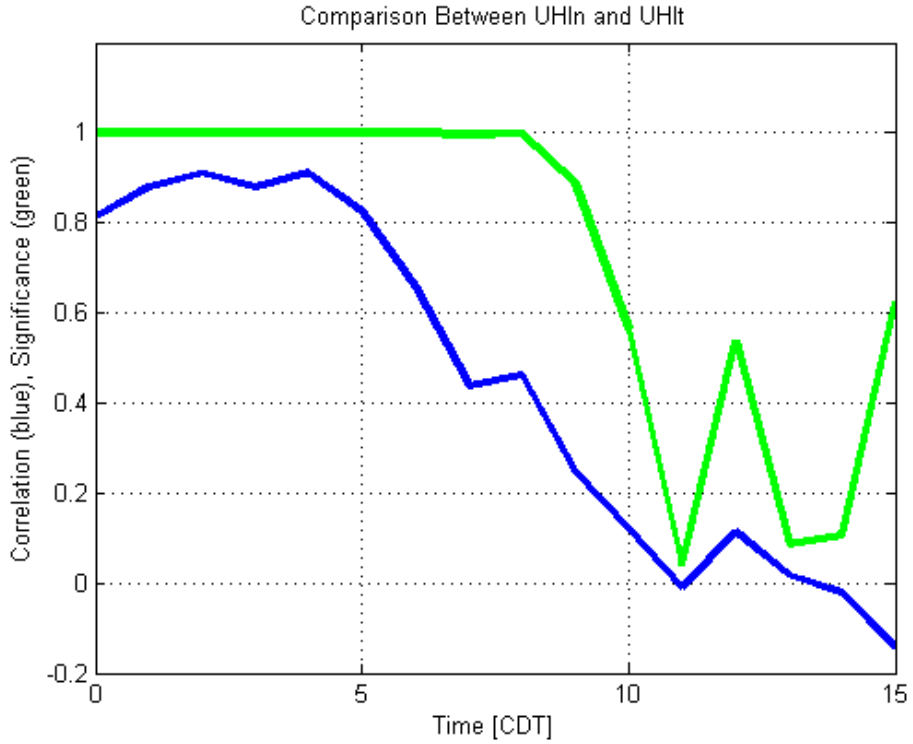

Figure 4.5. Comparison between the maximum nighttime Urban Heat Island magnitude (UHIn), and the UHI magnitude at a given time later the same day for days with lake-breezes (UHIt). Pearson's linear correlation coefficient is shown by the blue line and the significance (1 – P[correlation by random chance]) is shown by the green line.

Previous studies have found that UHI circulations are stronger during the daytime, despite the presence of a stronger thermal forcing the previous night (Vukovich et al., 1979; Hidalgo et al., 2008). Accordingly, the maximum nighttime UHI magnitude was also compared to the hourly UHI magnitude (Figure 4.5) and hourly u component of the wind in Aurora, IL (Figure 4.6) for days with lake-breezes. Not surprisingly, the maximum nighttime UHI magnitude and hourly UHI magnitude were highly correlated through 05 CDT with correlation coefficient values near 0.8 to 0.9 and significance near 1.0. This correlation dropped substantially later in the morning, possibly due to the lake-breeze passing through Midway Airport. Example scatter plots of the maximum nighttime UHI magnitude and UHIt are shown for 05 and 10 CDT in Figures 4.7 and 4.8, respectively.

The correlation coefficient between the maximum nighttime UHI magnitude and hourly u component of the wind in Aurora (Figure 4.6) ranged from approximately 0.2 – 0.35 with a significance above 0.8 through 04 CDT. Similar to the hourly UHI magnitude comparison to the u component of the wind (Figure 4.2), the maximum nighttime UHI magnitude and hourly u component of the wind were much less correlated in the post dawn hours. These weak, and generally statistically insignificant, correlations between the UHI magnitude and wind are indicative of the difficulty in directly observing the UHI circulation. In order to overcome this limitation of the current observational network, the UHI circulation was approximated by the UHI forcing, as defined in Chapter 2.

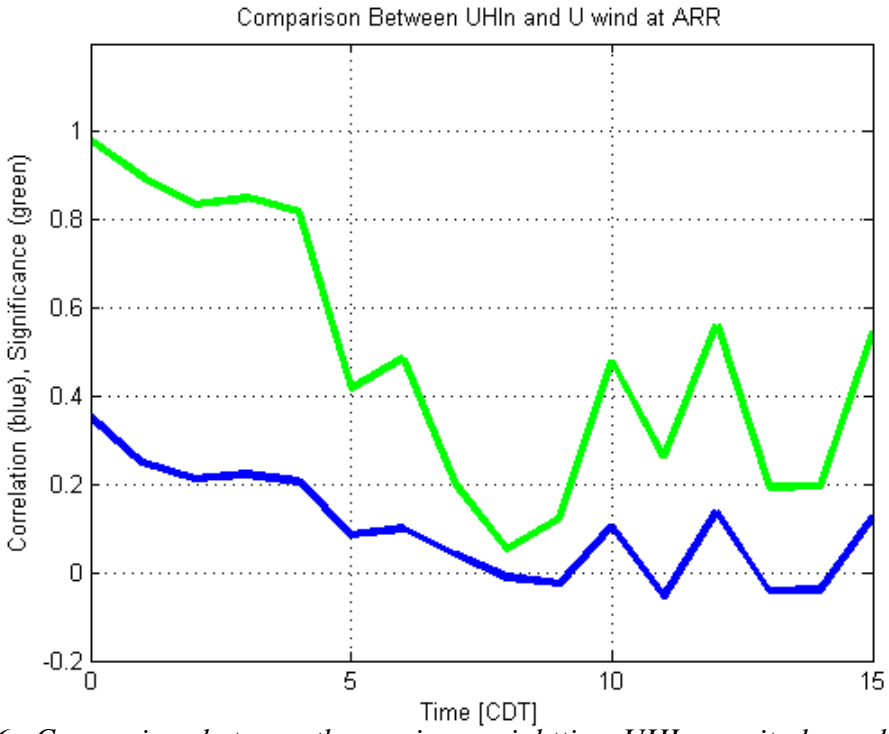

Figure 4.6. Comparison between the maximum nighttime UHI magnitude, and the u component of the wind at a given time later the same day for days with lake-breezes. Pearson's linear correlation coefficient is shown by the blue line and the significance (1 – P[correlation by random chance]) is shown by the green line.

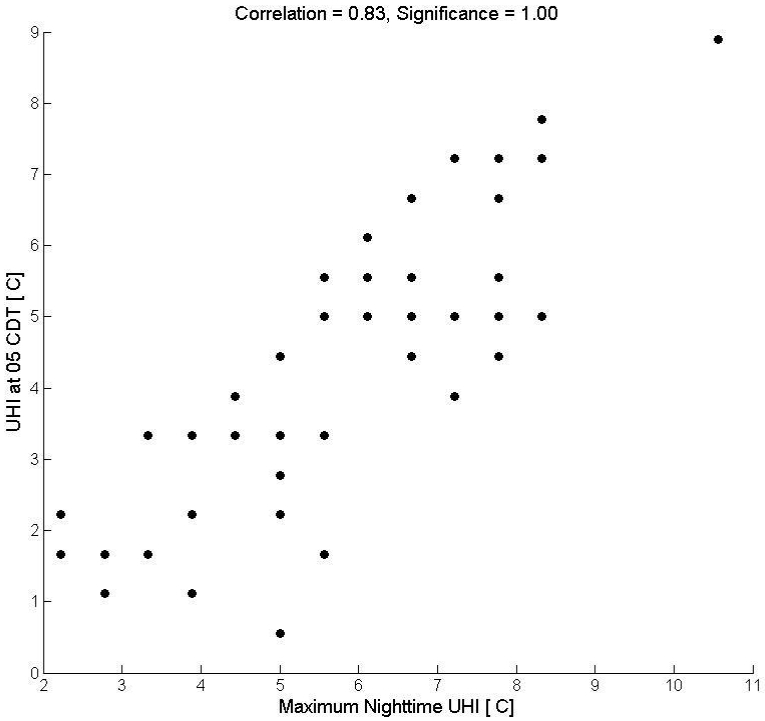

Figure 4.7. Scatter plot of the maximum nighttime UHI magnitude and the UHI magnitude at 05 CDT for all lake-breeze dates.

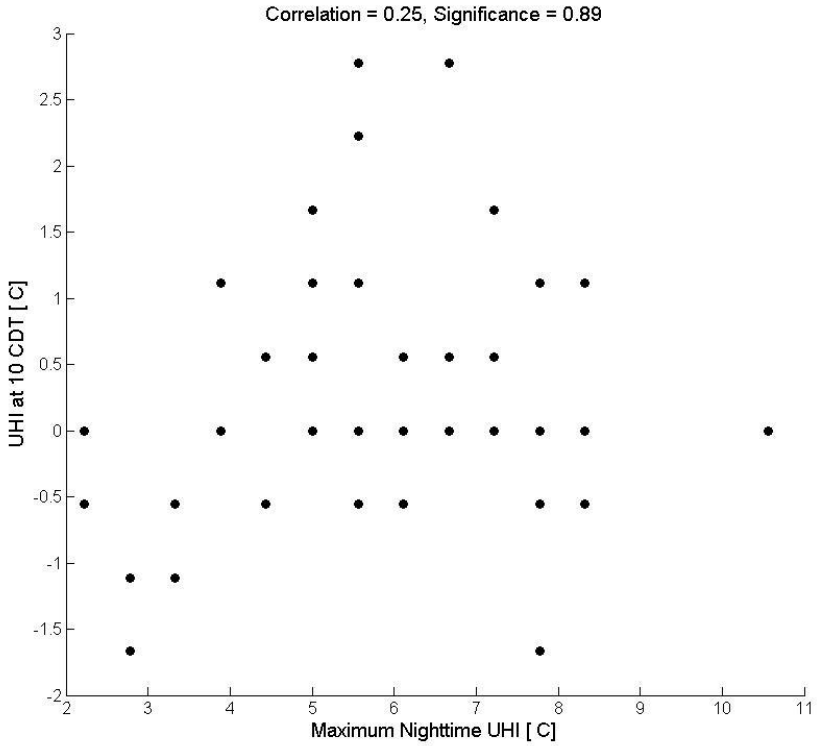

Figure 4.8. Scatter plot of the maximum nighttime UHI magnitude and the UHI magnitude at 10 CDT for all lake-breeze dates

2. Urban Heat Island and Lake-Breeze Interaction

The effect of Chicago's UHI on the lake-breeze was examined as the lake-breeze front progressed inland through downtown Chicago and its suburbs. If the UHI circulation did affect the inland motion of the lake-breeze front in 2005, one would expect that significant correlations between the UHI magnitude and inland motion of the lake-breeze front would only be present in the vicinity of Chicago. The correlations near the northern and southern suburbs should be weak, since the surface flow of the UHI would be parallel to the lake-breeze front, and thus have little effect on the inland motion of the lake-breeze front.

The hourly inland motion of the lake-breeze front along the individual cross sections was compared to the UHI magnitude at the time of lake-breeze initiation (UHI_D)

for the hours during which the lake-breeze front passed Midway Airport, and the I-294 – I-55 and I-355 – I-55 intersections. For the purposes of this study, lake-breeze initiation was defined as the hour in which the radar fine line was first manually discernable from ground clutter. These calculations allowed for comparison of lake-breeze frontal movement along all cross sections when the lake-breeze front was passing through specific geographic locations in the Chicago area. The daytime UHI magnitude is not a good predictor of how the lake-breeze front will move through the Chicago area, as is indicated by low correlations between UHI_D and lake-breeze frontal movement through Chicago (Figures 4.10 – 4.12).

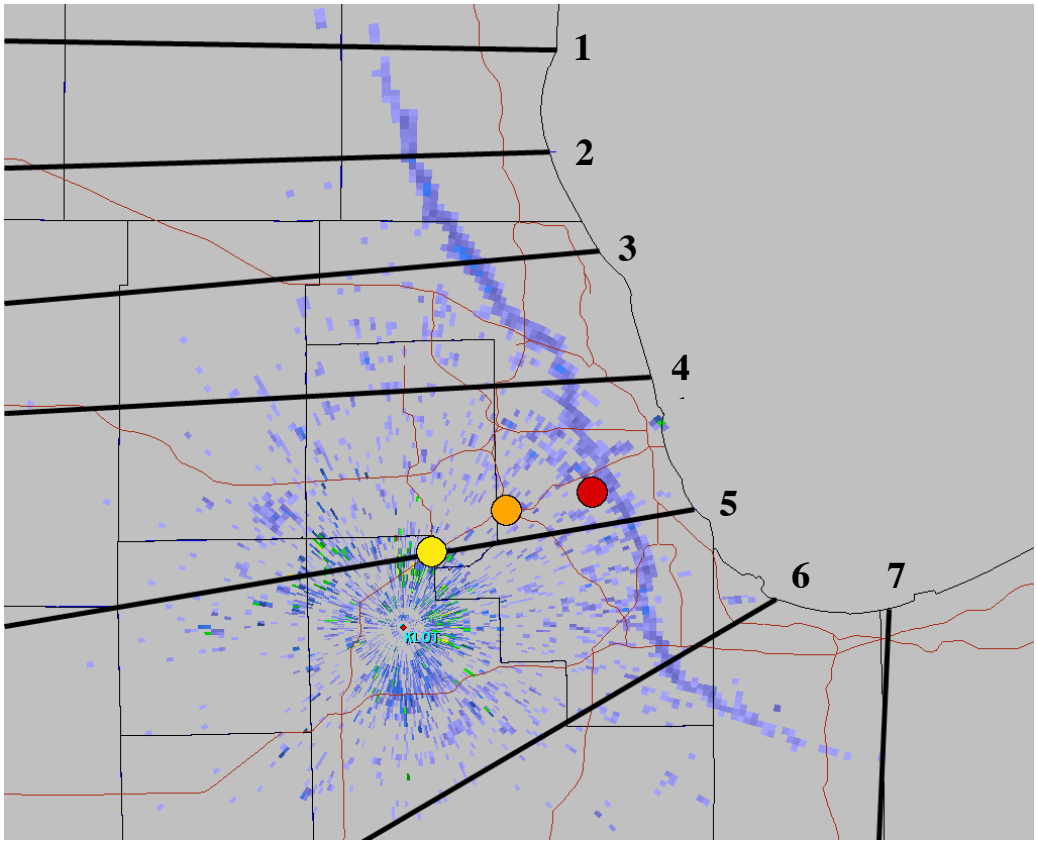

Figure 4.9. Cross sections along which the speed of inland motion of the lake-breeze front was calculated overlaid on an example image of radar base reflectivity (6/21/05, 1930 UTC). Geographic locations discussed in this chapter are noted by the circles (Midway Airport, red; I-55 – I-294 intersection, orange; I-55 – I-355 intersection, yellow).

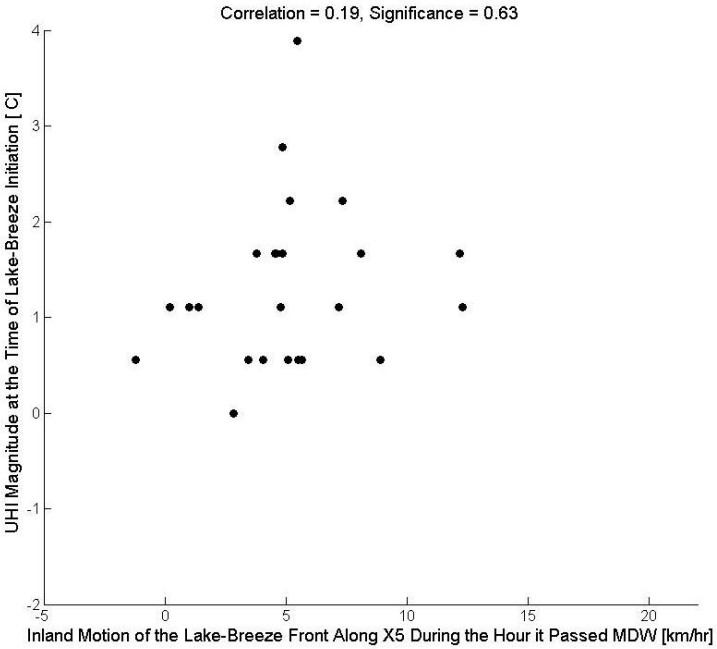

Figure 4.10. Comparison between the UHI magnitude at lake-breeze initiation and the average speed at which the lake-breeze front was moving inland along cross section 5 during the hour that the lake-breeze front passed over Midway Airport. Pearson's linear correlation coefficient and the significance (1 – P[correlation by random chance]) are shown.

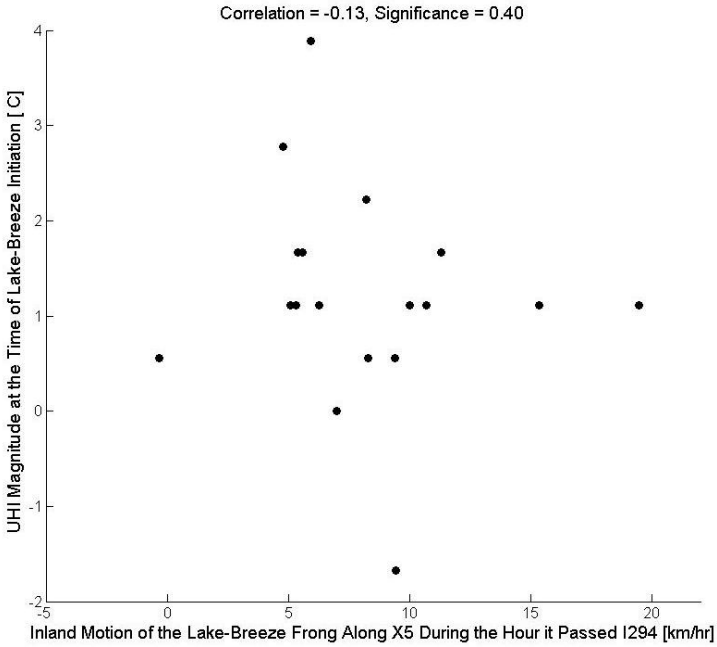

Figure 4.11. Comparison between the UHI magnitude at lake-breeze initiation and the average speed at which the lake-breeze front was moving inland along cross section 5 during the hour that the lake-breeze front passed over the I-55 – I-294 intersection. Pearson's linear correlation coefficient and the significance (1 – P[correlation by random chance]) are shown.

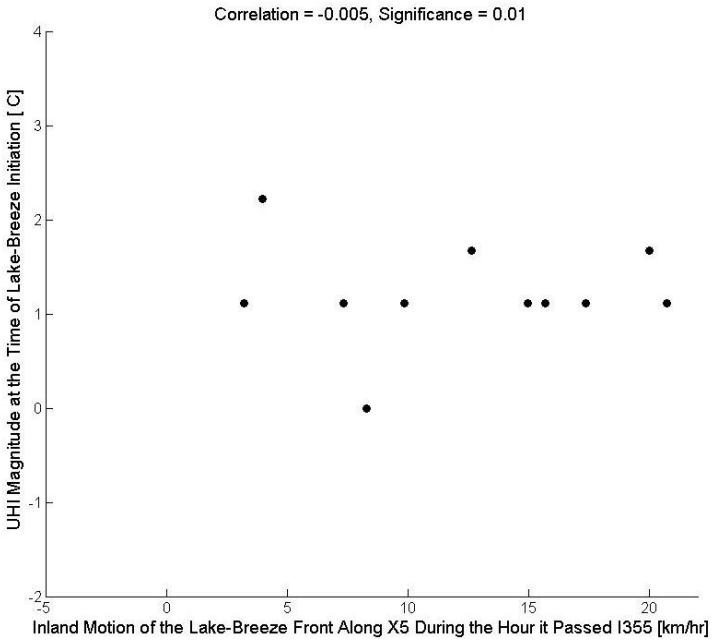

Figure 4.12. Comparison between the UHI magnitude at lake-breeze initiation and the average speed at which the lake-breeze front was moving inland along cross section 5 during the hour that the lake-breeze front passed over the I-55 – I-355 intersection. Pearson's linear correlation coefficient and the significance (1 – P[correlation by random chance]) are shown.

Since previous studies (Vukovich et al., 1979; Hidalgo et al., 2008) have found stronger daytime UHI circulations despite the maximum thermal forcing existing overnight, the same correlations were calculated based on the maximum nighttime UHI magnitude (UHI_N). Figures 4.13 and 4.14 show a weak tendency towards slower inland motion of the lake-breeze front along cross section 5 for days with stronger UHI_N. The significance of these correlations, particularly in figure 4.14, is substantially higher than in Figures 4.10, 4.11, and 4.12, however it is still below 0.95. A scatter plot of inland motion of the lake- breeze along cross section 5 and UHI_N for the hour the lake-breeze front passed over the I-55 – I-355 intersection is shown as Figure 4.15. A clear relationship can be seen between UHI_N and lake breeze frontal movement, with a correlation of -0.68 and a significance of 0.98. This indicates that lake-breeze fronts tend

to move more slowly inland along cross section 5 (while the lake-breeze front passes over I-355) when the maximum nighttime UHI magnitude is greater.

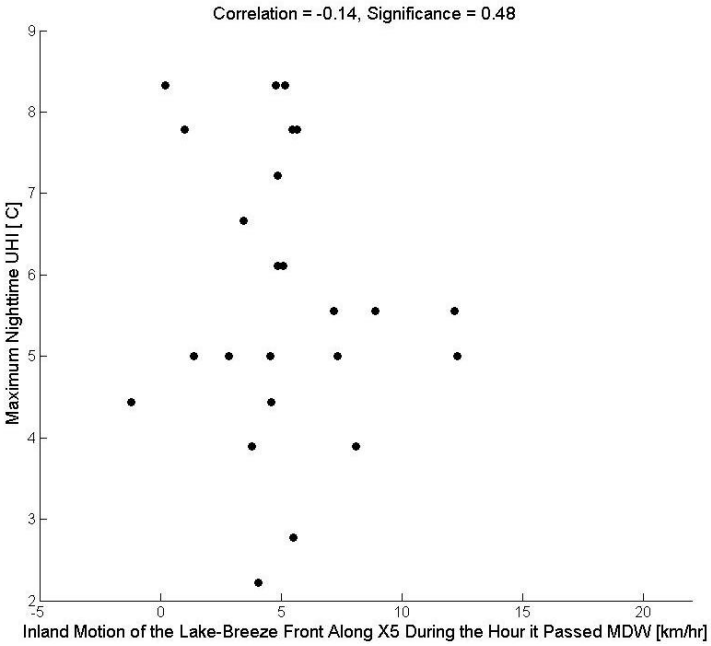

Figure 4.13. Comparison between the maximum nighttime UHI magnitude and the average speed at which the lake-breeze front was moving inland along cross section 5 during the hour that the lake-breeze front passed over Midway Airport. Pearson's linear correlation coefficient and the significance (1 – P[correlation by random chance]) are shown.

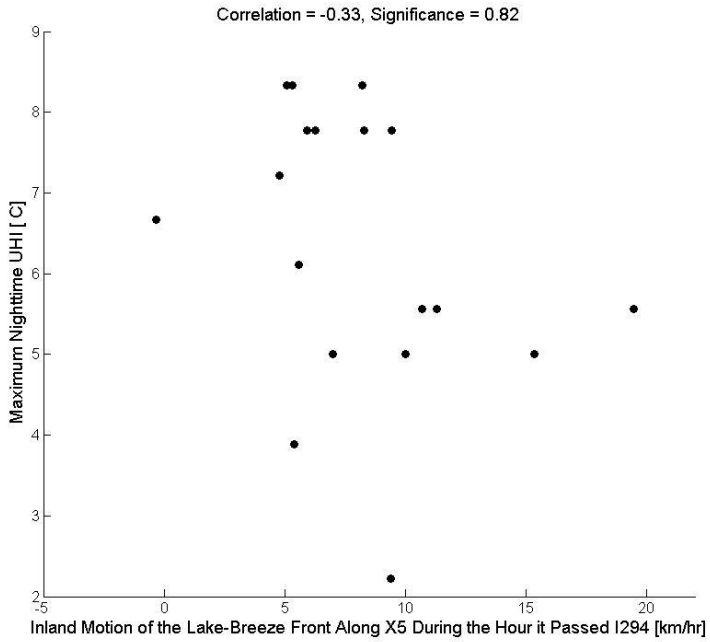

Figure 4.14. Comparison between the maximum nighttime UHI magnitude and the average speed at which the lake-breeze front was moving inland along cross section 5 during the hour that the lake-breeze front passed over the I-55 – I-294 intersection. Pearson's linear correlation coefficient and the significance (1 – P[correlation by random chance]) are shown.

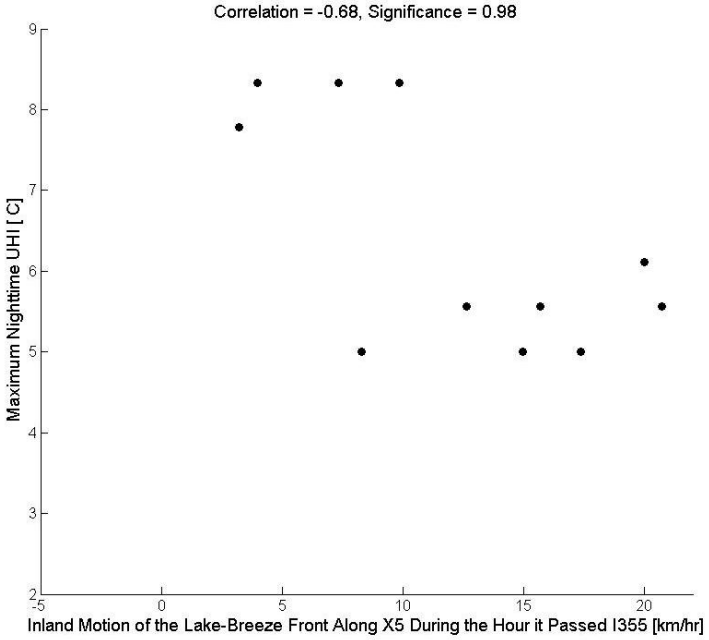

Figure 4.15. Comparison between the maximum nighttime UHI magnitude and the average speed at which the lake-breeze front was moving inland along cross section 5 during the hour that the lake-breeze front passed over the I-55 – I-355 intersection. Pearson's linear correlation coefficient and the significance (1 – P[correlation by random chance]) are shown.

Correlation Between UHI and Inland Motion of the Lake-Breeze Front						
	MDW		I-294		I-355	
	UHI_D	UHI_N	UHI_D	UHI_N	UHI_D	UHI_N
1	0.07	-0.32	-0.27	0.05	NaN	NaN
2	0.12	-0.28	-0.09	-0.18	0.27	-0.44
3	-0.08	-0.31	-0.04	0.30	0.38	-0.24
4	-0.06	-0.32	-0.02	-0.38	0.27	-0.52
5	0.19	-0.14	-0.13	-0.33	-0.01	-0.68
6	0.15	-0.25	0.39	0.07	-0.35	-0.52
7	0.06	-0.19	0.41	-0.29	0.01	-0.49

Significance	
0.50 – 0.59	
0.60 – 0.69	
0.70 – 0.79	
0.80 – 0.89	
0.90 – 0.99	

Figure 4.16. Comparison between the UHI (UHI_D, UHI magnitude at the time of lake-breeze initiation; UHI_N, maximum nighttime magnitude UHI) and the speed at which the lake-breeze front was moving inland along the individual cross sections during the hour in which it passed over Midway Airport, I-294, and I-355 (exact locations shown in Figure 4.9). Numerical values are Pearson's linear correlation coefficient and the significance (1 – P[correlation by random chance]) is shaded.

3. Discussion

Despite the clear correlation between UHI_N and lake-breeze frontal movement through Chicago, figures 4.5 and 4.6 illustrate that there is a statistically insignificant relationship between UHI_N and both the UHI magnitude and circulation by the afternoon. However, as discussed below, the UHI circulation above the surface may persist well into the day. Correlations between the UHI magnitude and lake-breeze frontal movement along all 7 cross sections (for the hours when the lake-breeze front passed through Midway, and the I-294 – I-55 and I-355 – I-55 intersections) are given in Figure 4.16. In general, UHI_N had a much stronger and more statistically significant correlation with the inland motion of the lake-breeze than UHI_D. The highest correlation and significance were often associated with cross sections near downtown Chicago, primarily cross sections 4, 5 and 6. An increase in both the magnitude of correlation and significance

occurred as the lake-breeze fronts progressed further inland, particularly for when they passed the I-355 – I-55 intersection.

These results are consistent with the findings of Vukovich et al. (1979) and Hidalgo et al. (2008), that despite the UHI magnitude being stronger at night, the UHI circulation is stronger during the day. Vukovich et al. (1979) attributed this increase in the UHI circulation strength during the day to destabilization of the boundary layer as a result of surface heating. This could help explain why the maximum nighttime UHI magnitude has a stronger correlation and significance to lake-breeze frontal movement through Chicago and its suburbs than the UHI magnitude at the time of lake-breeze initiation. In addition, the precise location of the UHI center is known to fluctuate due to the larger-scale wind (Vukovich, 1971; Wong and Dirks, 1978). If the UHI center is over or to the east of a particular location, such as Midway Airport, the u component of the wind associated with the UHI circulation would be zero or negative, respectively. Thus, it makes physical sense that the highest correlation between the UHI magnitude and inland motion of the lake-breeze front is further inland.

CHAPTER 5

CONCLUSIONS

Sea- and lake-breezes are known to have a substantial effect on local climate (Scott and Huff, 1996), precipitation (Byers and Rodebush, 1948; Laird et al., 1995; Baker et al., 2001), dispersion of pollutants (Lyons and Cole, 1976; Keen and Lyons, 1978; Bornstein and Thompson, 1981; Hastie et al., 1999), heat wave relief (Kunkel et al., 1996), and energy use. The implications of these effects are accentuated in coastal cities, due to their high population density. Therefore, a thorough understanding of sea- and lake-breeze systems near urban areas is highly valuable due to their societal impact and implications in local climate and forecasting.

Several recent numerical model simulations have suggested that sea- or lake-breezes should move more slowly through urban areas than in the surrounding suburbs due to the Urban Heat Island (UHI) circulation (Yoshikado, 1992; Sarkar et al., 1998; Kusaka et al., 2000). However, there have been few fine-scale observations of the spatial and temporal variations in lake-breeze movement to evaluate these results. Accordingly, this research utilized high-resolution WSR-88D observations to determine the effect of the UHI on lake-breeze frontal movement through Chicago and nearby suburban areas for lake-breezes which occurred during April – September 2005.

For dates in the study period, archived data from the WSR-88D radar in Romeoville, IL were visually inspected for the presence of radar fine lines (in base reflectivity, velocity, or spectral width fields) using GR2Analyst software. Radar fine lines have been utilized as a proxy for the location of sea- or lake-breeze fronts for more

than 50 years (Atlas, 1960), and is a well-accepted practice. Once a radar fine line was identified, archived surface temperature and wind data were analyzed to confirm that the fine line was indicative of a lake-breeze front and not another feature (such as convective outflow, or horizontal convective rolls). In order to be considered a lake-breeze front, the fine line must have been collocated with a surface convergence zone, and cooler surface temperatures had to be present on the side of the fine line closer to Lake Michigan. This methodology resulted in the identification of 49 lake-breeze dates during the April – September 2005 period.

Based on a climatology of lake-breezes on Lake Michigan (Laird et al., 2001), 2005 was a typical year in terms of monthly and overall lake-breeze frequency. The monthly lake-breeze frequency gradually increased from 5 days in April to 12 days August, then decreased slightly to 10 days in September. Similar to what was found by Laird et al., the increase in lake-breeze frequency later in the summer appeared to be the result of weaker synoptic-scale wind. The majority of lake-breezes (32 of 49 lake-breeze days) occurred from late June through September, when the half-monthly mean wind speed in Rockford, IL remained near or below 3.0 m s^{-1}. Lake-breeze start time, defined as the first hour that the radar fine line was discernable in radar reflectivity, velocity, or spectral width fields, had a linear correlation coefficient of 0.16 with the 12 UTC u-component of the wind in Rockford (Table 3.2). However the statistical significance (1 – P[correlation due to random chance]) was only 0.69. Lake-breeze duration, defined as the number of hours the fine line was discernable from ground clutter, was weakly correlated with the 12 UTC u-component of the wind (-0.14). The significance of this correlation was only 0.61. These correlations and their significance suggest that a weak

relationship between the u-component of the wind and lake-breeze start time/duration near southern Lake Michigan is possible, but other factors may play more important roles.

The average speed of inland motion of the lake-breeze front, calculated along seven shore perpendicular cross sections (Figure 2.3), was 5.0 km hr^{-1}. In general, the lake-breeze front moved inland more quickly north of Chicago (5.9 km hr^{-1} near Evanston, IL), than on the south side (4.0 km hr^{-1} near Gary, IN). Analysis of North American Regional Reanalysis (NARR) data (Figures 3.10, 3.11) indicated that surface troughs located in the Midwest (to the north or west of Chicago) were often associated with increased inland motion of the lake-breeze front. NARR data also indicated that surface high pressure centered to the southwest of Chicago was associated with decreased inland motion of the lake-breeze front. Of interest were two cases where the lake-breeze persisted despite the passage of a cold front and one case where the lake-breeze front retrograded to over Lake Michigan due to a larger-scale wind shift from along-shore to offshore during the day.

Chicago's hourly Urban Heat Island magnitude was calculated by subtracting the 2 m air temperature in Aurora, IL (ARR) from the 2 m air temperature at Midway Airport (MDW). This temperature perturbation, similar to an approximation for the UHI used by Ackerman (1985), had considerable diurnal variability with an average nighttime maximum near 4.5°C and afternoon minimum near 0°C (Figure 4.1). The surface UHI circulation is known to be difficult to observe directly due to its juxtaposition with strong microscale circulations around numerous obstacles (such as individual buildings). Not surprisingly, correlations between the wind in ARR and the UHI magnitude were weak

and often statistically insignificant (Figures 4.2 – 4.8). Therefore, the UHI magnitude was henceforth used as a proxy for the strength of the UHI circulation.

The effect of Chicago's UHI on the lake-breeze was examined along all seven cross sections (Figure 4.9) as the lake-breeze front progressed inland through downtown Chicago and its suburbs. The relationship between UHI magnitude at the time of lake-breeze initiation (UHI_D) and the inland motion of the lake-breeze front along the individual cross sections for the hours during which the lake-breeze front passed over Midway Airport, and the I-294 – I-55 and I-355 – I-55 intersections was examined. Surprisingly, these correlations (Figures 4.10 – 4.12) were weak and statistically insignificant, contradicting the findings reported in much of the current literature.

Keeping in mind that the UHI circulation takes longer to develop in larger cities (Richiardone and Brusaca, 1989) and that stronger daytime UHI circulations have been observed despite stronger forcing at night (Vukovich et al., 1979; Hidalgo et al., 2008), the same correlations were calculated with the maximum nighttime UHI magnitude (UHI_N), instead of UHI_D. Along cross section 5, which cuts through the core of downtown Chicago, the correlation between UHI_N and inland motion of the lake-breeze front remained weak and statistically insignificant for the hour during which the lake-breeze front passed over Midway Airport (Figure 4.13). However, the correlation and significance increased along cross section 5 as the lake-breeze front progressed further inland (Figures 4.14 – 4.15). By the time the lake-breeze front reached the I-355 – I-55 intersection, the inland motion of the lake-breeze front along cross section 5 had a -0.68 correlation coefficient with UHI_N and significance of 0.98. A summary of the correlations between lake-breeze movement along each of the cross sections and UHI

magnitude is shown in Figure 4.16. In general, higher correlations with the UHI magnitude are present along cross sections near downtown Chicago. The lake-breeze front tended to move inland more slowly through the southwest suburbs of Chicago on days with stronger UHI_N.

Further research on the UHI circulation and its relationship to UNI_N is recommended. Idealized numerical simulations of the diurnal cycle of UHI circulations could help determine the implications of stronger UHI_N on characteristics of the following day's UHI circulation. These simulations would be particularly valuable if carried out under a variety of atmospheric conditions.

REFERENCES

Ackerman, B., 1985: Temporal march of the Chicago heat island. *J*. *Appl*. *Meteor*., **24**, 547–554.

Arritt, R. W., 1993: Effects of the large-scale flow on characteristic features of the sea breeze. *J*. *Appl*. *Meteor*., **32**, 116–125.

Atkins, N.T., R.M. Wakimoto, and T.M. Weckwerth, 1995: Observations of the sea-breeze front during CaPE. Part II: dual-doppler and aircraft analysis. *Mon*. *Wea*. *Rev*., **123**, 944–969.

Atlas, D., 1960: Radar detection of the sea breeze. *J*. *Atmos*. *Sci*., **17**, 244–258.

Aviation Digital Data Service (ADDS), cited 2005: [Available online at http://adds.aviationweather.gov/satellite/.]

Baker, R. D., B. H. Lynn, A. Boone, W.-K. Tao, and J. Simpson, 2001: The influence of soil moisture, coastline curvature, and land-breeze circulations on sea-breeze-initiated precipitation. *J*. *Hydrometeor*., **2**, 193-211.

Barbato, J. P., 1978: Areal parameters of the sea breeze and its vertical structure in the Boston basin. *Bull*. *Amer*. *Meteor*. *Soc*., **59**, 1420–1431.

Biggs, W. G., and M. E. Graves, 1962: A lake breeze index. *J*. *Appl*. *Meteor*., **1**, 474 – 480.

Bornstein, R.D., 1968: Observations of the urban heat island effect in New York City. *J*. *Appl*. *Meteor*., **7**, 575–582.

Bornstein, R. D., and W.T. Thompson, 1981: Effects of frictionally retarded sea breeze and synoptic frontal passages on sulfur dioxide concentrations in New York City. *J*. *Appl*. *Meteor*., **20**, 843–858.

Byers, H. R., and H. R. Rodebush, 1948: Causes of thunderstorms of the Florida peninsula. *J*. *Meteor*., **5**, 275-280.

Cenedese, A., and P. Monti, 2003: Interaction between an inland urban heat island and a sea-breeze flow: a laboratory study. *J*. *Appl*. *Meteor*., **42**, 1569–1583.

Comrie, A.C., 2000: Mapping a wind–modified urban heat island in Tucson, Arizona (with comments on integrating research and undergraduate learning). *Bull*. *Amer*. *Meteor*. *Soc*., **81**, 2417–2431.

Crum, T.D., and R.L. Alberty, 1993: The WSR-88D and the WSR-88D operational support facility. *Bull*. *Amer*. *Meteor*. *Soc*., **74**, 1669–1687.

Hage, K., 1972: Nocturnal temperatures in Edmonton, Alberta. *J*. *Appl*. *Meteor*., **11**, 123–129.
Hastie, D. R., J. Narayan, C. Schiller, H. Niki, P. B. Shepson, D. M. L. Sills, P. A. Taylor, W. J. Moroz, J. W. Drummond, N. Reid, R. Taylor, R. B. Roussel, and O. T. Melo, 1999: Observational evidence for the impact of the lake breeze circulation on ozone concentrations in Southern Ontario. *Atmos*. *Environ*., **33**, 323-335.

Hidalgo, J., G. Pigeon, and V. Masson, 2008: Urban-breeze circulation during the CAPITOUL experiment: observational data analysis approach. *Meteorol*. *Atmos*. *Phys*., **102**, 223–241.
Keen, C. S., and W. A. Lyons, 1978: Lake/land breeze circulations on the western shore of Lake Michigan. *J*. *Appl*. *Meteor*., **17**, 1843–1855.

Kim, Y.H., and J.J. Baik, 2005: Spatial and temporal structure of the urban heat island in Seoul. *J*. *Appl*. *Meteor*., **44**, 591–605.

Kunkel, K. E., S. A. Changnon, B. C. Reinke, and R. W. Arritt, 1996: The July 1995 heat wave in the Midwest: a climatic perspective and critical weather factors. *Bull*. *Amer*. *Meteor*. *Soc*., **77**, 1507–1518.

Kusaka, H., F. Kimura, H. Hirakuchi, and M. Mizutori, 2000: The effects of land-use alteration on the sea breeze and daytime heat island in the Tokyo metropolitan area. *J*. *Meteor*. *Soc*. *Japan*, **78(4)**, 405-420.

Laird, N.F., D.A. Kristovich, R.M. Rauber, H.T. Ochs, and L.J. Miller, 1995: The Cape Canaveral sea and river breezes: kinematic structure and convective initiation. *Mon*. *Wea*. *Rev*., **123**, 2942–2956.

Laird, N.F., D.A.R. Kristovich, X.Z. Liang, R.W. Arritt, and K. Labas, 2001: Lake Michigan lake breezes: climatology, local forcing, and synoptic environment. *J*. *Appl*. *Meteor*., **40**, 409–424.

Lyons, W. A., and H. S. Cole, 1976: Photochemical oxidant transport: mesoscale lake breeze and synoptic-scale aspects. *J*. *Appl*. *Meteor*., **15**, 733–743.

McPherson, R.D., 1970: A numerical study of the effect of a coastal irregularity on the sea breeze. *J*. *Appl*. *Meteor*., **9**, 767–777.

Mesinger, F., G. DiMego, E. Kalnay, K. Mitchell, P.C. Shafran, W. Ebisuzaki, D. Jović, J. Woollen, E. Rogers, E.H. Berbery, M.B. Ek, Y. Fan, R. Grumbine, W. Higgins, H. Li, Y. Lin, G. Manikin, D. Parrish, and W. Shi, 2006: North American Regional Reanalysis. *Bull*. *Amer*. *Meteor*. *Soc*., **87**, 343–360.

Midwestern Regional Climate Center, cited 2008: [Available online at http://mcc.sws.uiuc.edu/prod_serv/prodserv.htm.]

Miller, S.T.K., B.D. Keim, R.W. Talbot, and H. Mao, 2003: Sea breeze: structure, forecasting, and impacts, *Rev*. *Geophys*., 41(3), 1011, doi:10.1029/2003RG000124.

Mitchell, J. M., 1961: The temperature of cities. *Weatherwise*, **14**, 224–229.

Moderate Resolution Imaging Spectroradiometer (MODIS), cited 2010: [Available online at http://modis.gsfc.nasa.gov/gallery/#.]

Moroz, W.J., 1967: A lake breeze on the eastern shore of Lake Michigan: observations and model. *J*. *Atmos*. *Sci*., **24**, 337–355.

Munn, R.E., M.S. Hirt, and B.F. Findlay, 1969: A climatological study of the urban temperature anomaly in the lakeshore environment at Toronto. *J*. *Appl*. *Meteor*., **8**, 411–422.

National Climatic Data Center (NCDC), cited 2008: [Available online at http://hurricane.ncdc.noaa.gov/pls/plhas/HAS.FileAppSelect?datasetname=6500.]

National Data Buoy Center (NDBC), cited 2008: [Available online at http://www.ndbc.noaa.gov/station_page.php?station=45007.]

National Oceanic and Atmospheric Administration – Earth Systems Research Laboratory, cited 2008: [Available online at http://www.esrl.noaa.gov/psd/cgi-bin/data/narr/plotday.pl.]

Ohashi, Y., and H. Kida, 2002: Local circulations developed in the vicinity of both coastal and inland urban areas: a numerical study with a mesoscale atmospheric model. *J*. *Appl*. *Meteor*., **41**, 30–45.

Richiardone, R., and G. Brusasca, 1989: Numerical experiments on urban heat island intensity. *Quart*. *J*. *Roy*. *Meteor*. *Soc*., **115,** 983–995.

Sarkar, A., R. S. Saraswat, and A. Chandrasekar, 1998: Numerical study of the effects of urban heat island on the characteristic features of the sea breeze circulation. *Proc*. *Indian Acad*. *Sci*. *(Earth Planet*. *Sci*.*)*, **107**, 127-137.

Scott, R. W., and F. A. Huff, 1996: Impacts of the Great Lakes on regional climate conditions. *J*. *Great Lakes Res*., **22**, 845-863.

Vukovich, F.M., 1971: Theoretical analysis of the effect of mean wind and stability on a heat island circulation characteristic of an urban complex. *Mon*. *Wea*. *Rev*., **99**, 919–926.

Vukovich, F.M., W.J. King, J.W. Dunn, and J.J.B. Worth, 1979: Observations and simulations of the diurnal variation of the urban heat island circulation and associated variations of the ozone distribution: a case study. *J*. *Appl*. *Meteor*., **18**, 836–854.

Wakimoto, R.M., and N.T. Atkins, 1994: Observations of the sea-breeze front during CaPE. Part I: single-doppler, satellite, and cloud photogrammetry analysis. *Mon. Wea. Rev.*, **122**, 1092–1114.

Wong, K.K., and R.A. Dirks, 1978: Mesoscale perturbations on airflow in the urban mixing layer. *J. Appl. Meteor.*, **17**, 677–688.

Yoshikado, H., 1992: Numerical study of the daytime urban effect and its interaction with the sea breeze. *J. Appl. Meteor.*, **31**, 1146–1164.

APPENDIX A

HOURLY LAKE-BREEZE FRONT LOCATIONS

The hourly locations of the lake-breeze front were documented for all 44 lake-breezes identified from April – September 2005. Radar fine lines in base reflectivity, base velocity, and spectral width fields were used as a proxy for the lake-breeze front location. These figures document the great deal of temporal (day-to-day, intraday) and spatial (urban versus suburban) variability of inland motion of the lake-breeze front.

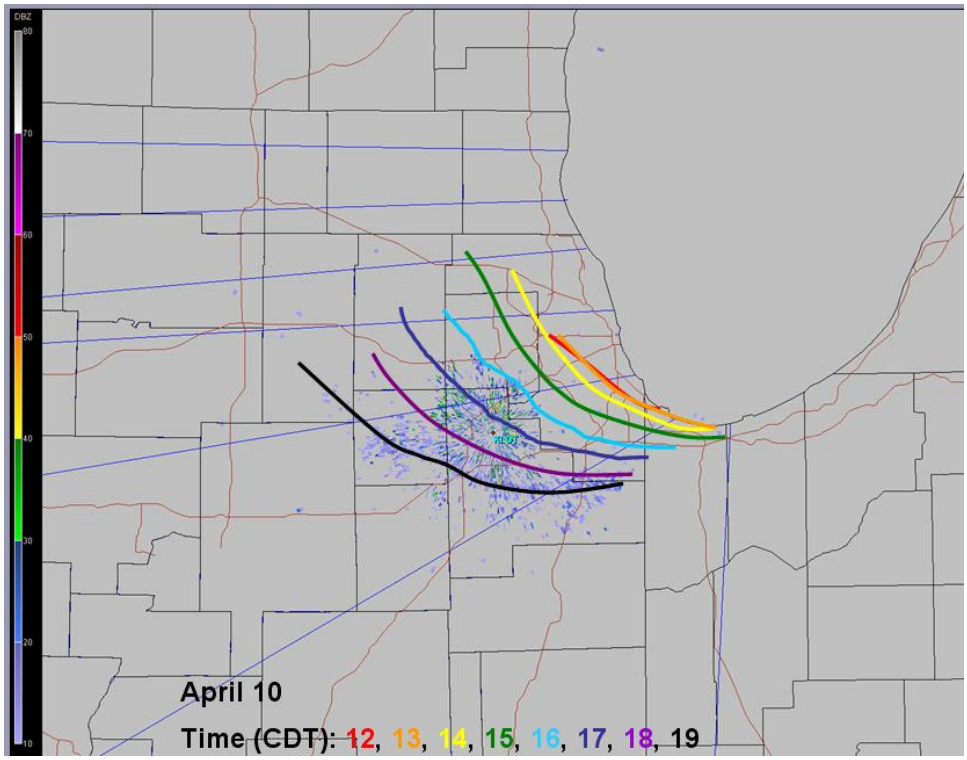

Figure A.1. Hourly locations of the lake-breeze front, based on the radar fine line location, for 4/10/05 overlaid on the 1905 CDT base reflectivity Plan Position Indicator (PPI).

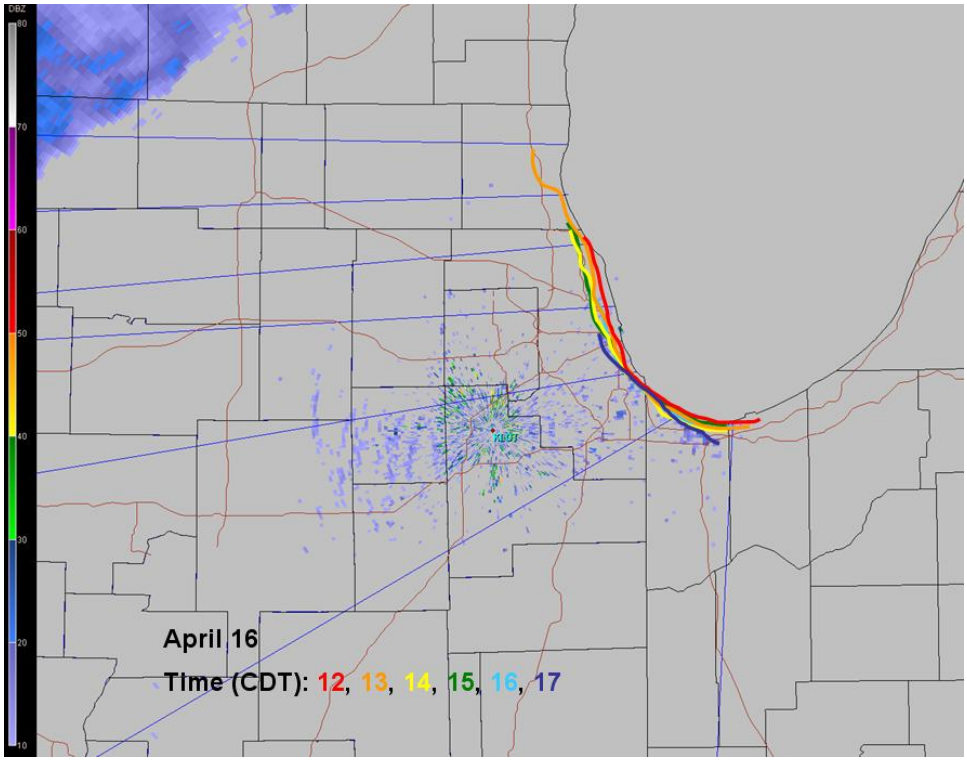

Figure A.2. Same as Figure A.1, except for 4/16/05 overlaid on the 1703 CDT base reflectivity PPI.

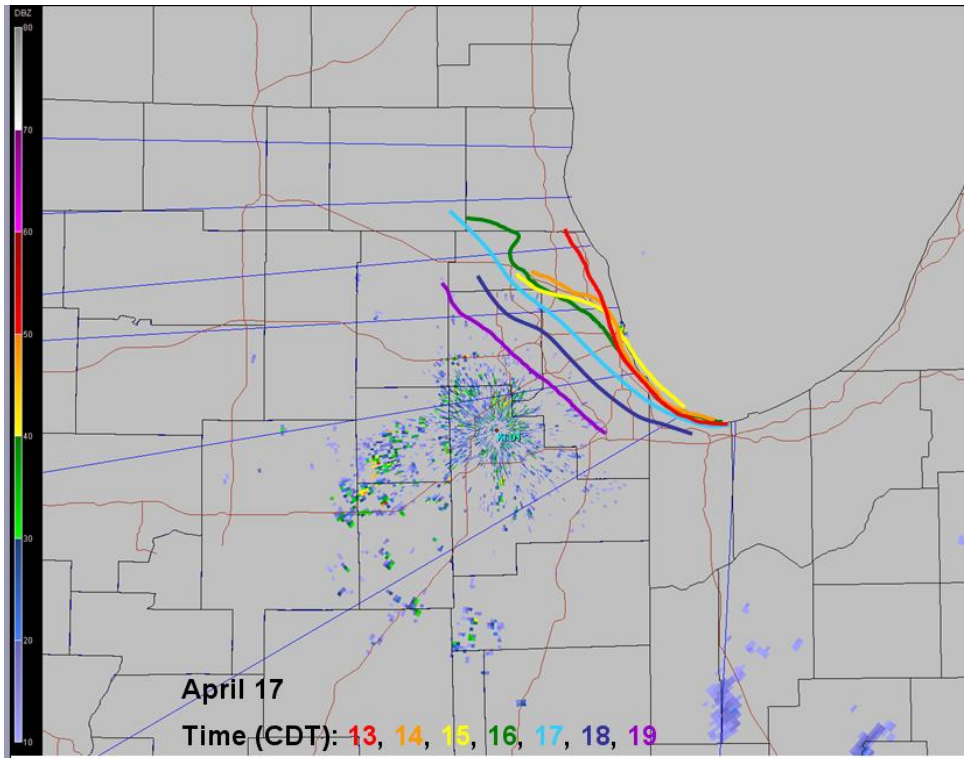

Figure A.3. Same as Figure A.1, except for 4/17/05 overlaid on the 1906 CDT base reflectivity PPI.

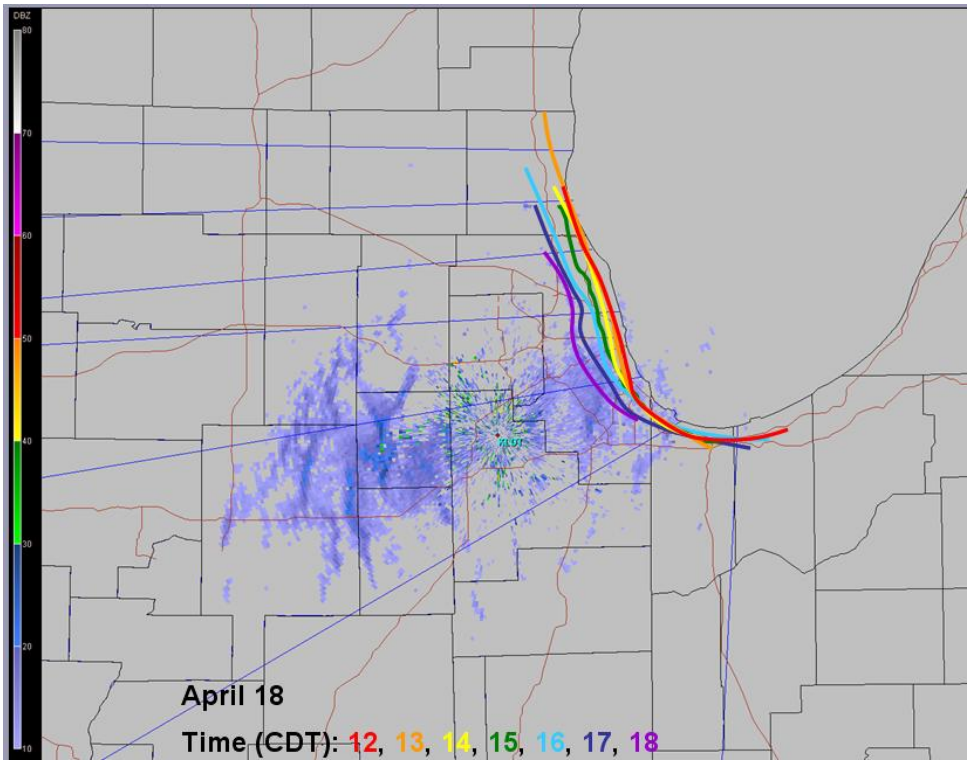

Figure A.4. Same as Figure A.1, except for 4/18/05 overlaid on the 1807 CDT base reflectivity PPI.

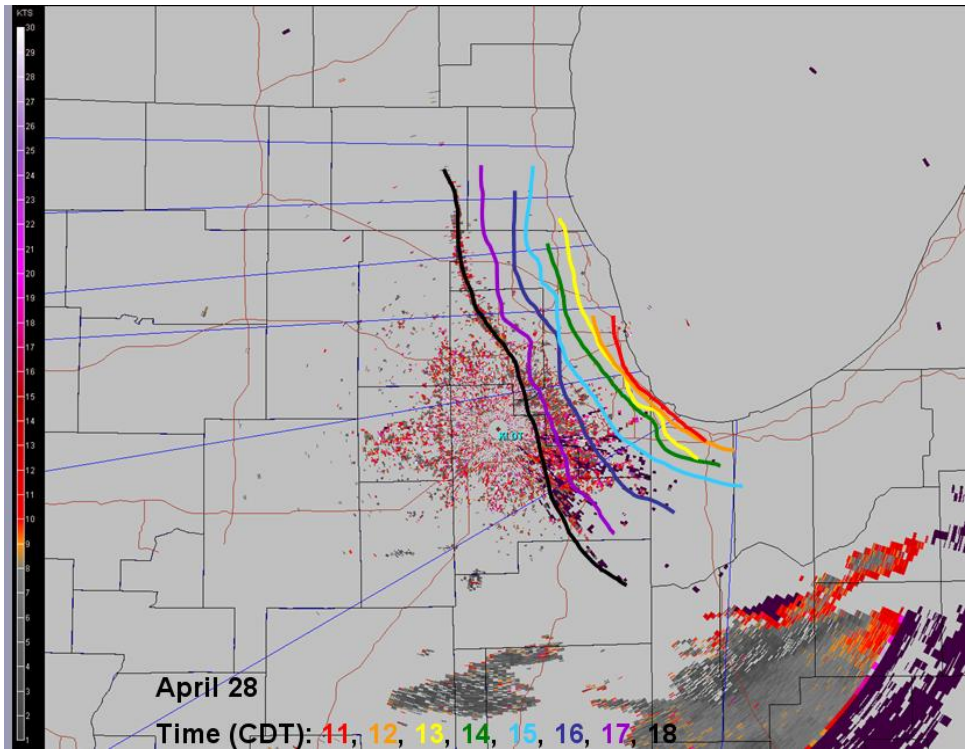

Figure A.5. Same as Figure A.1, except for 4/28/05 overlaid on the 1803 CDT spectral width PPI.

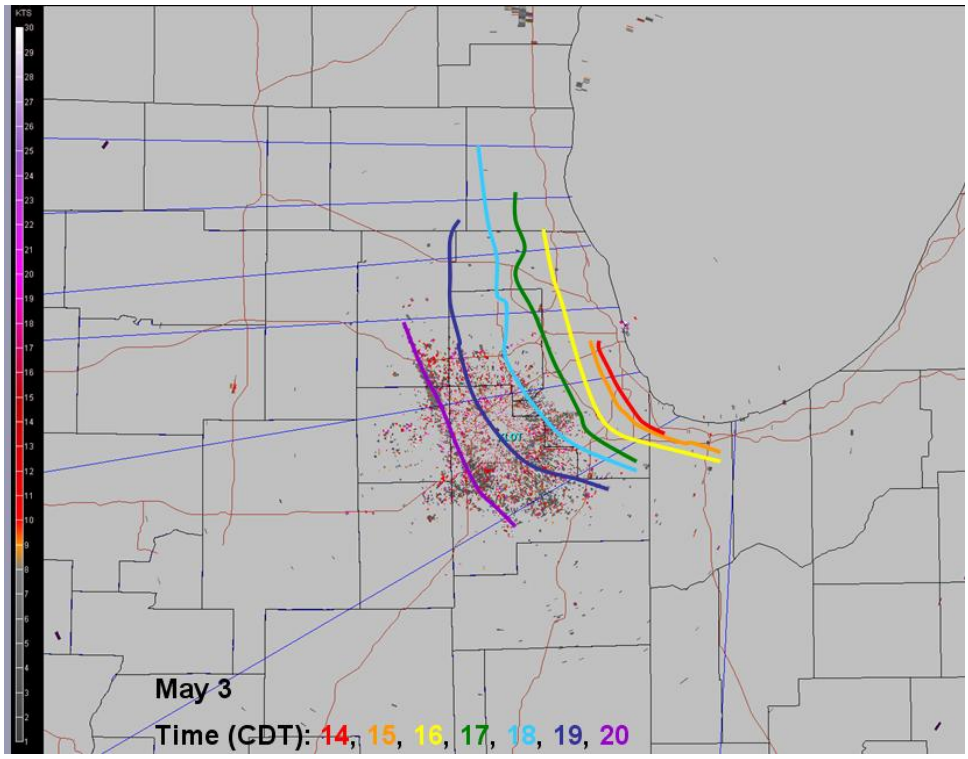

Figure A.6. Same as Figure A.1, except for 5/3/05 overlaid on the 2009 CDT spectral width PPI.

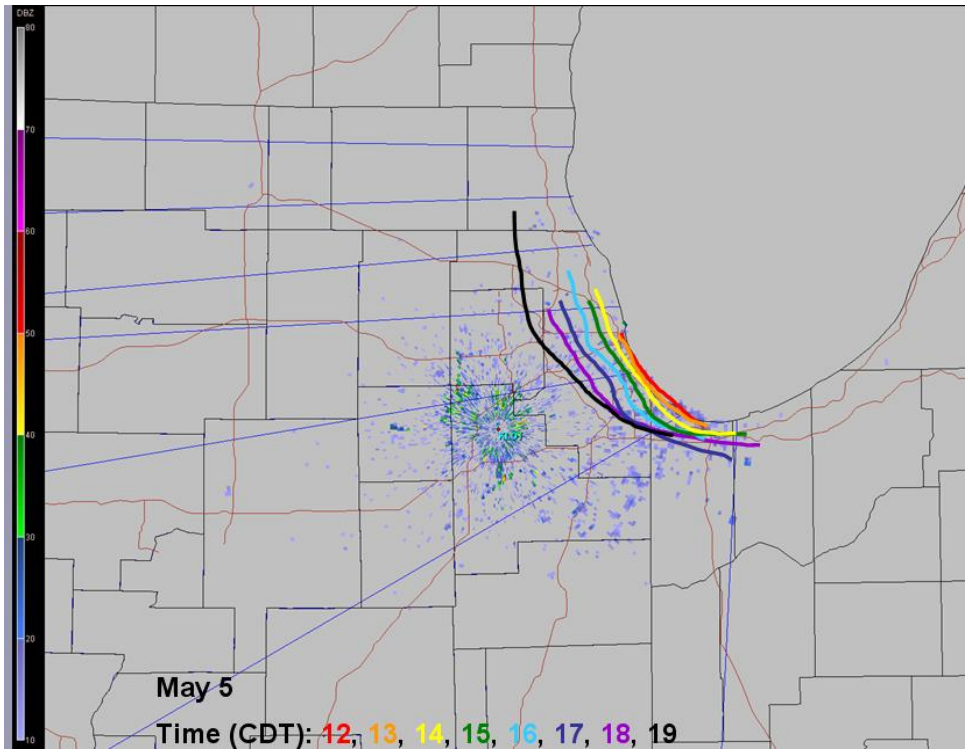

Figure A.7. Same as Figure A.1, except for 5/5/05 overlaid on the 1305 CDT base reflectivity PPI.

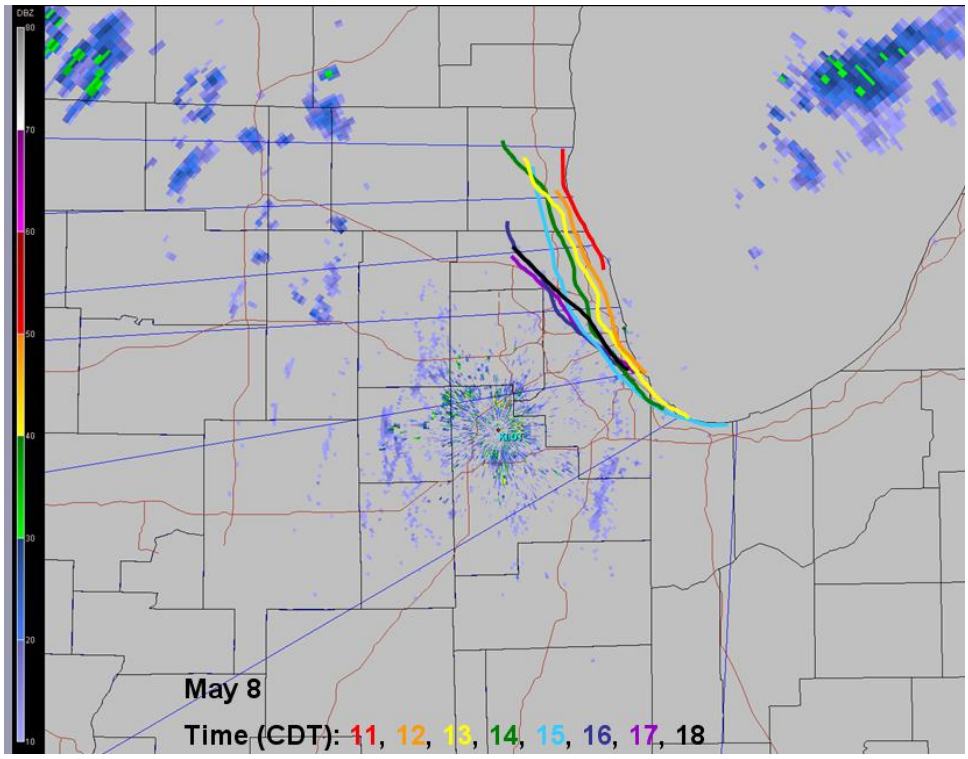

Figure A.8. Same as Figure A.1, except for 5/8/05 overlaid on the 1809 CDT base reflectivity PPI.

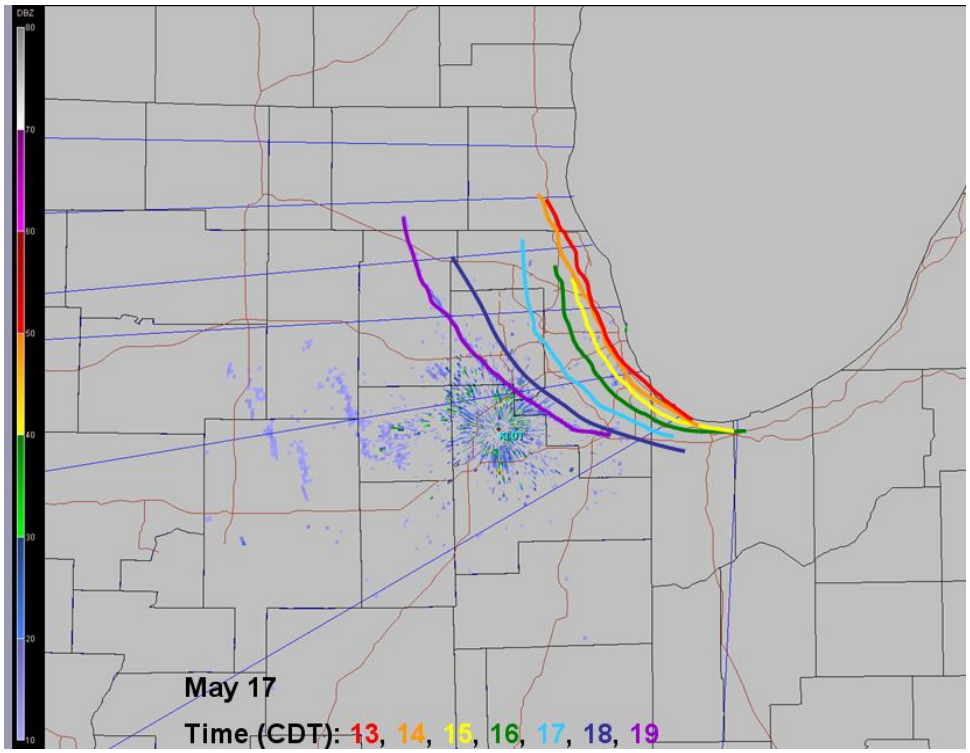

Figure A.9. Same as Figure A.1, except for 5/17/05 overlaid on the 1902 CDT base reflectivity PPI.

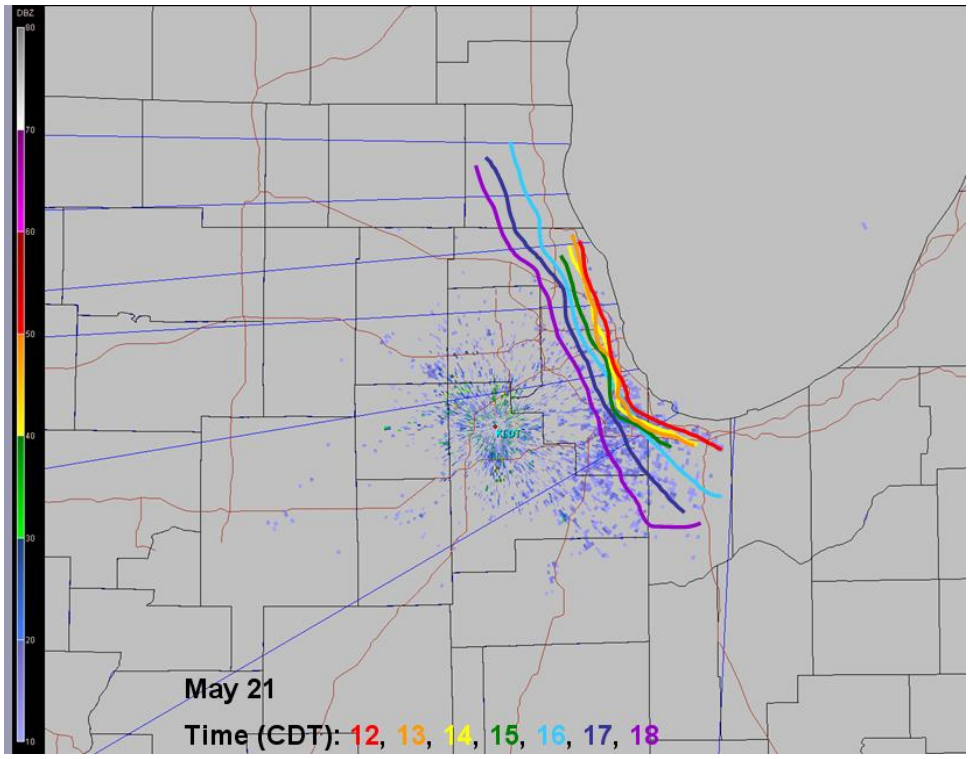

Figure A.10. Same as Figure A.1, except for 5/21/05 overlaid on the 1208 CDT base reflectivity PPI.

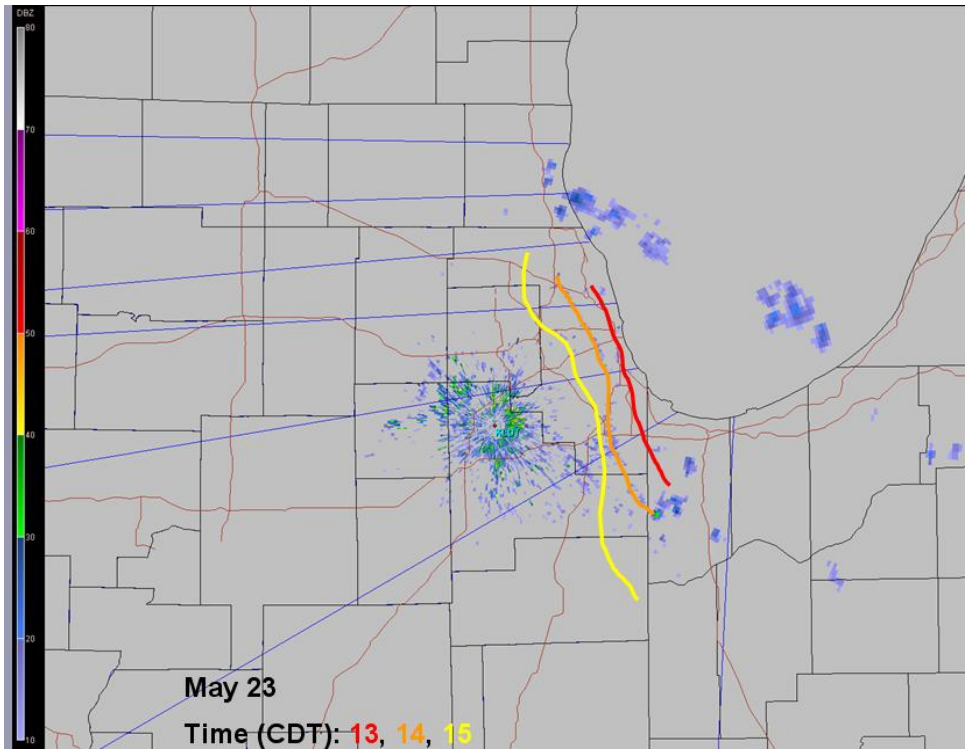

Figure A.11. Same as Figure A.1, except for 5/23/05 overlaid on the 1404 CDT base reflectivity PPI.

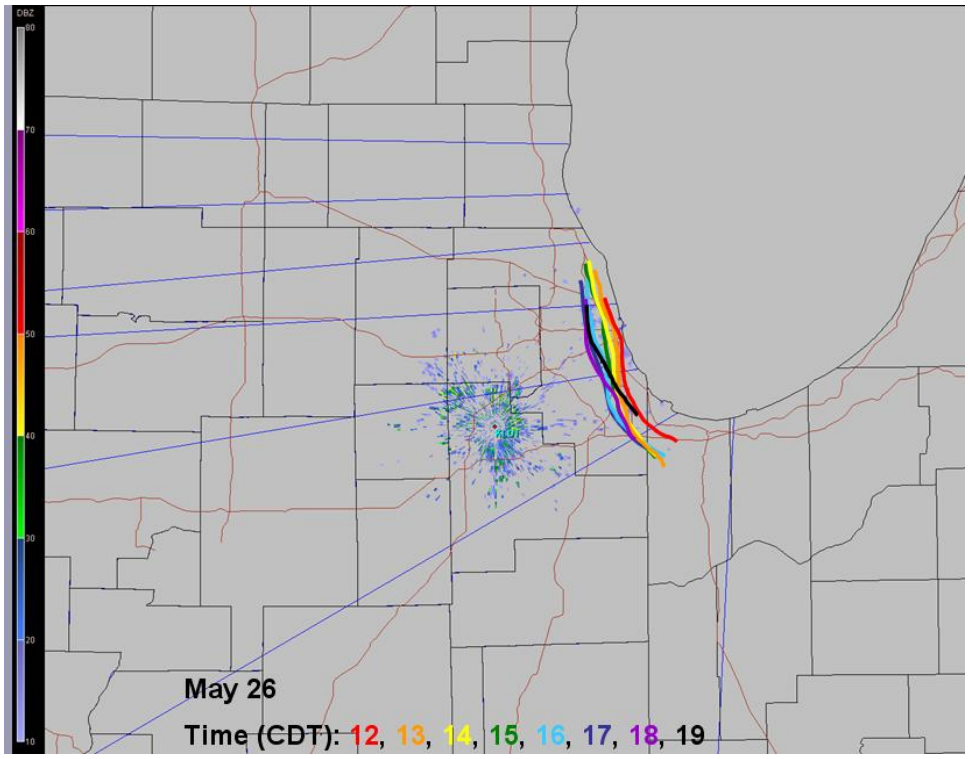

Figure A.12. Same as Figure A.1, except for 5/26/05 overlaid on the 1905 CDT base reflectivity PPI.

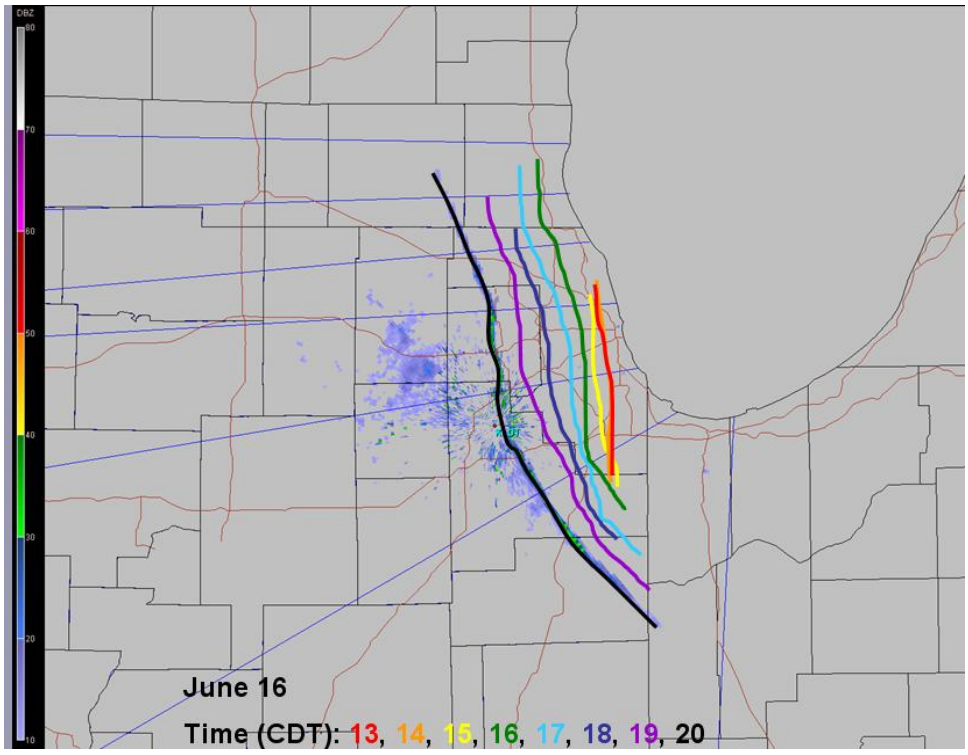

Figure A.13. Same as Figure A.1, except for 6/16/05 overlaid on the 2000 CDT base reflectivity PPI.

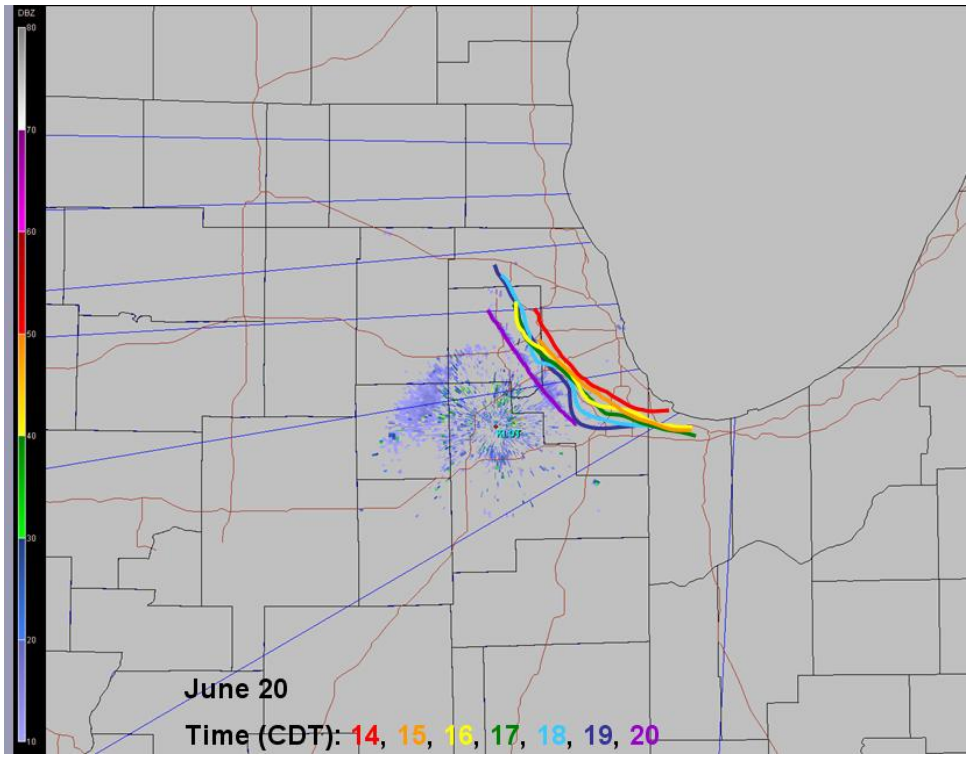

Figure A.14. Same as Figure A.1, except for 6/20/05 overlaid on the 2007 CDT base reflectivity PPI.

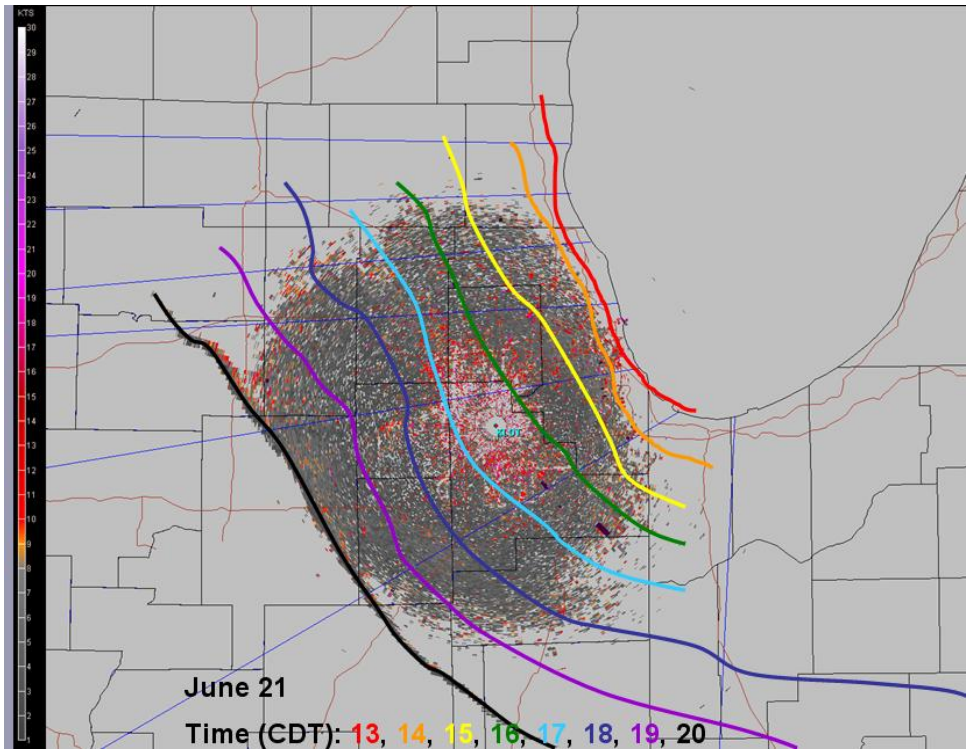

Figure A.15. Same as Figure A.1, except for 6/21/05 overlaid on the 2003 CDT spectral width PPI.

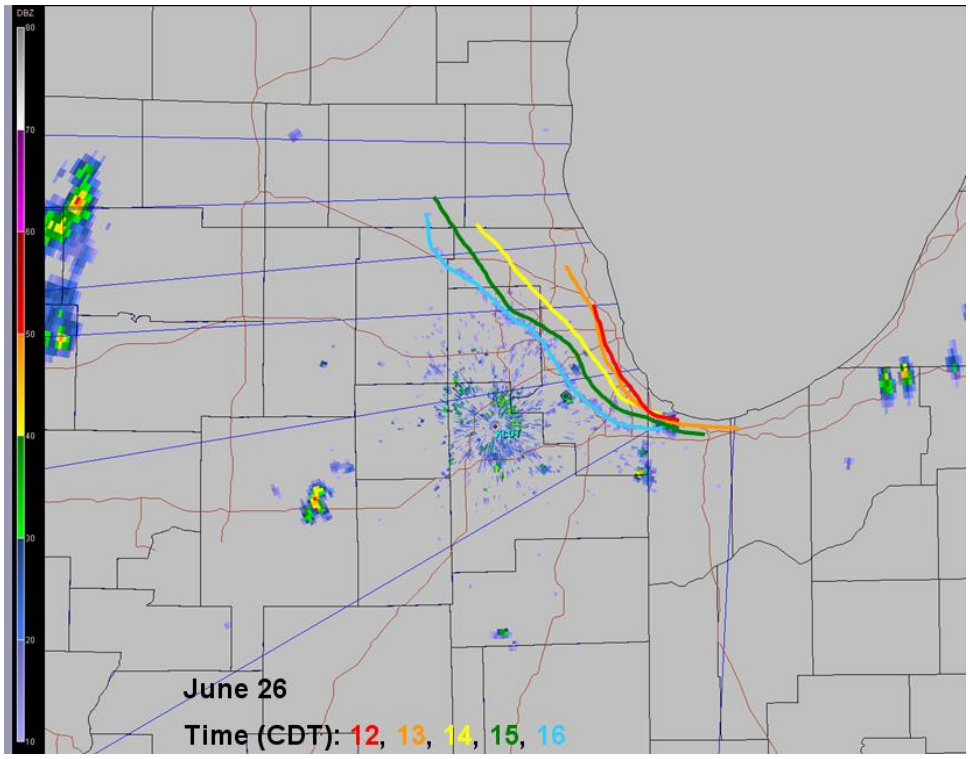

Figure A.16. Same as Figure A.1, except for 6/26/05 overlaid on the 1601 CDT base reflectivity PPI.

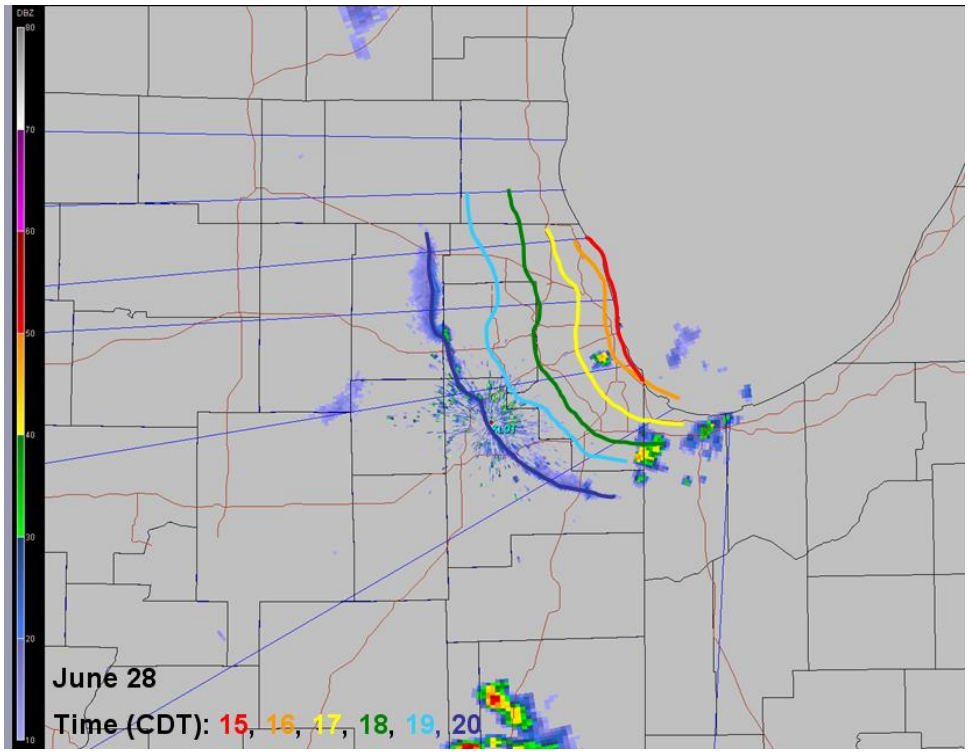

Figure A.17. Same as Figure A.1, except for 6/28/05 overlaid on the 2000 CDT base reflectivity PPI.

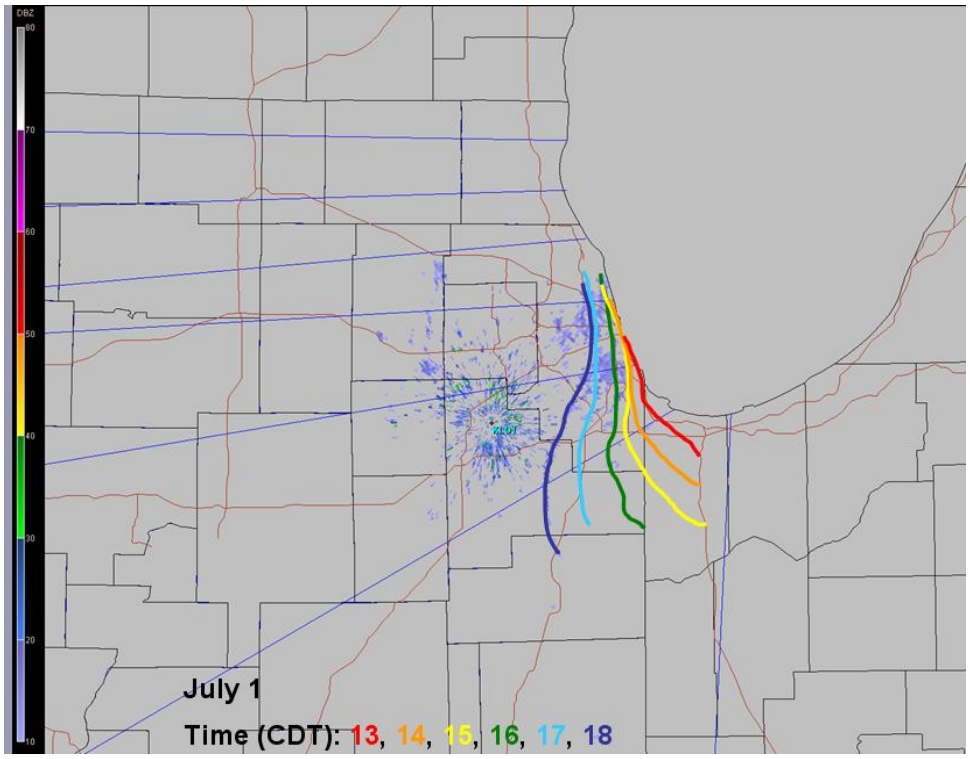

Figure A.18. Same as Figure A.1, except for 7/1/05 overlaid on the 1806 CDT base reflectivity PPI.

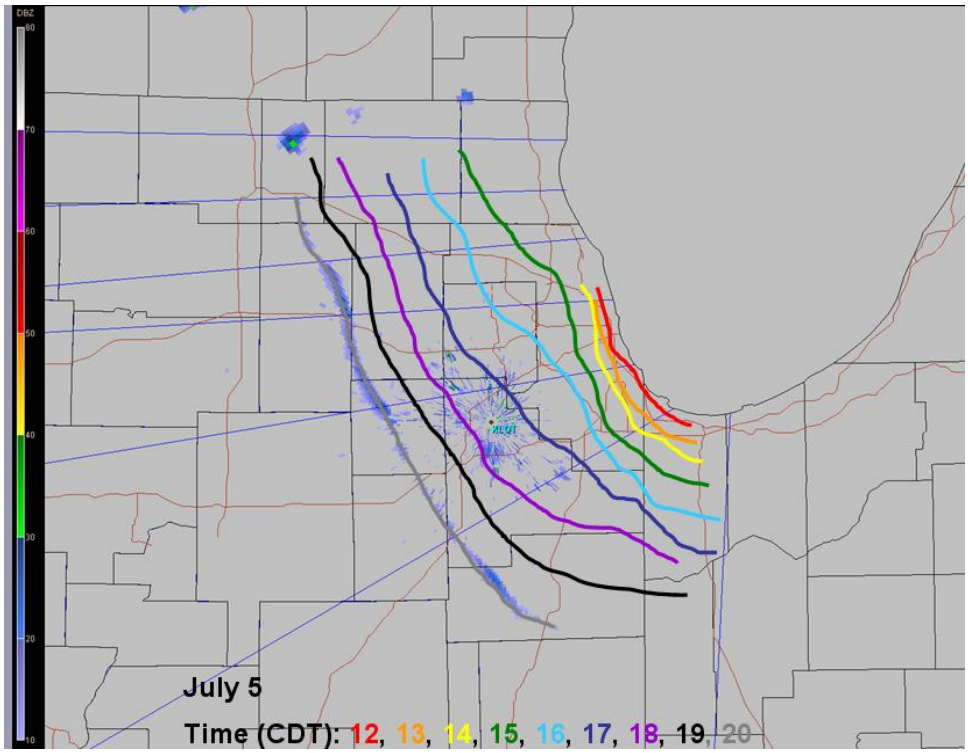

Figure A.19. Same as Figure A.1, except for 7/5/05 overlaid on the 2004 CDT base reflectivity PPI.

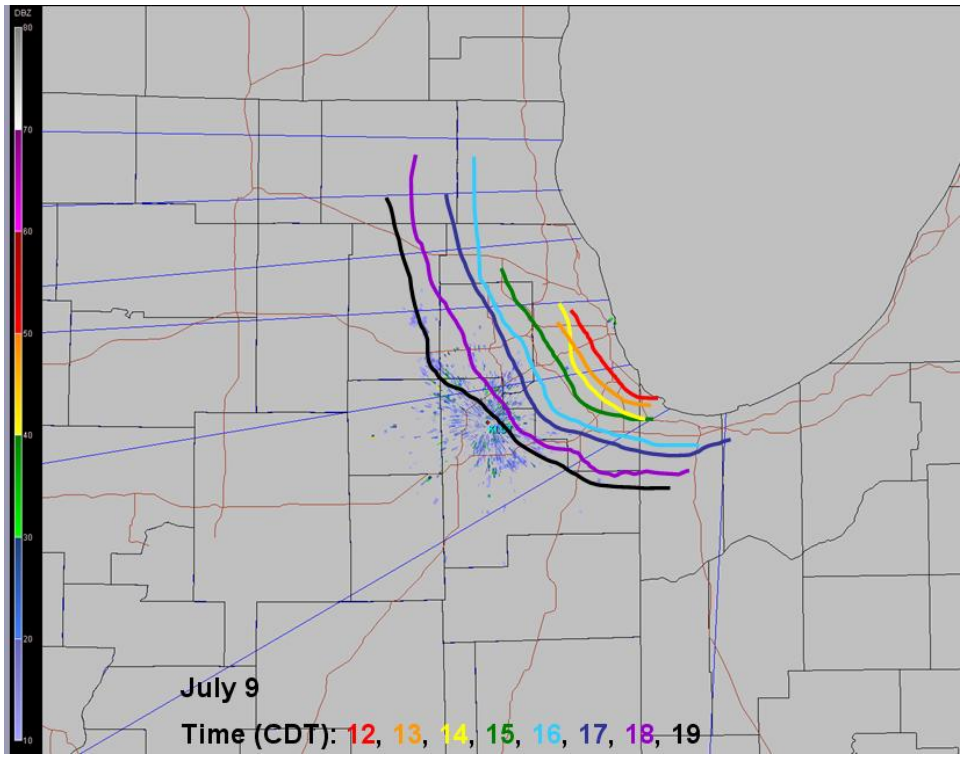

Figure A.20. Same as Figure A.1, except for 7/9/05 overlaid on the 1909 CDT base reflectivity PPI.

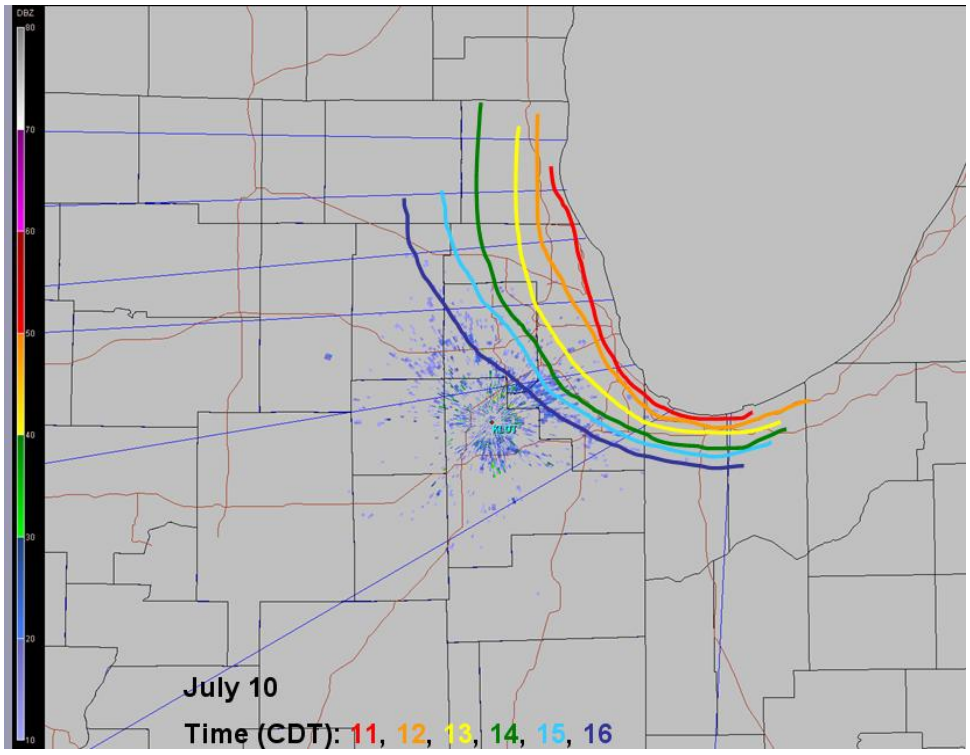

Figure A.21. Same as Figure A.1, except for 7/10/05 overlaid on the 1601 CDT base reflectivity PPI.

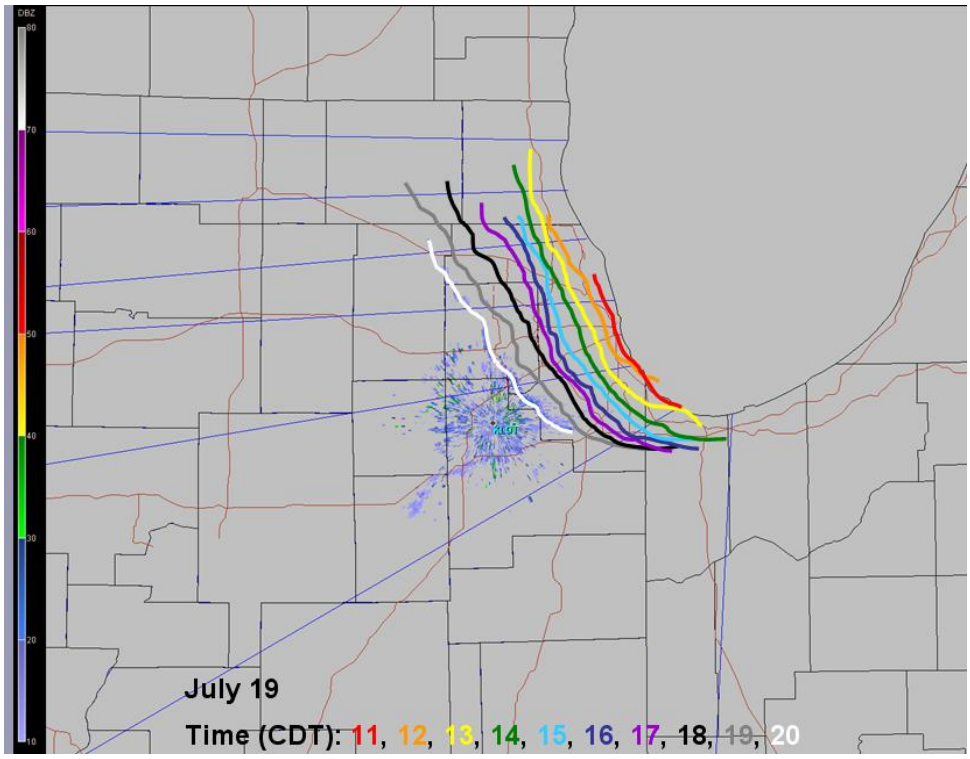

Figure A.22. Same as Figure A.1, except for 7/19/05 overlaid on the 2003 CDT base reflectivity PPI.

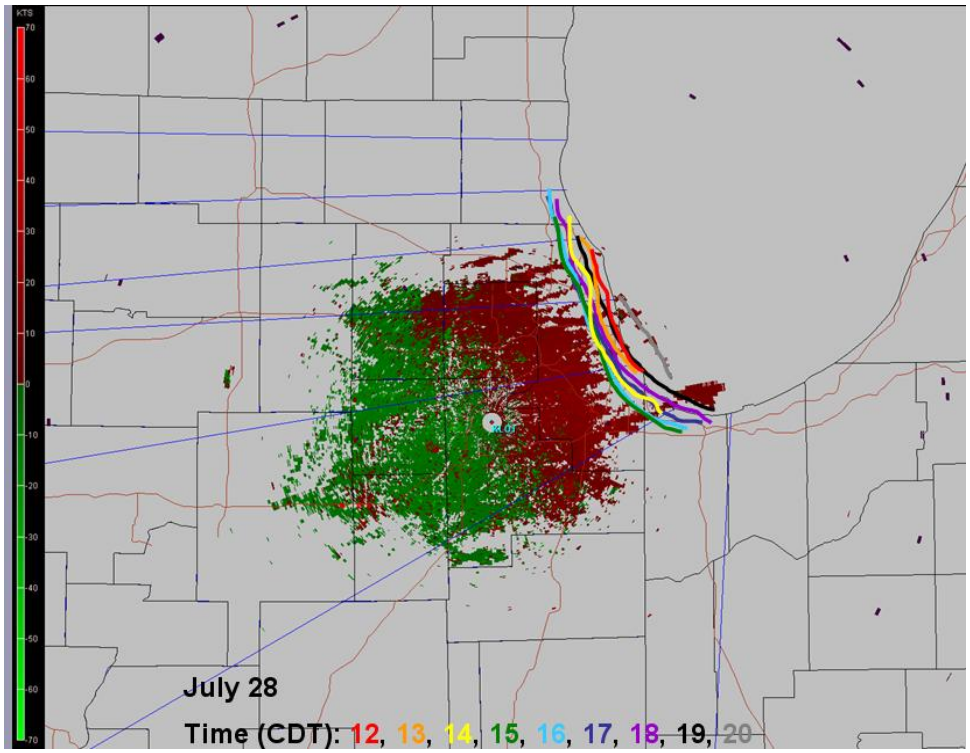

Figure A.23. Same as Figure A.1, except for 7/28/05 overlaid on the 2002 CDT base velocity PPI.

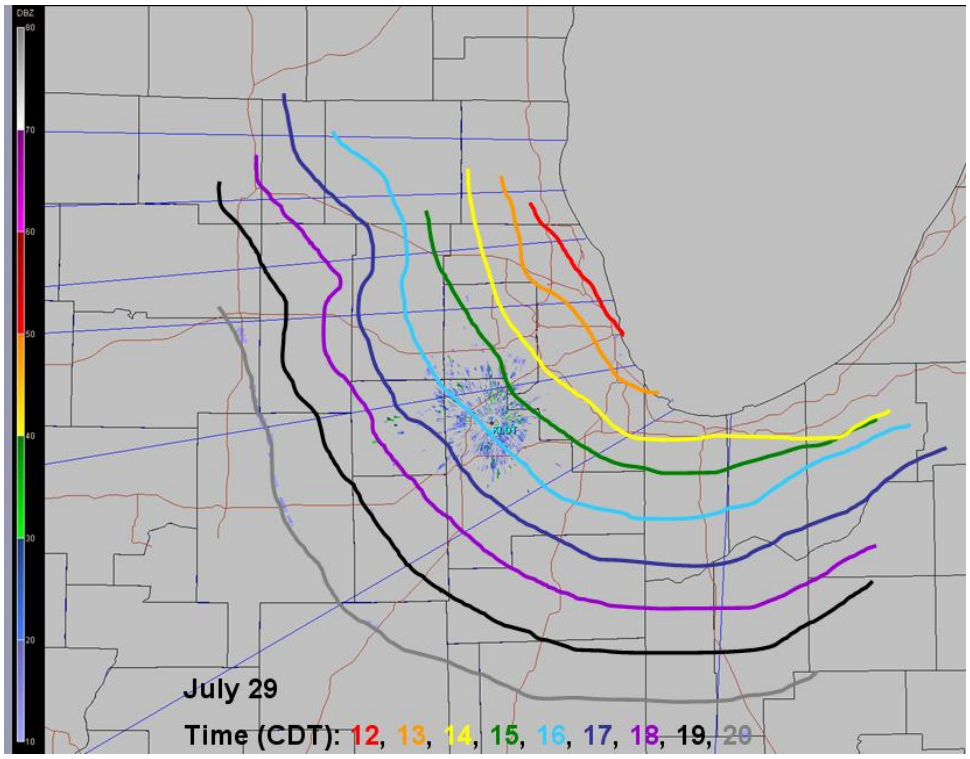

Figure A.24. Same as Figure A.1, except for 7/29/05 overlaid on the 2001 CDT base reflectivity PPI.

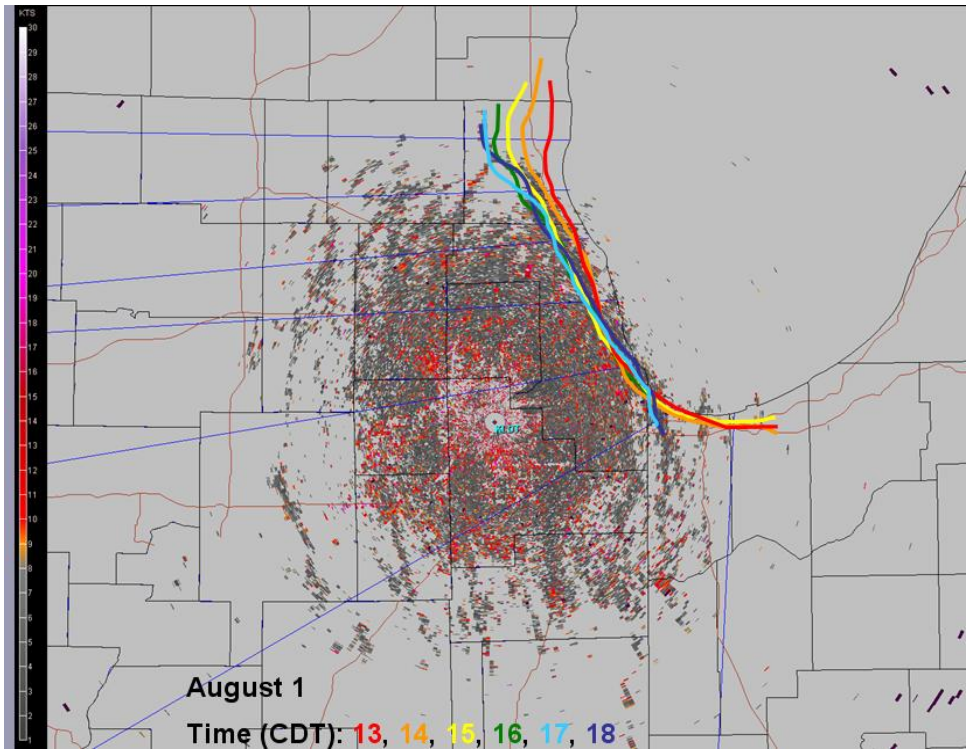

Figure A.25. Same as Figure A.1, except for 8/1/05 overlaid on the 1807 CDT spectral width PPI.

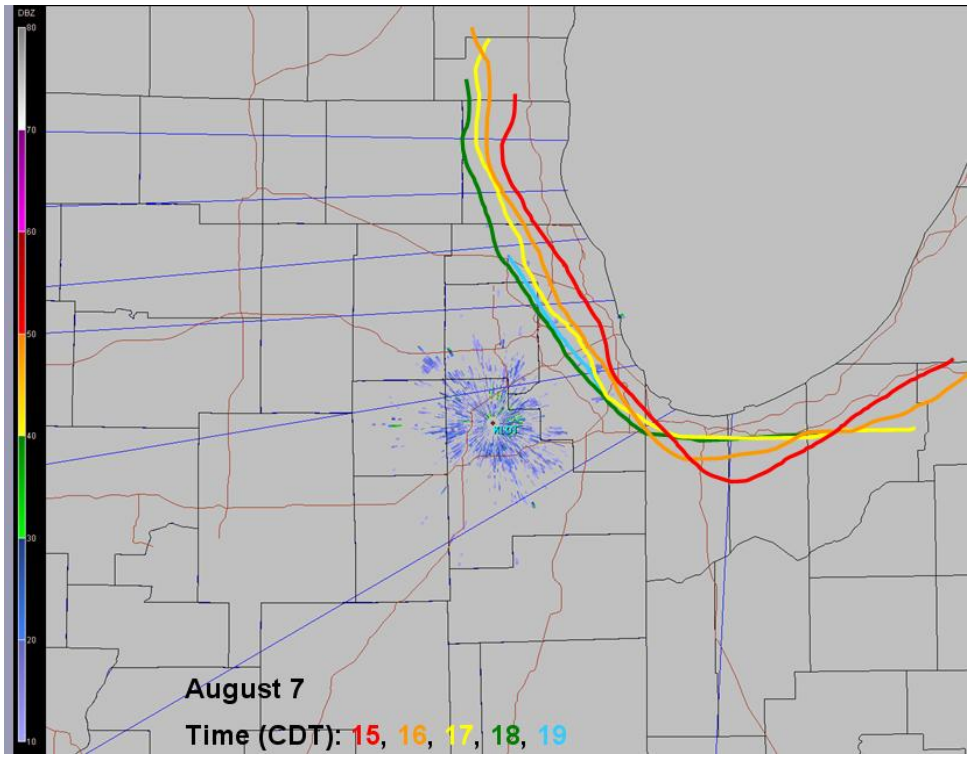

Figure A.26. Same as Figure A.1, except for 8/7/05 overlaid on the 1908 CDT base reflectivity PPI.

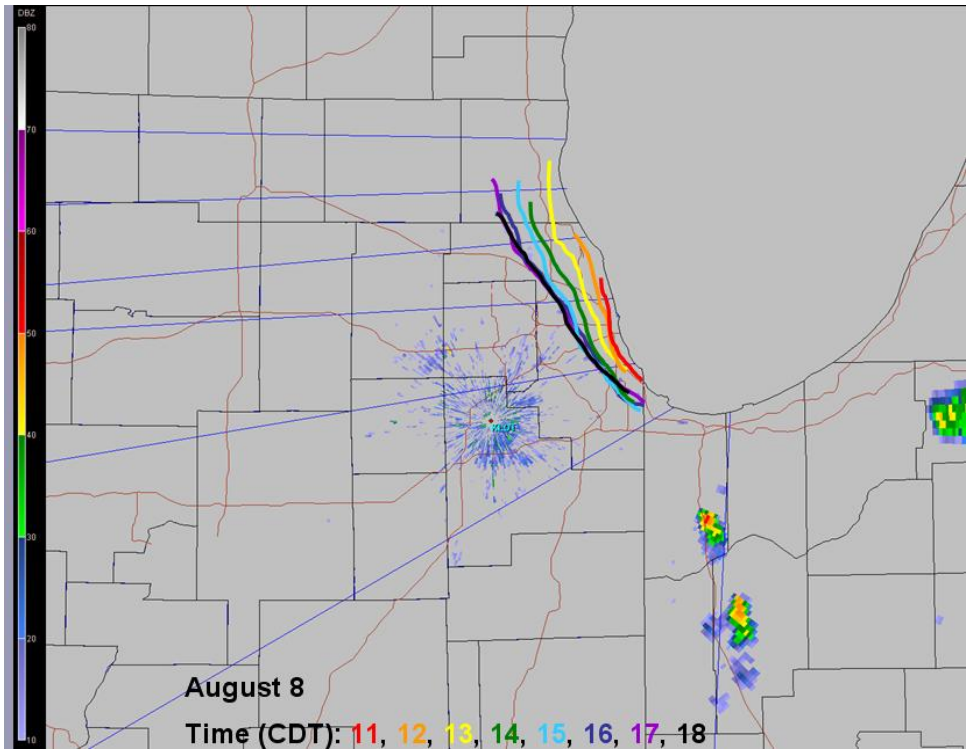

Figure A.27. Same as Figure A.1, except for 8/8/05 overlaid on the 1801 CDT base reflectivity PPI.

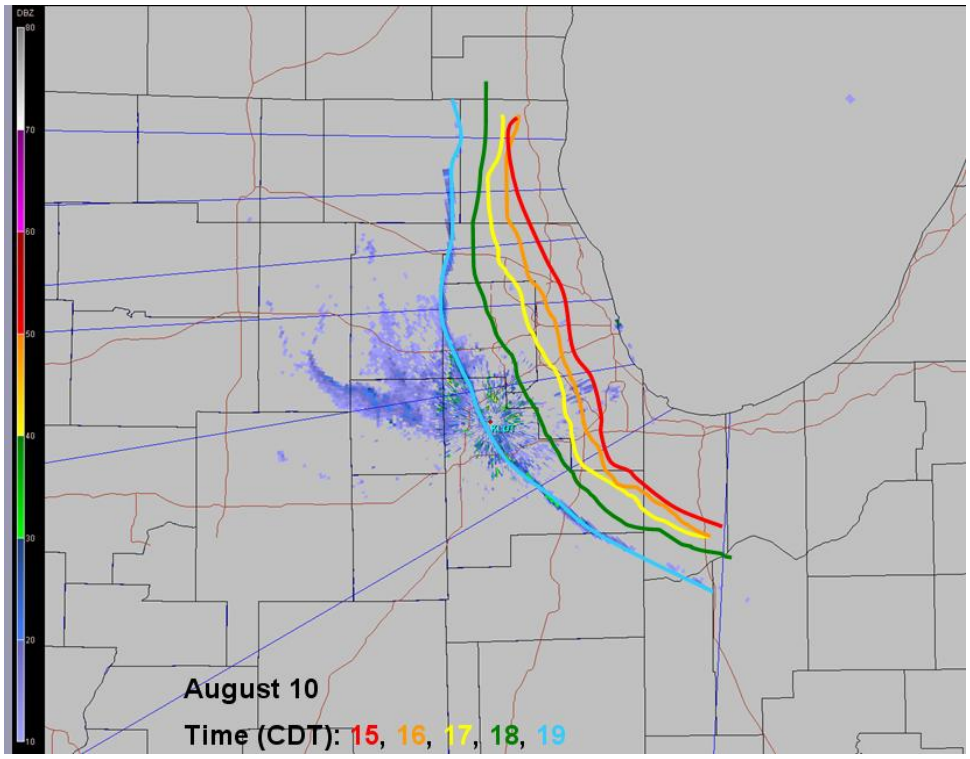

Figure A.28. Same as Figure A.1, except for 8/10/05 overlaid on the 1900 CDT base reflectivity PPI.

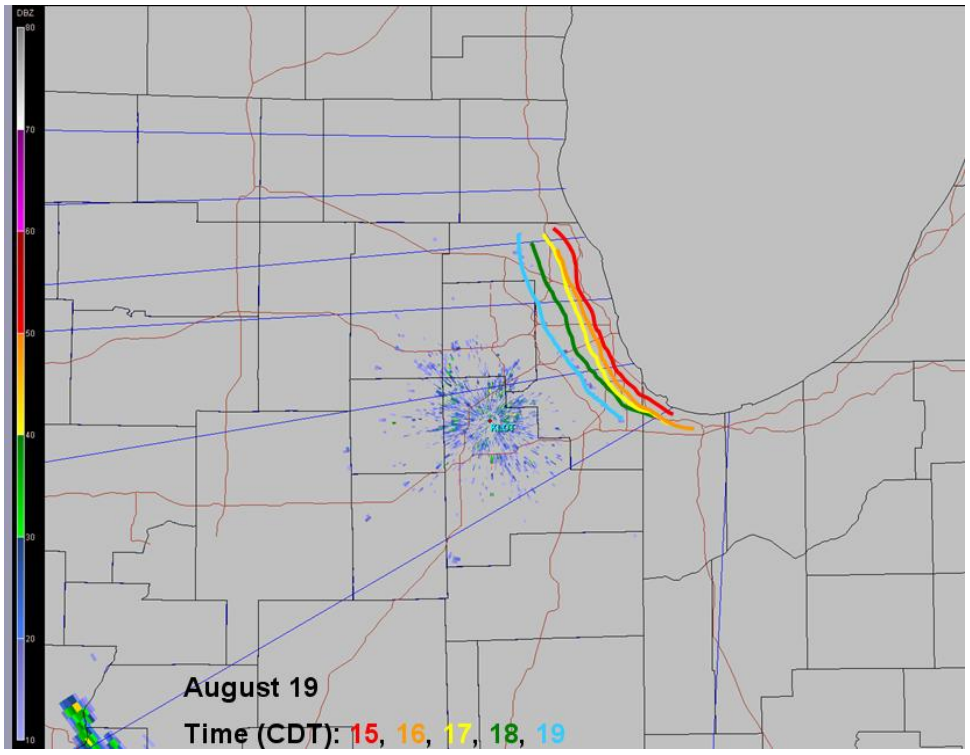

Figure A.29. Same as Figure A.1, except for 8/19/05 overlaid on the 1908 CDT base reflectivity PPI.

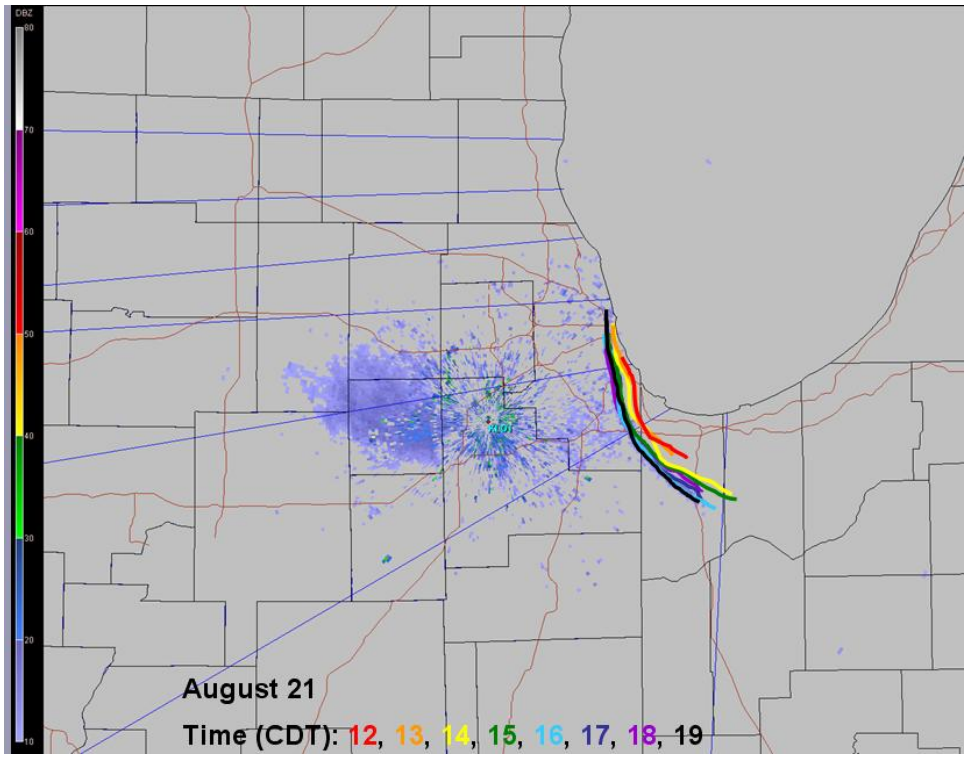

Figure A.30. Same as Figure A.1, except for 8/21/05 overlaid on the 1904 CDT base reflectivity PPI.

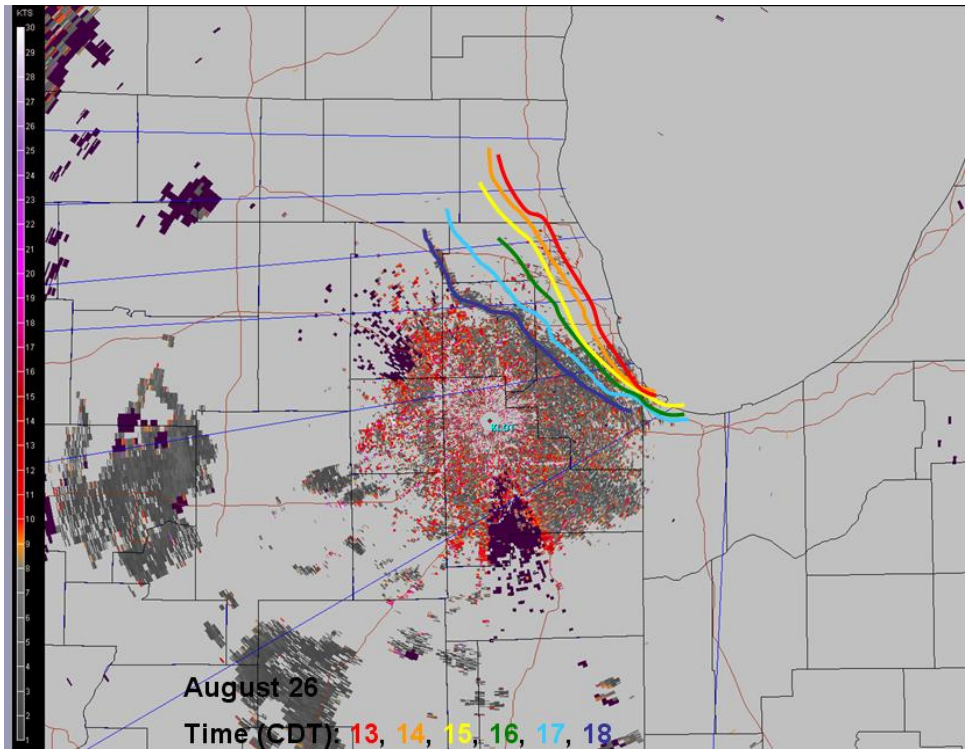

Figure A.31. Same as Figure A.1, except for 8/26/05 overlaid on the 1803 CDT spectral width PPI.

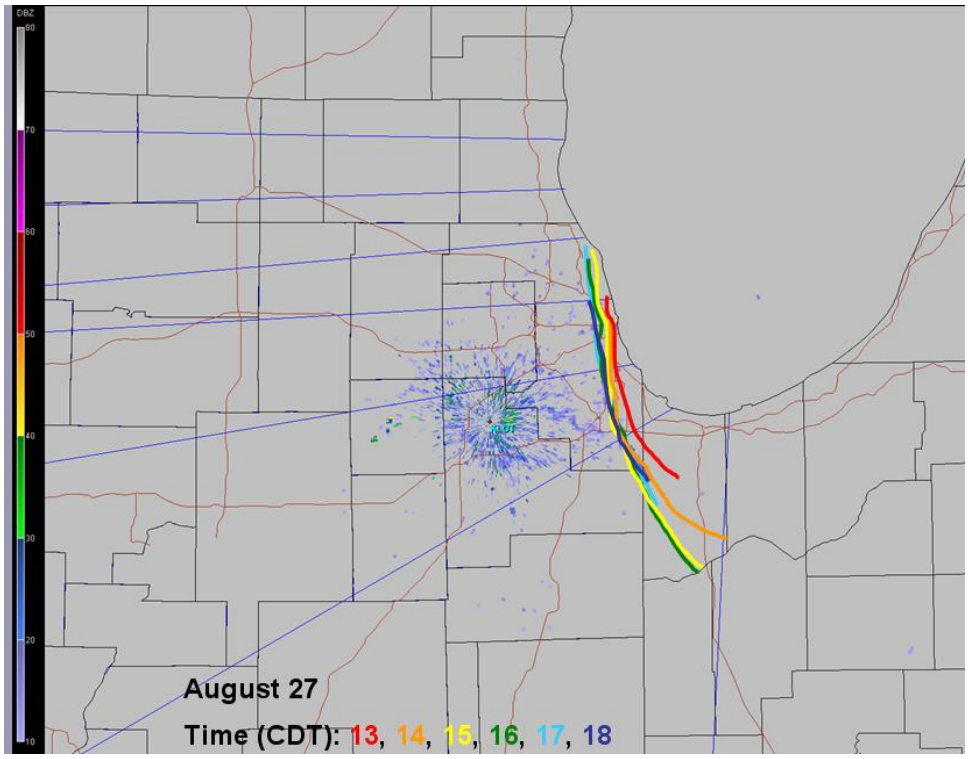

Figure A.32. Same as Figure A.1, except for 8/27/05 overlaid on the 1805 CDT base reflectivity PPI.

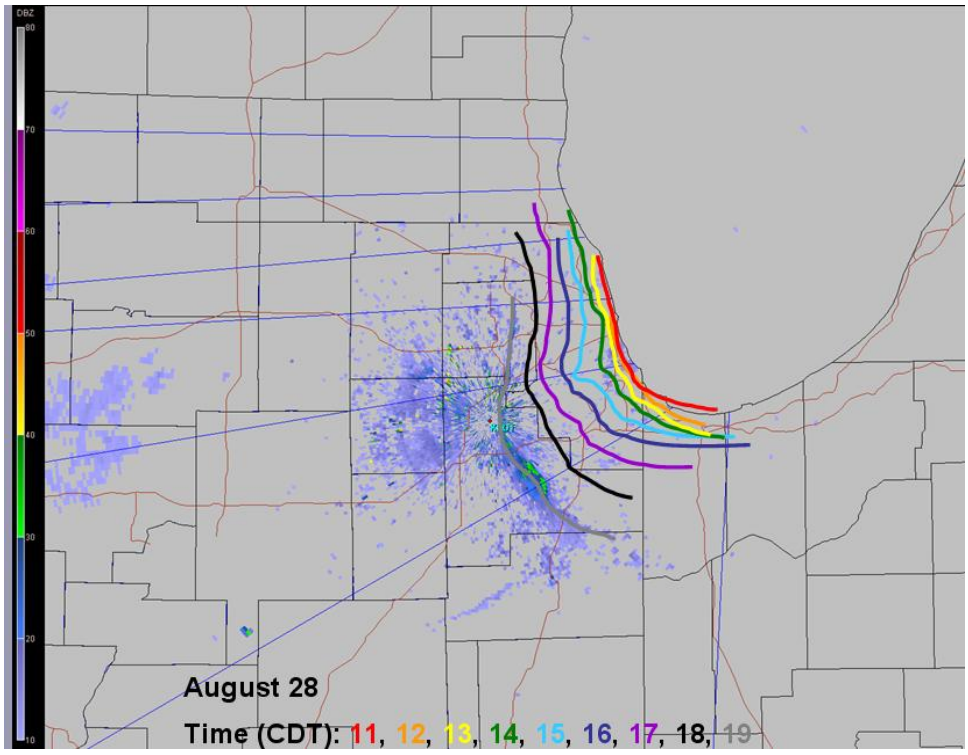

Figure A.33. Same as Figure A.1, except for 8/28/05 overlaid on the 1904 CDT base reflectivity PPI.

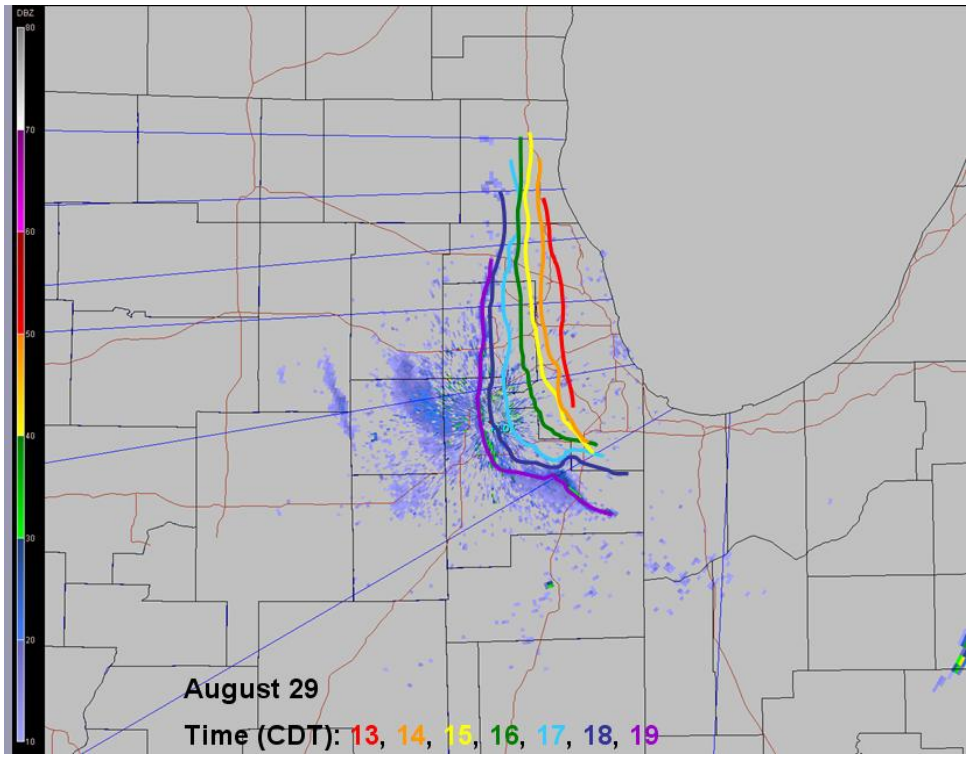

Figure A.34. Same as Figure A.1, except for 8/29/05 overlaid on the 1904 CDT base reflectivity PPI.

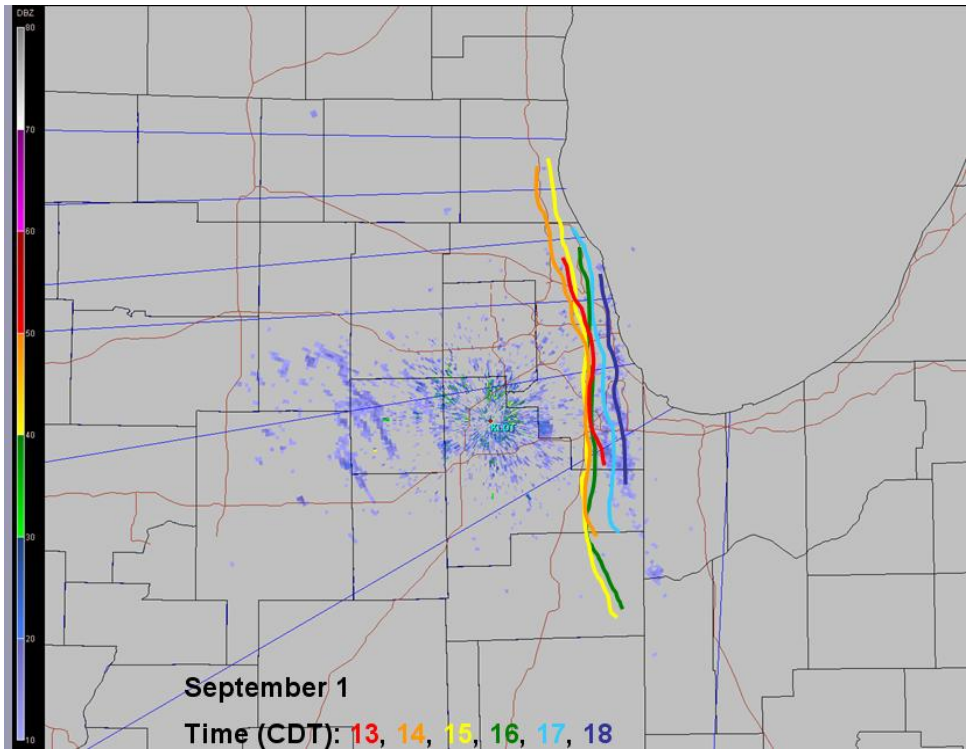

Figure A.35. Same as Figure A.1, except for 9/1/05 overlaid on the 1800 CDT base reflectivity PPI.

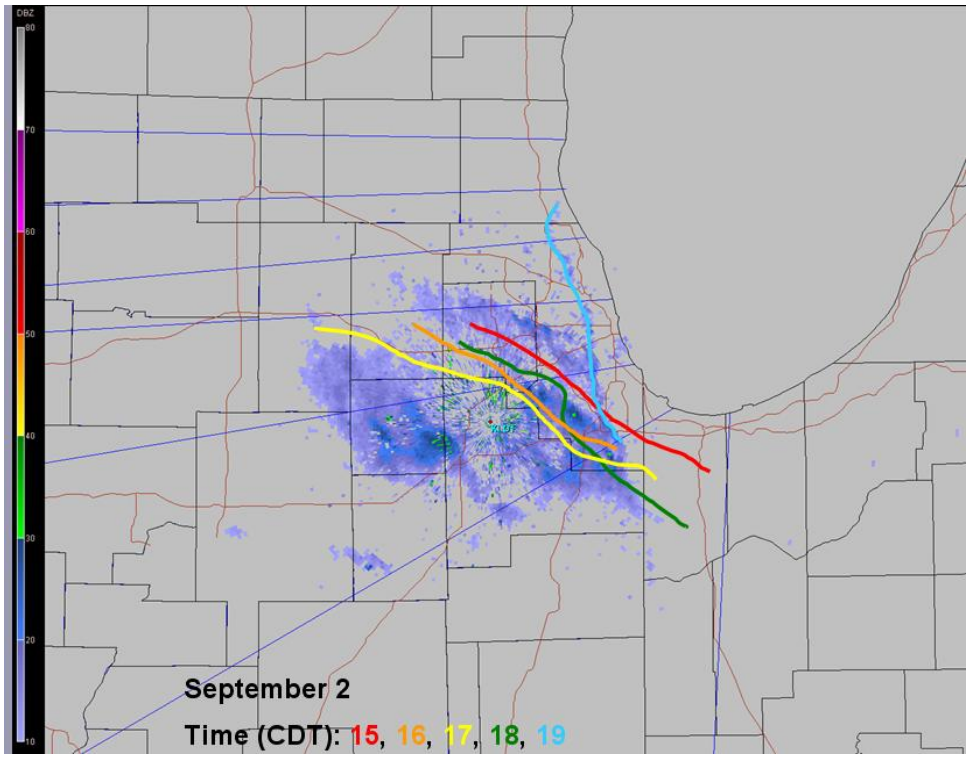

Figure A.36. Same as Figure A.1, except for 9/2/05 overlaid on the 1908 CDT base reflectivity PPI.

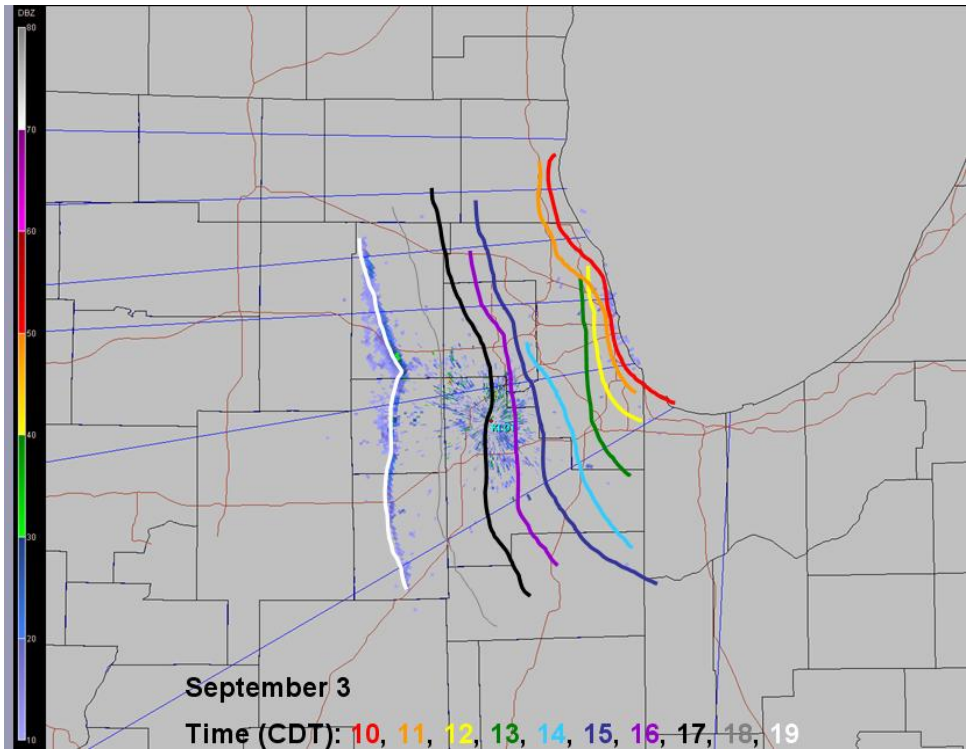

Figure A.37. Same as Figure A.1, except for 9/3/05 overlaid on the 1908 CDT base reflectivity PPI.

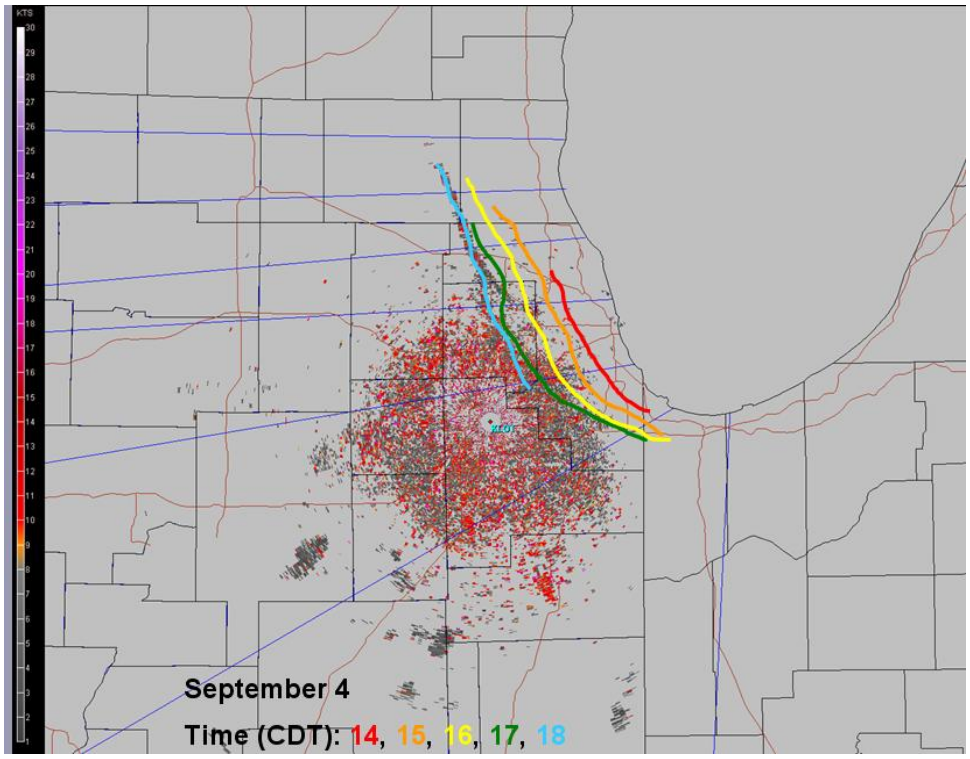

Figure A.38. Same as Figure A.1, except for 9/4/05 overlaid on the 1803 CDT spectral width PPI.

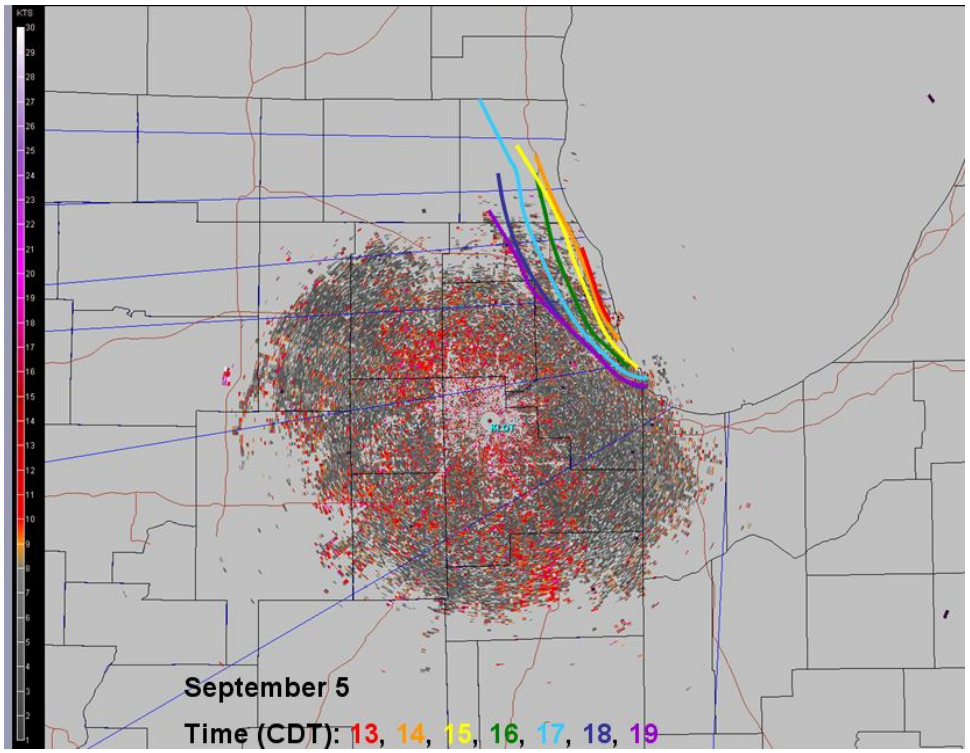

Figure A.39. Same as Figure A.1, except for 9/5/05 overlaid on the 1902 CDT spectral width PPI.

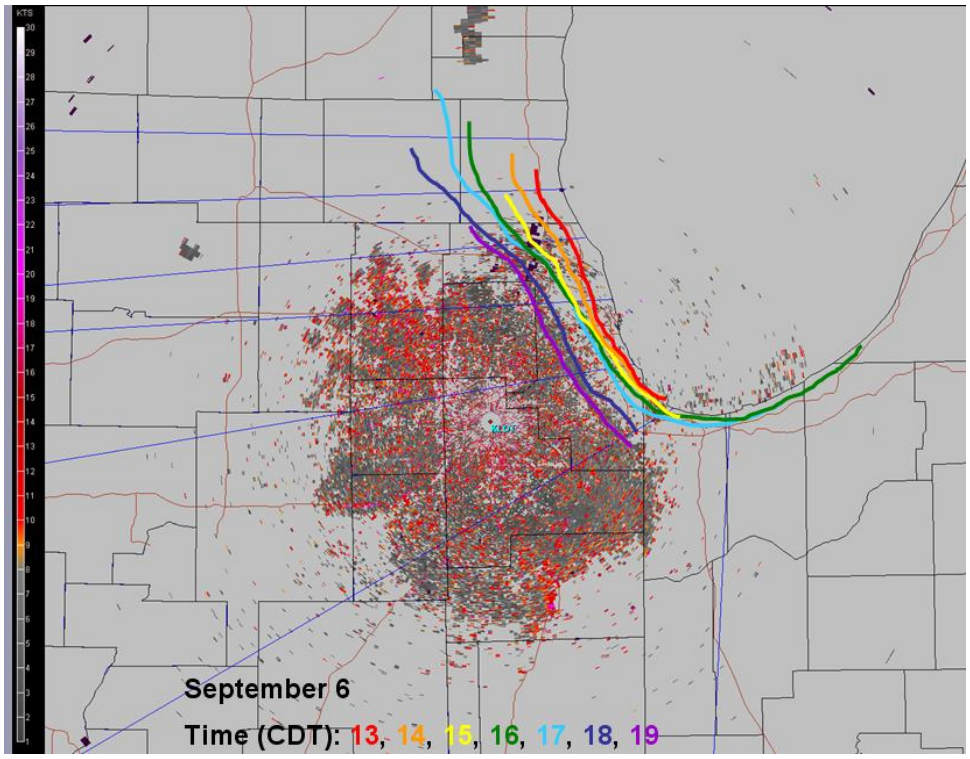

Figure A.40. Same as Figure A.1, except for 9/6/05 overlaid on the 1902 CDT spectral width PPI.

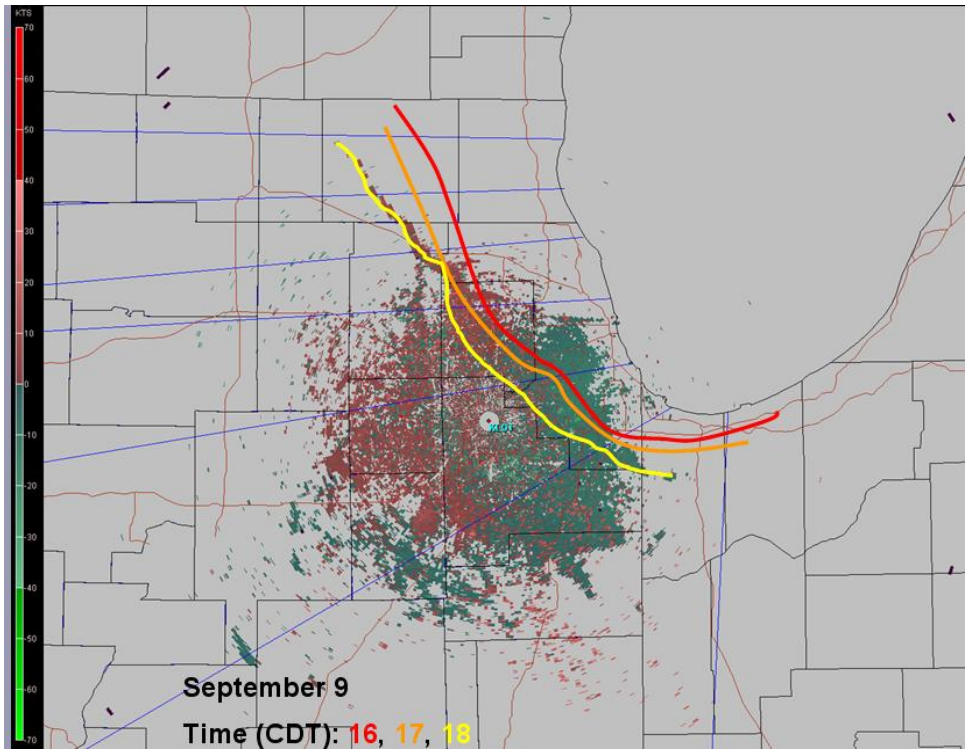

Figure A.41. Same as Figure A.1, except for 9/9/05 overlaid on the 1808 CDT base velocity PPI.

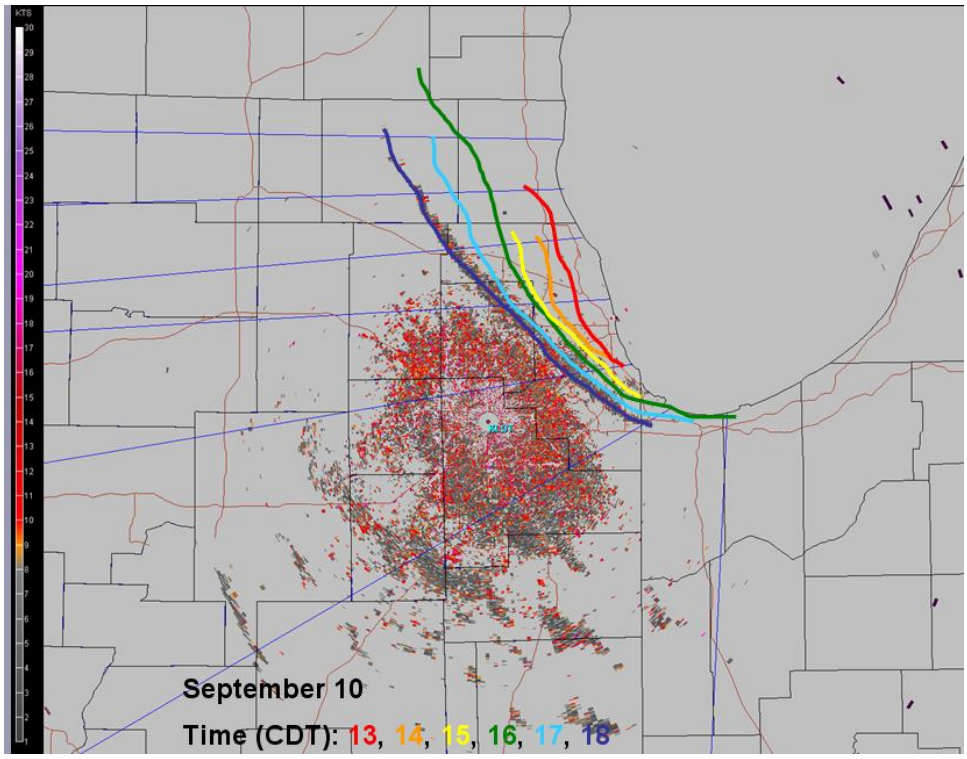

Figure A.42. Same as Figure A.1, except for 9/10/05 overlaid on the 1808 CDT spectral width PPI.

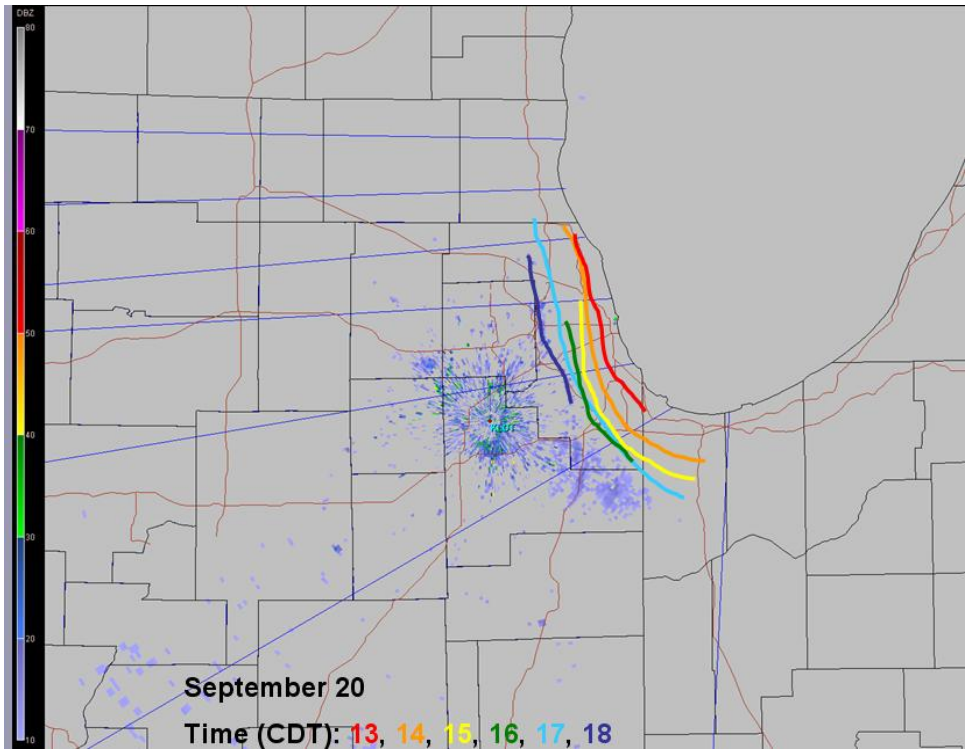

Figure A.43. Same as Figure A.1, except for 9/20/05 overlaid on the 1800 CDT base reflectivity PPI.

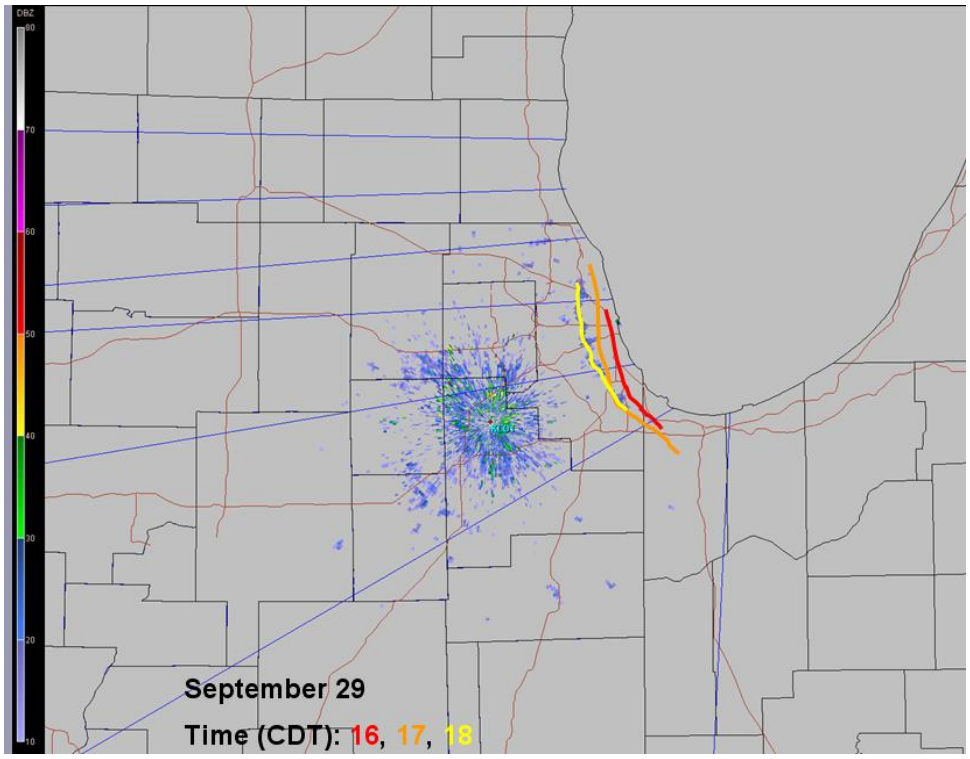

Figure A.44. Same as Figure A.1, except for 9/29/05 overlaid on the 1800 CDT base reflectivity PPI.